AD-A036 120 ARMY ENGINEER WATERWAYS EXPERIMENT STATION VICKSBURG MISS F/G 8/13
EFFECT OF HORIZONTAL REINFORCEMENT ON STABILITY OF EARTH MASSES--ETC(U)
SEP 76 M M AL-HUSSAINI, E B PERRY

UNCLASSIFIED WES-TR-S-76-11 NL

1 OF 2
AD A036120

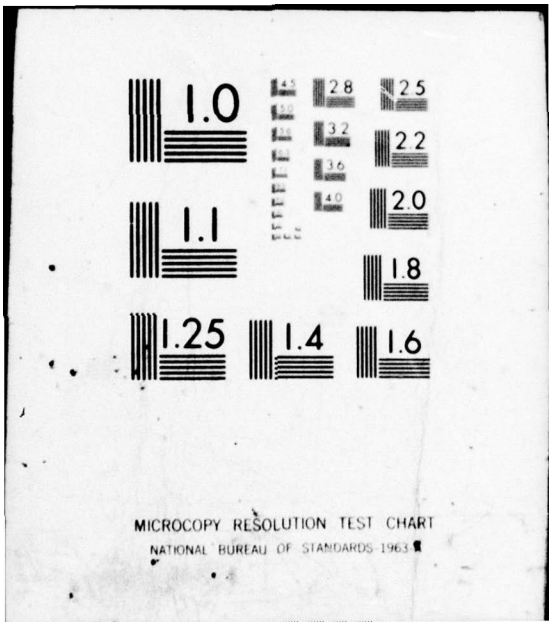
1.0
1.1
1.25
1.4
1.6
1.8
2.0
2.2
2.5
2.8
3.2
3.6
4.0
MICROCOPY RESOLUTION TEST CHART
NATIONAL BUREAU OF STANDARDS 1963-A

TECHNICAL REPORT S-76-11

EFFECT OF HORIZONTAL REINFORCEMENT ON STABILITY OF EARTH MASSES

by

Nabil A. Al-Hussaini, Edward B. Perry

Soils and Pavements Laboratory
U. S. Army Engineer Waterways Experiment Station
P. O. Box 631, Vicksburg, Miss. 39180

September 1976
Final Report

Unclassified

SECURITY CLASSIFICATION OF THIS PAGE (When Data Entered)

REPORT DOCUMENTATION PAGE

READ INSTRUCTIONS BEFORE COMPLETING FORM

1. REPORT NUMBER: Technical Report S-76-11

2. GOVT ACCESSION NO.

3. RECIPIENT'S CATALOG NUMBER

(14) WES-TR-S-76-11

4. TITLE (and Subtitle)

(6) EFFECT OF HORIZONTAL REINFORCEMENT ON STABILITY OF EARTH MASSES

5. TYPE OF REPORT & PERIOD COVERED

(9) Final report Jul 74 - Jun 76

6. PERFORMING ORG. REPORT NUMBER

7. AUTHOR(s)

(10) Mosaid M. Al-Hussaini, Edward B. Perry

8. CONTRACT OR GRANT NUMBER(s)

(16)

9. PERFORMING ORGANIZATION NAME AND ADDRESS

U. S. Army Engineer Waterways Experiment Station
Soils and Pavements Laboratory
P. O. Box 631, Vicksburg, Miss. 39180

(17)

10. PROGRAM ELEMENT, PROJECT, TASK AREA & WORK UNIT NUMBERS

Project 4A161102AT22
Task A2 Work Unit 004

11. CONTROLLING OFFICE NAME AND ADDRESS

Office, Chief of Engineers, U. S. Army
Washington, D. C. 20314

(11)

12. REPORT DATE

September 1976

13. NUMBER OF PAGES

104

(12) 120

14. MONITORING AGENCY NAME & ADDRESS(if different from Controlling Office)

15. SECURITY CLASS. (of this report)

Unclassified

15a. DECLASSIFICATION/DOWNGRADING SCHEDULE

16. DISTRIBUTION STATEMENT (of this Report)

Approved for public release; distribution unlimited.

17. DISTRIBUTION STATEMENT (of the abstract entered in Block 20, if different from Report)

18. SUPPLEMENTARY NOTES

19. KEY WORDS (Continue on reverse side if necessary and identify by block number)

Membrane strips
Reinforced earth
Reinforcing materials
Retaining walls
Soil stability
Steels
Stress-strain relations (Soils)

20. ABSTRACT (Continue on reverse side if necessary and identify by block number)

Reinforced earth consists primarily of soil whose engineering properties and performance have been improved by the introduction of small quantities of frictional material that possesses a relatively high tensile strength and modulus of elasticity. The design concept of reinforced earth is based on the assumption that the induced lateral force of a restrained soil mass under load will be resisted by frictional forces that develop between the reinforcement and the surrounding soil. This practical concept has been applied to

next page

(Continued)

DD FORM 1 JAN 73 1473 EDITION OF 1 NOV 65 IS OBSOLETE

Unclassified

SECURITY CLASSIFICATION OF THIS PAGE (When Data Entered)

038 100

6 pg

20. ABSTRACT (Continued).

cont.

the problem of stabilizing slopes, retaining walls, pavements, and other applications as described in the literature review.

The objectives of this study were: (a) to investigate the uncertainties concerning the stress-strain distribution and the interrelation between the reinforcement and the surrounding soil, and (b) to evaluate the performance of neoprene-coated nylon fabric (membrane) versus galvanized steel as reinforcing material within a cohesionless soil mass. These two objectives were directed toward the feasibility of using the concept of reinforced earth in Corps of Engineers projects.

The objectives were achieved by constructing two instrumented retaining walls, each 16 ft long, 12 ft high, and 10 ft deep; the first wall was reinforced with membrane ties, and the second with galvanized steel ties. The membrane ties were 4 in. wide, 0.08 in. thick, and 10 ft long, spaced at intervals of 2 and 4 ft in the vertical and horizontal directions, respectively. The galvanized steel ties had the same width and length as the membrane ties but were 0.024 in. thick and spaced 2.5 ft apart along the wall. Three galvanized steel ties along the center line of the wall and located at 1, 5, and 9 ft above the bottom of the wall were instrumented with complete SR-4 strain gage bridges on both surfaces at points 1, 2.5, 5, and 7.5 ft from the face of the wall. At the elevation of each instrumented tie and 1 ft away from the surface of the wall, two pressure cells were placed to measure the induced vertical and horizontal pressures within the backfill soil. A similar pressure cell arrangement was used for the membrane-reinforced wall. The skin element which comprised the exposed surface of the wall was made of Alcoa T11 high-strength aluminum landing mat panels similar to those used for construction of expedient airfield [illegible]. Although the membrane-reinforced wall failed before it reached 10 ft high, the steel-reinforced wall was constructed to the full height of 12 ft and uniformly surcharge loaded, using 1- and 2-ton lead weights, to surface pressure in excess of 1500 psf. Deflection of the skin elements was measured during construction and surcharge loading. It is probable that failure of the reinforced earth retaining wall was initiated by failure of the connection which joined the reinforcing ties to the skin element or by failure of the skin element due to buckling and shear.

Based on the instrumentation measurements collected during construction and during loading of the structure to failure, it appears that the Rankine earth pressure theory provides a good approximation for the measured lateral pressure when the wall is carrying little or no surcharge load. Prior to failure under a substantial surcharge loading, the measured lateral earth pressure was maximum at the middle third of the wall and varied from 1.0 to 1.2 times the earth pressure predicted by the Rankine theory for the active case. The curve connecting the points where maximum tensile stress occurred in the reinforcing ties did not coincide with the theoretical Rankine failure surface. An improved method of defining the effective length of reinforcing tie, compatible with full-scale field test results, to be used in computing tie pullout should be developed.

The field test conducted at the U. S. Army Engineer Waterways Experiment Station indicated that the reinforced earth concept provides another alternative for constructing earth structures which may prove to be more economical when compared with conventional methods under certain conditions.

PREFACE

The study reported herein was conducted at the U. S. Army Engineer Waterways Experiment Station (WES) under the sponsorship of the Office, Chief of Engineers (OCE), Project No. 4A161102AT22, "Theory and Principles of Reinforced Earth," Task A2, Work Unit 004.

The field and laboratory studies described were performed during the period July 1974 through June 1976 by Drs. M. M. Al-Hussaini and E. B. Perry, both of the Soil Mechanics Division, Soils and Pavements Laboratory, assisted by Mr. C. L. Rone of the Pavement Investigation Division, Soils and Pavements Laboratory, and Mr. V. Agostinelli of the Technical Engineering Branch, Lower Mississippi Valley Division. The literature review portion of this report was written by Dr. Perry and the remaining parts were written by Dr. Al-Hussaini under the general direction of Mr. C. L. McAnear, Chief, Soil Mechanics Division, and Mr. J. P. Sale, Chief, Soils and Pavements Laboratory. OCE technical monitor for this study was Mr. A. F. Muller.

Directors of WES during the conduct of this study and the preparation of this report were COL G. H. Hilt, CE, and COL J. L. Cannon, CE. Technical Director was Mr. F. R. Brown.

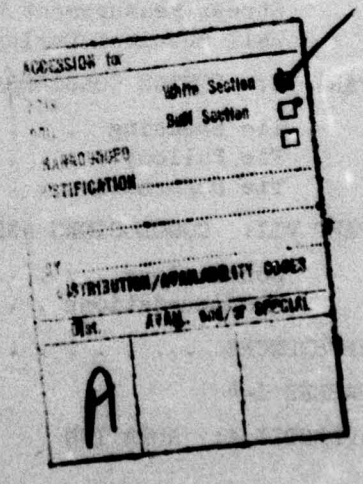

CONTENTS

CONVERSION FACTORS, U. S. CUSTOMARY TO METRIC (SI) UNITS OF MEASUREMENT

U. S. customary units of measurement used in this report can be converted to metric (SI) units as follows:

Multiply	By	To Obtain
mils	0.0254	millimetres
inches	25.4	millimetres
feet	0.3048	metres
square feet	0.09290304	square metres
pounds (mass)	0.4535924	kilograms
tons (2000 lb, mass)	907.1847	kilograms
pounds (force)	4.448222	newtons
ounces (mass) per square yard	0.03390575	kilograms per square metre
pounds (mass) per cubic foot	16.01846	kilograms per cubic metre
pounds (force) per square inch	6894.757	pascals
pounds (force) per square foot	47.88026	pascals
kips (force) per square inch	6894.757	kilopascals
tons (force) per square foot	95.76052	kilopascals
inches per minute	25.4	millimetres per minute
degrees (angular)	0.01745329	radians

EFFECT OF HORIZONTAL REINFORCEMENT ON STABILITY OF EARTH MASSES

PART I: INTRODUCTION

The Reinforced Earth Concept

1. Reinforced earth may be defined as a construction material composed primarily of soil whose performance has been improved by the introduction of small quantities of other material in a form of bars, strips, or fibers to resist tensile forces that soil alone is unable to resist. The concept of reinforced earth is very old. Ancient Egypt and Babylon and many other civilizations used straw in clay to improve the quality of building material in the construction of their dwellings, roads, and other structures. However, this concept remained a craft carried from one generation to the other until 1969 when Henri Vidal developed and patented his concept of reinforced earth. His basic concept is to assume that a differential tensile force develops in a reinforcement, creating a linkage between soil grains such that the tensile forces are resisted by a frictional force between the reinforcement and soil grains. Vidal patented (U. S. Patent No. 3,421,326, 14 January 1969) his concept with regard to reinforced earth with reference to its application to practical problems. An earlier patent by Andress Munster (U. S. Patent No. 1,762,343, 10 June 1930) provides for tension members which unify an earth fill to form a substantially solid mass, thereby making it practical to construct a retaining wall of the earth fill itself.

2. The general design principles of reinforced earth and applications outside the U. S. have been presented by Vidal and co-workers.[1-18] The first reinforced earth structure was completed in Europe in 1964.[16] Reinforced earth came to the U. S. in 1971 with the establishment of the Reinforced Earth Company, Washington, D. C., as the U. S. licensee for the process. More than 100 reinforced earth structures have been built in countries throughout the world.

Reinforced earth applications have included retaining walls, platforms on sloping ground, quay walls, foundation slabs, walls or piers including foundation footings, and bridge abutments.[14,17] Potential reinforced earth applications include embankment dams, beams, and tunnels in embankments. Military applications to date, both in France, include military atomic shelters[7] and the Long Island merlon at Brest.[17] Reinforced earth has also been suggested for use in constructing missile silos.[17]

3. Three general types of application of reinforced earth have been employed in the U. S.:[19-31] (a) reinforced earth fill supporting a highway, (b) foundation slab supporting a highway, and (c) retaining wall in a marine environment supporting a railroad. One of each of these three applications will be described to show a spectrum of reinforced earth projects in the U. S. Reinforced earth was approved in November 1974 by the Federal Highway Administration of the U. S. Department of Transportation as an acceptable standard highway construction practice.[32,33]

Reinforced earth fill

4. The first reinforced earth project in the U. S. was a reinforced earth fill located on Route 39 near Crystal Lake in the San Gabriel Mountains, Los Angeles County, California.[19-20,23-30] The reinforced earth fill was constructed over a random fill embankment founded on slide debris. A toe buttress was built at the bottom of the slide debris to act as a stabilizing embankment. The reinforced earth embankment had a maximum height of 55 ft* and a length of 528 ft. An extensive drainage system consisting of a 3-ft-thick permeable interceptor blanket behind the wall and a herringbone pattern of 8- to 18-in.-diam perforated metal pipes backfilled with permeable filter material within the fill material was used to remove surface water and seepage.

5. Consolidated-drained triaxial tests on the embankment material compacted to field density (85 percent relative compaction) gave an apparent angle of internal friction of 44 deg. Shear box tests gave an

* A table of factors for converting U. S. customary units of measurement to metric (SI) units is shown on page 3.

angle of skin friction between the embankment material and the reinforcing ties of 31 deg. The reinforcing ties and skin elements were constructed of galvanized steel with a yield strength of 37,000 psi, ultimate strength of 50,000 psi, Young's modulus of 28,500,000 psi, and Poisson's ratio of 0.28. The ties had a thickness of 0.118 in., width of 2.362 in., and length of 22.8 to 46 ft. The skin elements were semi-elliptical in shape with a height of 10 in. along the major axis and 3.7 in. along the minor axis, 0.118 in. thick, and 6.5 to 39.4 ft long.

6. In order to monitor the behavior of the completed structure, a comprehensive instrumentation program was planned and implemented under the auspices of the Federal Highway Administration of the U. S. Department of Transportation. The instrumentation included slope indicators to measure the internal movement of the fill and slide debris, settlement platforms to measure vertical settlements, extensometers to measure soil strains, soil pressure cells to measure soil stresses, strain gages to measure the stresses developed in the reinforcing ties and skin elements, and gage points to measure the deformations of the skin elements and the wall face. Based on the results obtained from the instrumented reinforced earth structure and the analysis of performance, it was concluded that the basic mechanism of behavior could be explained by Rankine stress theory. For design purposes, it was recommended that the active earth pressure coefficient be used for calculating stresses for the end portions of the reinforcing ties and that the coefficient of earth pressure at rest be used for calculating stresses for the middle portion of the reinforcing ties.

7. The Heart O' the Hills road, as described by Munoz,[34] is located in the Olympic National Park just south of Port Angeles, Washington. In 1970 a major landslide occurred and approximately 200 ft of the road dropped vertically about 30 ft. A comprehensive study of the area showed that the site consisted of highly weathered fragments of clay, silt, and sandstone. Several underground springs were also found which could have triggered the landslide. Three design alternatives were considered:

a. Earth embankment with buttress and berms.

b. Reinforced earth retaining wall.

c. Bridge structure.

8. After studying these three alternatives, it was found that while reinforced earth was slightly more expensive than the earth embankment, it would require less working time to construct and provide more flexibility to accommodate considerable differential settlement. The bridge structure was found to be the most expensive. Therefore, two reinforced earth structures were designed. The bottom wall (40 ft high, 256 ft long, and 55 ft wide) was located on stable ground and used as a buttress for stabilizing the landslide. The top wall (25 ft high, 378 ft long, and 22 ft wide) was used to carry the road. Pumping wells were installed to reduce the danger of pore pressure buildup during construction.

9. Precast concrete panels approximately 5 ft square were used as facing elements. The reinforcing strips were bolted to the panels and the backfill material was placed in 10-in. lifts, spread, and compacted with a steel-wheel compactor.

10. Another reinforced earth retaining wall was constructed by the Tennessee Bureau of Highways to correct a slide on Interstate 40, on the side of Walden Ridge near Rockwood, Tennessee.[35,36] The affected section of the highway is located in an extremely unstable area where several major landslides occurred during construction of the roadway. Materials greatly affecting the slope stability of the highway along the Cumberland Escarpment are clay shales, residual clays, colluvium, and water. Two alternatives were studied as remedial measures:

a. Rock buttress.

b. Reinforced earth structure.

It was found that the cost of rock buttress would be almost twice that of reinforced earth. Consequently, a reinforced earth retaining wall about 800 ft long and 39 ft high was selected as the method to correct the slide. Cruciform-shaped precast panels, 5 ft square and varying in thickness from 7-1/8 to 8-5/8 in., were used as facing elements. Polyurethane-foam strips (2 by 2 in.) were used to seal the vertical joints between the panels. Galvanized steel strips, 1/8 in. thick with

varying width and length, were used as reinforcing strips. Each row of strips was covered with approximately 30 in. of sand compacted in 8- to 10-in. lifts.

Reinforced earth slab

11. A reinforced earth slab was constructed to support a 1200-ft-long highway section near Philadelphia, Pennsylvania.[22] The slab was 3 ft thick and ranged in width from 80 to 160 ft supporting a 15-ft-thick soil embankment and pavement for a 4-lane, divided highway. Before constructing the slab, the contractor filled existing voids of cavernous limestone bedrock with grout. The reinforced earth slab was designed to bridge an assumed 50-ft void in the bedrock. Galvanized steel reinforcing ties were placed at 6-in. intervals in alternate layers of longitudinal and transverse strips sandwiched within a granular backfill. All bidders on the highway section selected reinforced earth as more economical than concrete for the slab construction.

12. Binquet and Lee[37] conducted model tests with strip footings on reinforced sand foundation to investigate the potential benefits of using reinforced earth slabs to improve the bearing capacity of soils.

Reinforced earth wall in marine environment

13. The first reinforced earth structure to be constructed in a marine environment in the United States was constructed along the navigable tidal estuary, Academy Creek, in Brunswick, Georgia.[31] The reinforced earth wall allowed the widening of a primary State Highway and relocation of a railroad freight spur in the vicinity of Highway I-95. The center line of the railroad was located 14 ft from the vertical face of the reinforced earth wall. The wall was constructed in the dry behind a temporary earth dike. The retaining wall, constructed of interlocking precast concrete panels and aluminum-magnesium alloy reinforcing ties, was 1100 ft long and 28 ft high when completed. Since much of the wall facing would be under water, Polyfilter X was glued across the joints on the inside of the concrete facing panels to prevent the sand backfill from washing out into the estuary. Recently, in England and Australia, glass-reinforced concrete facing panels, which

weigh only 36 lb and can be lifted into place manually, have been used.[3]

Review of Previous Research on Reinforced Earth

14. Since the application of the reinforced earth concept in Europe by Vidal[16] in 1964, many research and governmental organizations have initiated research programs on reinforced earth. A summary review of some of the research work on reinforced earth follows.

Previous research in Europe and Japan

15. The Central Laboratory of Ponts et Chaussees in Paris, France, initiated research on reinforced earth in 1967 with two-dimensional model tests.[38-40] These model tests, which employed steel cylinders to simulate the soil and aluminum reinforcement ties, were conducted to study modes of failure. Small-scale model walls were built in Japan at the Japanese National Railway Research Laboratory[41] using galvanized steel reinforcement and sand backfill. These model walls were failed by releasing the reinforcement ties a few at a time while measuring the wall displacement. An instrumented reinforced earth retaining wall, 165 ft long and 33 ft high, was constructed at Incarville, France, in 1968.[14,42] The results obtained from this wall were limited in scope because an unknown quantity of clayey silt was intermingled with the gravelly sand backfill. Long and co-workers[43] at the Central Laboratory of Ponts et Chaussees conducted triaxial tests on samples of sand reinforced with regularly spaced aluminum disks to determine the effect of reinforcements on the failure characteristics of reinforced earth. Schlosser and Long[40] conducted consolidated-drained direct shear tests on mixtures of Loire sand and Provins clay to determine the development of the angle of internal friction and the short-term cohesion as a function of the different proportions of the soil constituents. Behnia[44] has conducted a study of reinforced earth tunnels at the University of Paris.

Previous research in the U. S.

16. An early study on reinforced earth in the U. S. was reported

by Pratap[45] in 1970. Pratap conducted small-scale laboratory reinforced earth retaining wall tests using dry Ottawa sand and aluminum alloy wire mesh reinforcement ties. The skin elements composing the vertical face of the retaining wall were constructed of steel shaped into channel sections. Strains were measured along the top of the reinforcement ties. Surcharge loads (uniform stress over a strip) were applied along the top surface of the sand using a hydraulic jack and a loading plate. The results of the study indicated that Rankine stress theory could be used to compute the in situ stresses (zero surcharge) in the soil mass. In each surcharge test, bearing capacity failure of the top sand surface occurred before the failure of the retaining wall could take place.

17. Lee and co-workers have conducted several research studies on reinforced earth since 1971.[41,46-51] They conducted small-scale laboratory reinforced earth retaining wall tests using dry Ottawa sand and aluminum ties under static loading conditions.[41,46,49] Measurements were made of strain in the reinforcement ties, stresses in the sand backfill, and wall deflection. Both tie pullout and tie breaking modes of failure were studied. The results of the study indicated that design procedures using either Rankine or Coulomb stress theory were adequate for design purposes. Unanswered questions resulting from the study include reduction from the ideal Rankine pressure distribution near the base of the box and the small difference in observed failure heights between loose and dense sand backfills which is in variance with Rankine stress theory.

18. Another study was conducted by Richardson and co-workers[47,48,52] on small-scale reinforced earth retaining walls subjected to horizontal sinusoidal seismic loading with a shaking table. The results of the tests showed that reinforced earth retaining walls subjected to seismic loadings could be designed using an empirical design force envelope and a base acceleration determined by response spectra modal participation factor analysis. Yang[50,51] conducted triaxial tests on samples of dry sand reinforced with regularly spaced horizontal layers of fiberglass nets. The results of the tests showed that the deformation modulus of reinforced sand was higher than that of unreinforced

sand and that the strength of the reinforced sand could increase from several hundred percent to that of a state where the applied deviator stress, however large, could not fail the specimen without causing tensile failure in the reinforcement or crushing of the sand grains. Circular plate loading tests, conducted on reinforced sand foundations prepared by introducing circular fiberglass nets lying horizontally in the sand, showed that the reinforced sand foundation undergoes smaller settlement and has a greater ultimate bearing capacity than an unreinforced sand foundation.

19. Bell and his co-workers[53] have conducted laboratory tests at Oregon State University using a nonwoven synthetic porous fabric (installed as a continuous sheet in dry sand) as reinforcement for a small-scale retaining wall. The test results were used as input for a study on the use of the fabric as reinforcement for low-class forest roads over soft soils. Similar work has been reported by Yamanouchi[54] at Kyushu University in Japan.

General requirements for reinforced earth structure

20. Although concepts regarding the behavior of reinforced earth material are still in the developing stages, nevertheless rules and requirements have already been suggested[16,24] to ensure best material performance and overall structural stability. The reinforcing materials should possess high tensile strength and high resistance to environmental conditions. The backfill material should be primarily free-drainage granular material with not more than 15 percent passing the No. 200 sieve. The maximum particle size of the backfill should not exceed 10 in. There must be sufficient friction between the backfill and the reinforcement to generate the necessary tensile stresses in the reinforcement. The internal stability of reinforced earth structures has been designed using Rankine stress theory with active and/or at-rest earth pressure conditions within the backfill. Some general rules have been given for overall stability considerations:

a. The ratio of depth to height of a reinforced earth embankment is suggested to be in the range of 0.8 to 1.

b. The footing of the reinforced earth embankment is recommended to be embedded to 20 percent of the clear height of the embankment.

c. For walls higher than 15 ft, a berm should be constructed in front of the wall with maximum slope of 2:3 and minimum width of 5 ft.

21. The advantages reported for reinforced earth are:

a. It is economical compared to alternate types of construction. Reinforced earth retaining walls 0 to 15 ft high are competitive; 15 to 50 ft high are very competitive; greater than 50-ft-high reinforced earth is easy to design where other types might not be feasible.

b. It requires no additional earthwork equipment.

c. It can be erected much faster than conventional types of construction.

d. Reinforced earth structures are relatively flexible and can tolerate large differential settlements.

e. Structures can be built to large heights (reinforced earth structure built at Tarbela Damsite in West Pakistan to support a rock-crushing plant is 85 ft high and was constructed in six weeks).

One disadvantage of reinforced earth is that corrosion of the metal reinforcing ties occurs, particularly in marine environments. However, to combat corrosion, reinforcing ties can be made from an aluminum-magnesium alloy and coated with a coal-tar epoxy.

Concluding remarks

22. From the previous literature it appears that there are uncertainties with regard to the amount and spacing of the reinforcing material in relationship to the backfill. The majority of reinforced earth research was performed using small-scale models which have the advantage of being economical tools. However, such models impose difficulties in determining the influence of particle size, skin friction between reinforcing strips and backfill material, the internal friction within the backfill soil, and the boundary conditions which cannot be scaled properly. Consequently, small-scale models can only provide a crude approximation of the actual behavior of the modeled prototype. Because of the difficulties in exact scaling, it appears that the only reasonable way of providing a realistic approach for designing reinforced

earth material is by constructing large-scale models in the field and studying their performance at failure. This approach forms the base and purpose of the study reported herein.

Purpose and Scope of Study

23. The study is intended to stimulate research activity on reinforced earth as a construction material and to investigate the feasibility of using reinforced earth in Corps of Engineers projects as an alternative to other conventional construction methods. The study is also concerned with resolving some of the uncertainties with regard to the interrelation between the reinforcing material and the backfill soil in reinforced earth retaining walls. The main purpose of the study is to evaluate the behavior of fabric membrane versus steel reinforcement ties in granular soil mass.

24. To achieve the purposes, two instrumented reinforced earth retaining walls were constructed and surcharge loaded to failure at the U. S. Army Engineer Waterways Experiment Station (WES). Each wall was 16 ft long, 10 ft deep, and 12 ft high. The first wall was reinforced by strips made of heavy-duty neoprene-coated nylon fabric membrane, and the other wall was reinforced by galvanized steel strips; concrete sand was used as backfill material in both retaining walls.

PART II: THEORETICAL CONSIDERATION OF REINFORCED EARTH MATERIAL

25. The exact state of stress in a reinforced earth mass is not known and any attempt to solve the problem mathematically may involve several simplifying assumptions which may or may not be compatible with actual events. However, if soil deformation is considered, it may be possible to set a range within which soil behavior can be characterized.

Basic Concept

26. Let A be a soil element within a dry cohesionless semi-infinite homogeneous mass, as shown in Figure 1a, acted upon by vertical stress σ_v* and horizontal stress σ_h. If the vertical stress is increased without changing the lateral strain ϵ_h, then the horizontal stress may be increased proportionately to the vertical stress.

$$\sigma_h = k_o \sigma_v \tag{1}$$

where k_o is the coefficient of earth pressure at rest, and the state of stress with the element A is said to be under at-rest condition.

27. Theoretical study by Jaky[55] and subsequent experimental tests have shown that k_o can be expressed as

$$k_o = 1 - \sin \phi' \tag{2}$$

where ϕ' is the effective angle of internal friction.

28. If the vertical stress is increased such that the soil element A starts to compress in the vertical direction and expand in the horizontal direction, then the shear stress will increase and σ_h may change slightly as shown in Figure 1b. However, there is a limit beyond

---

* For convenience, symbols and unusual abbreviations are listed and defined in the Notation (Appendix A).

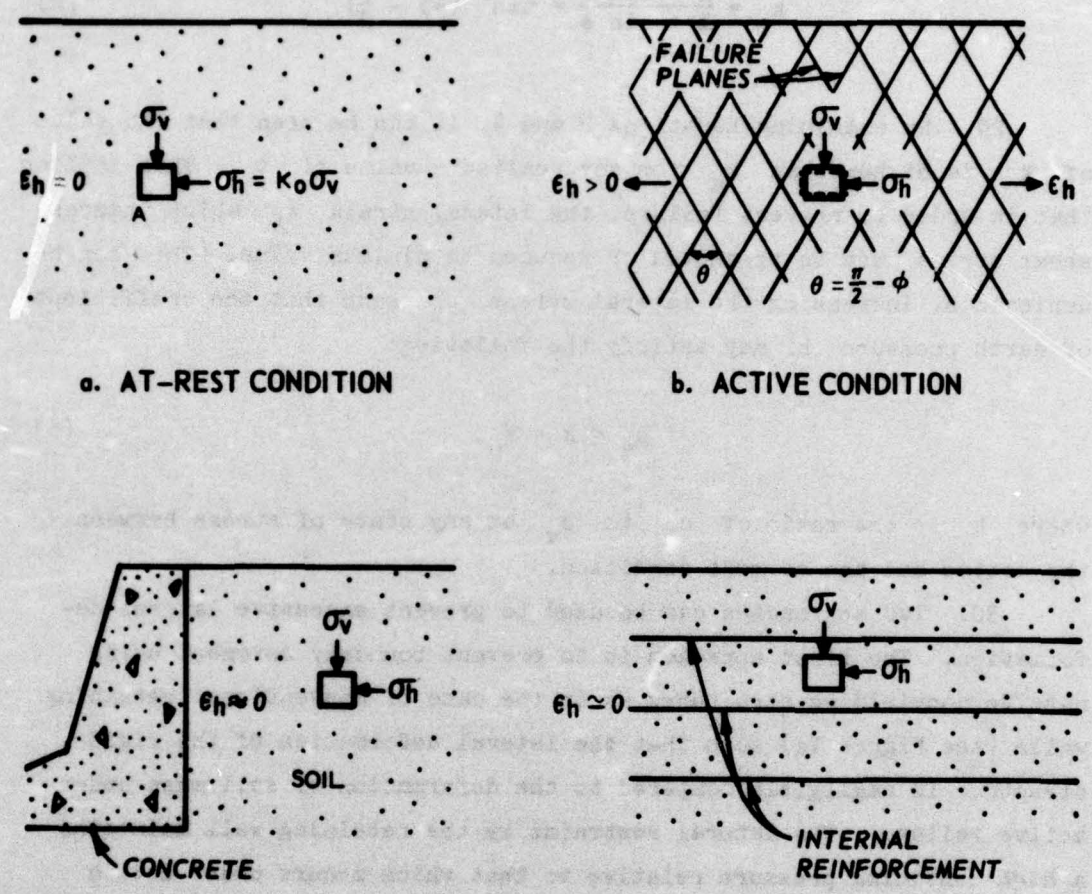

a. AT-REST CONDITION

b. ACTIVE CONDITION

c. RIGID LATERAL SUPPORT

d. REINFORCED EARTH

Figure 1. Schematic of soil element under different conditions

which any increment in the vertical stress may cause the soil to fail in shear, and the relationship between σ_h and σ_v under such limiting conditions may be expressed as

$$\sigma_h = k_a \sigma_v \tag{3}$$

where k_a is the coefficient of active earth pressure and the state of stress at point A is said to be in the active condition. For cohesionless soil k_a may be expressed as

$$k_a = \frac{1 - \sin \phi}{1 + \sin \phi} = \tan^2 (45 - \frac{\phi}{2}) \quad (4)$$

29. By examining Equations 2 and 4, it can be seen that the value of k_o is higher than k_a for any realistic value of ϕ. This implies that in order to prevent failure, the lateral strain ε_h which induces shear stress must be prevented or reduced to minimum value. This can be achieved by increasing the lateral stress σ_h such that the coefficient of earth pressure k may satisfy the following:

$$k_a < k < k_o \quad (5)$$

where k is the ratio of σ_h to σ_v at any state of stress between the active and the at-rest condition.

30. Two approaches can be used to prevent excessive lateral deformation. The first approach is to prevent boundary movement using massive nonyielding structures as in the case of conventional retaining walls (see Figure 1c) such that the lateral deformation of the rigid structure is negligible compared to the deformation of soil mass under active failure. The lateral restraint by the retaining wall maintains a high confining pressure relative to that which occurs under active conditions and results in shear stresses below that needed to create failure. The second approach is to restrain lateral deformation internally by reinforcing the soil with frictional and high-tension material. In this case (see Figure 1d) the needed confining pressure to offset lateral deformation is provided by the frictional forces between the reinforcing material and the soil. It must be noted that the problem of determining the stresses within the reinforced earth system is highly indeterminant and depends upon the physical properties and the geometry of both the soil and the reinforcing material and the interaction between them. Therefore, reasonable simplifying assumptions are necessary if rational practical solutions for reinforced earth problems are to be obtained.

Major Elements of Reinforced Earth Retaining Wall

31. The reinforced earth wall, shown schematically in Figure 2, consists of three major components: the backfill material, the

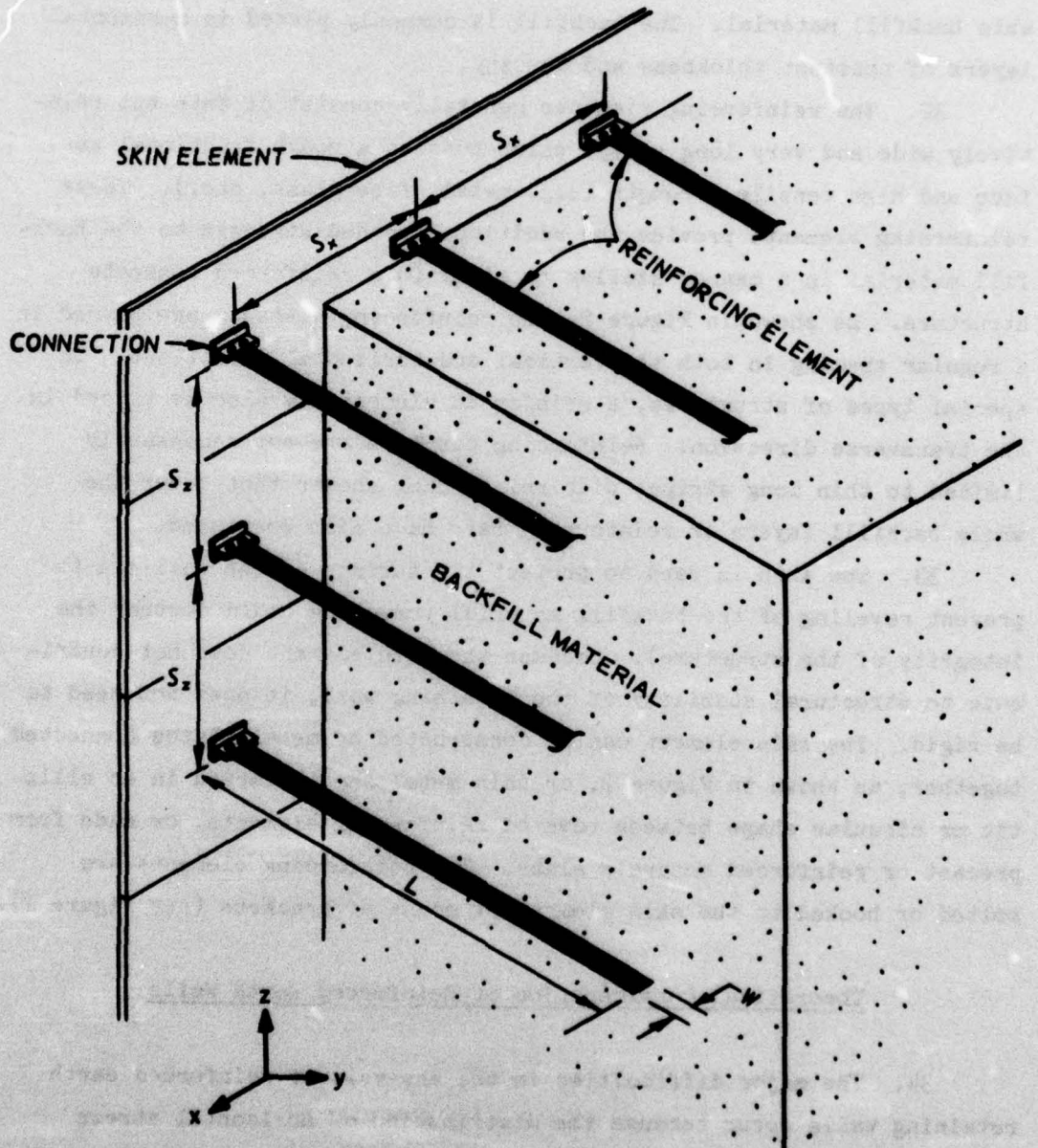

Figure 2. Schematic of major elements of reinforced earth wall

reinforcing elements, and the skin element. The backfill material usually consists of free-draining material whose strength depends on the frictional forces between the particles rather than the cohesion of the mass. Thus any material with a relatively high angle of internal friction such as sand and gravel with less than 15 percent fines is a suitable backfill material. The backfill is commonly placed in horizontal layers of constant thickness and density.

32. The reinforcing elements generally consist of thin but relatively wide and very long strips which possess a rough frictional surface and high tensile strength (e.g. metal, fiberglass, etc.). These reinforcing elements provide the additional needed strength to the backfill material in a manner similar to steel in a reinforced concrete structure. As shown in Figure 2, the reinforcing elements are placed in a regular spacing in both the vertical and horizontal directions. In special types of structures, a reinforced element may also be placed in the transverse direction. Reinforcing elements are not necessarily limited to thin long strips; wide reinforcing sheets that cover the whole backfill layers or reinforcing bars have also been used.

33. The skin is used to protect the surface of the wall and to prevent raveling of the backfill material (raveling could destroy the integrity of the structure). Because the skin element does not contribute to structural stability of the retaining wall, it does not need to be rigid. The skin element can be constructed of metal plates connected together, as shown in Figure 2, or thin metal sheets curved in an elliptic or circular shape between rows of reinforcing elements, or made from precast or reinforced concrete slabs. The reinforcing elements are bolted or hooked to the skin element by means of brackets (see Figure 2).

Theoretical Consideration of Reinforced Earth Walls

34. The major difficulties in the analysis of reinforced earth retaining walls occur because the distribution of horizontal stress within the fill material and the influence of the reinforcing material on the distribution of these stresses are not known. Thus, in order to

arrive at an approximate determination of the horizontal thrust acting on the wall under static condition, it is necessary to make several simplifying assumptions:

a. During construction, the wall is free to move laterally a sufficient amount (0.0025 H) to create a limiting equilibrium condition within the backfill material behind the wall. This assumption permits use of the classical earth pressure theories such as those of Rankine and Coulomb.

b. The lateral movement of the wall, regardless of how small, may generate through friction enough confining pressure on the reinforcing elements such that the net shear stress within the backfill is less than its maximum strength.

c. The wall is frictionless so that there is no significant transfer of vertical stresses from the backfill material to the wall. Under such conditions, the vertical and horizontal stresses are equivalent to the major principal stress σ_1 and minor principal stress σ_3, respectively.

d. The shear stress generated from the frictional forces is fully mobilized along the effective length of the reinforcing elements.

e. The backfill material is level and surcharge load exerts uniformly distributed pressure.

The validity of these assumptions and their practical significance will be discussed later herein.

Stress Analysis Using Rankine Theory

35. Rankine theory is based on the assumption that a conjugate relationship exists between the vertical and lateral stresses within the soil adjacent to the retaining wall. It assumes that the presence of the retaining wall introduces no change in the shearing stress at the surface of contact between the backfill material and the wall. Thus the theory is applicable to vertical retaining walls with smooth surfaces.

36. Assume that Figure 3 represents a wall with a smooth frictionless contact surface inclined at an angle α from the vertical, retaining a homogeneous cohesionless fill, with its surface inclined at an angle i with the horizontal, and supporting a surcharge with

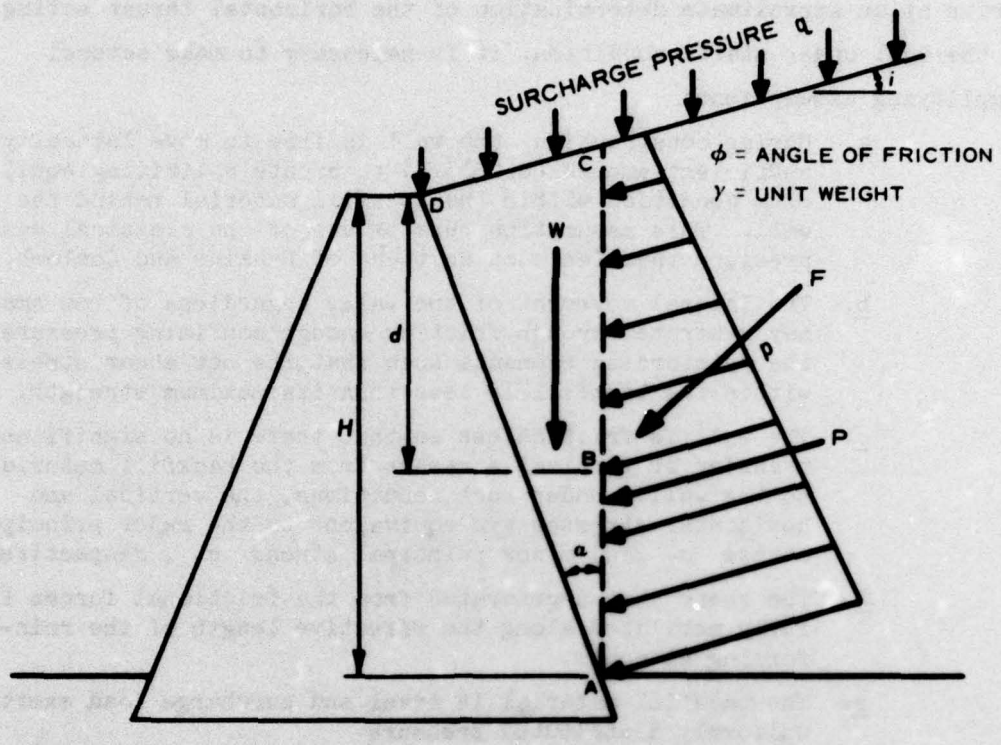

Figure 3. Pressure distribution according to Rankine theory

uniform intensity q. The thrust acting on the wall F is the resultant of two forces: the gravity force W acting downward which represents the weight of the wedge ACD and the surcharge load acting on it, and a force P representing the total pressure acting on the vertical plane AC.

$$P = \int_A^C p\,dH \tag{6}$$

According to Rankine's theory, the pressure p at any point B at depth d is conjugate to the vertical pressure σ_v at that point where

$$\sigma_v = \gamma d + q \tag{7}$$

where γ is the unit weight of the backfill material. Using Mohr's

theory and the concept of conjugate stresses, it is possible to show that

$$p = (\gamma d + q) \cos i \frac{\cos i - \sqrt{\cos^2 i - \cos^2 \phi}}{\cos i + \sqrt{\cos^2 i - \cos^2 \phi}} \tag{8}$$

where ϕ is the angle of internal friction and p acts parallel to the slope of the backfill soil. The horizontal component of p may be expressed as

$$\sigma_h = p \cos i = (\gamma d + q) \cos^2 i \frac{\cos i - \sqrt{\cos^2 i - \cos^2 \phi}}{\cos i + \sqrt{\cos^2 i - \cos^2 \phi}} \tag{9}$$

If the backfill material has a horizontal slope, then $\cos i$ becomes unity and Equation 9 becomes

$$\sigma_h = (\gamma d + q)\frac{1 - \sin \phi}{1 + \sin \phi} = k_a(\gamma d + q) \tag{10}$$

37. It must be noted that Rankine's theory is not applicable when there is friction between the surface of the wall and the backfill soil; consequently, it cannot provide a unique solution in the mathematical sense, nor is it kinematically admissible.

Stress Analysis Using Coulomb's Theory

38. Coulomb's theory considers the overall stability of the entire retaining wall. Thus it is much more general than the Rankine theory since it is not confined to any geometry or physical properties of the backfill material or the wall. The theory is based on two major assumptions: first, the failure surface is plane and acted upon by uniform shear stress; second, the backfill thrust on the wall acts in some known direction.

39. Assume the same retaining wall shown in Figure 3, which is redrawn in Figure 4, to be analyzed by Coulomb's theory. Let AC be

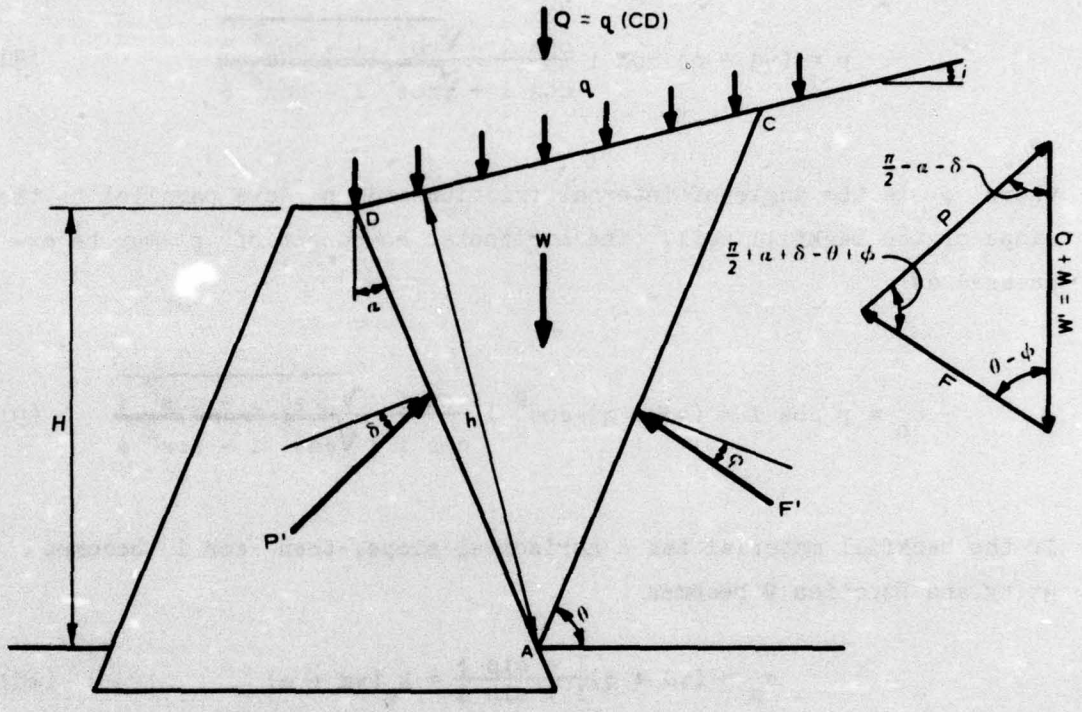

Figure 4. Force diagram for general Coulomb theory

any failure plane in the backfill mass inclined at an angle θ from the horizontal. Let δ be the angle between the thrust for P' and the normal to the wall and let h be the normal distance from the backfill surface CD to point A. Other variables have been defined previously. Since an active case is considered, the lateral force F' acts at angle ϕ to the normal of the failure plane. The force W' is the sum of vertical forces

$$W' = W + Q = \frac{1}{2} h \overline{DC} \gamma + q \overline{DC} = \frac{1}{2} h \overline{DC}(\gamma + \frac{2q}{h}) \qquad (11)$$

or

$$W' = \frac{1}{2} h \overline{DC} \gamma' \qquad (12)$$

where γ' is a composite unit weight which considers the influence of the dead weight of the soil and the surcharge.

40. With W' known in magnitude and direction, P' and F' are known in direction; the magnitude of P' and F' can be easily obtained from the force polygon shown in Figure 4. It must be noted that the direction of both P' and F' are known in terms of arbitrary angle θ. Using the law of sines, it can be shown that

$$P' = W' \frac{\sin (\theta - \phi)}{\sin (\frac{\pi}{2} + \alpha + \delta - \theta + \phi)} \tag{13}$$

41. The maximum value of P' can be obtained by setting the derivative of P' with respect to θ to be equal to zero. Using the procedure credited to Rebhann by Taylor,[55] the thrust P' acting on the wall can be expressed as

$$P' = \frac{1}{2} \gamma' H^2 K' \tag{14}$$

where K' is equal to

$$K' = \frac{\csc^2 (\phi - \alpha)}{\cos^2 \alpha \cos (\alpha + \delta) \left[1 + \sqrt{\frac{\sin (\phi + \delta) \sin (\phi - i)}{\cos (\alpha + \delta) \cos (i - \alpha)}}\right]^2} \tag{15}$$

Knowing the value of P' the value of θ can be determined using Equation 13.

42. If the backfill material is horizontal and the wall is vertical, then Equation 15 may be reduced to

$$K' = K'' = \frac{\cos^2 \phi}{\cos \delta \left[1 + \sqrt{\frac{\sin (\phi + \delta) \sin \phi}{\cos \delta}}\right]^2} \tag{16}$$

If the wall is smooth and frictionless, then $\delta = 0$ and Equation 16 becomes

$$K'' = \frac{\cos^2 \phi}{(1 + \sin \phi)^2} = \frac{1 - \sin \phi}{1 + \sin \phi} = k_a \qquad (17)$$

From Equation 17 it is clear that for a smooth vertical wall with horizontal backfill, both Rankine and Coulomb theories provide the same value for earth pressure coefficient.

Earth Pressure Theories and Reinforced Earth Wall

43. One of the major advantages of reinforced earth walls is that they are flexible. It has been indicated by Terzaghi[56] that outside movement on the order of 0.5-1.0 percent of the wall height is enough to create an active zone in the fill material. Consider a simple retaining wall with horizontal backfill and vertical frictionless wall as shown in Figure 5. According to both Rankine and Coulomb theories, the horizontal stress at any depth d from the surface of the backfill may be expressed as

$$\sigma_h = k_a (\gamma d + q) \qquad (18)$$

where γ is the unit weight of soil, q is intensity of surcharge load, and k_a is the coefficient of active earth pressure.

44. Assuming that the reinforcing ties are placed in a regular pattern, as shown in Figure 2, with horizontal and vertical spacing S_x and S_z, respectively, the total horizontal thrust F_h acting on an area bounded by $S_x S_z$ at d distance below the surface may be expressed as

$$F_h = \int_0^{S_x} \int_0^{S_z} \sigma_h \, dz \, dx = k_a (\gamma d + q) S_x S_z \qquad (19)$$

45. In order to satisfy equilibrium conditions along the y axis, the horizontal thrust of the backfill material at the surface of the

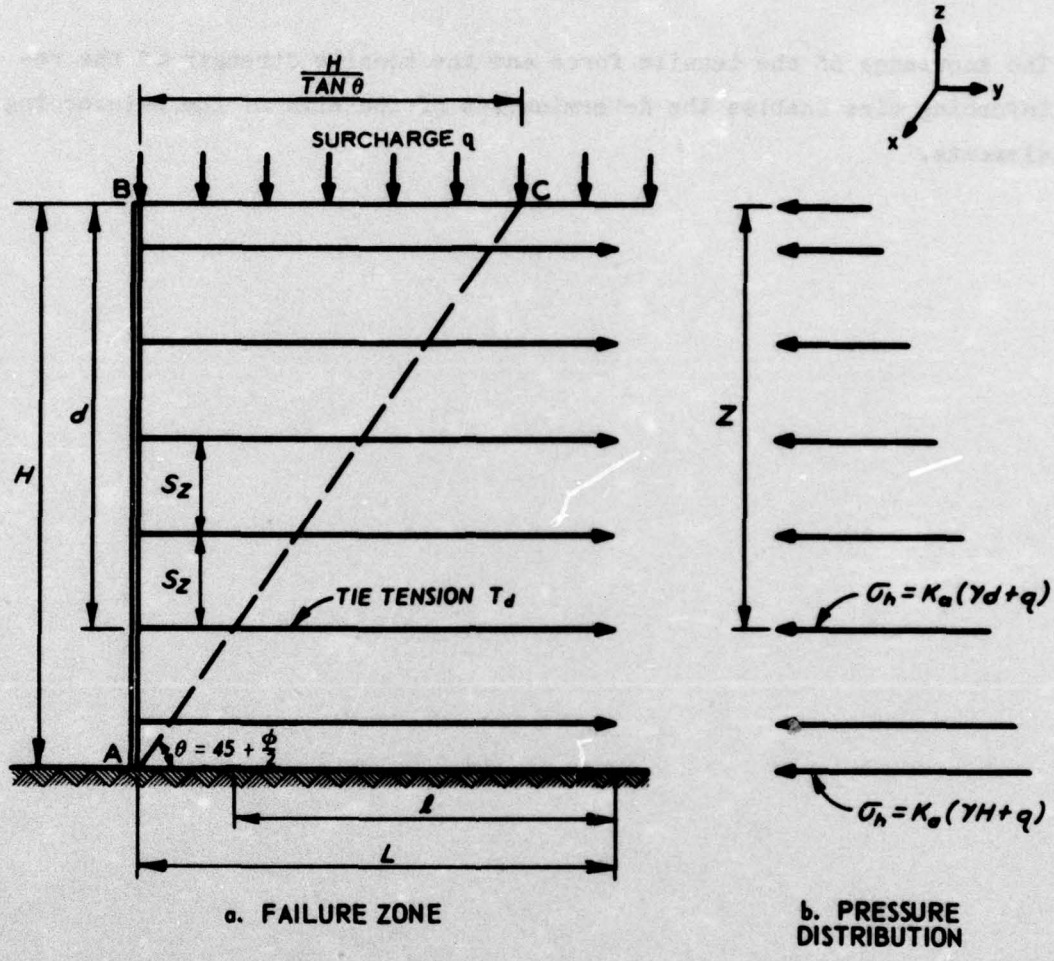

Figure 5. Pressure distribution according to Rankine theory

backfill should be equal to the tension force in the ties. Consequently, the tension force carried by a single tie at depth d is

$$T_d = F_h = k_a(\gamma d + q)S_x S_z \qquad (20)$$

where T_d is the tensile force in the reinforcing tie.

46. It is clear from Equation 20 that T_d takes a maximum value when the depth d assumes the full height of the wall H; thus,

$$T_{max} = k_a(\gamma H + q)S_x S_z \qquad (21)$$

The knowledge of the tensile force and the tensile strength of the reinforcing ties enables the determination of the size of the reinforcing elements.

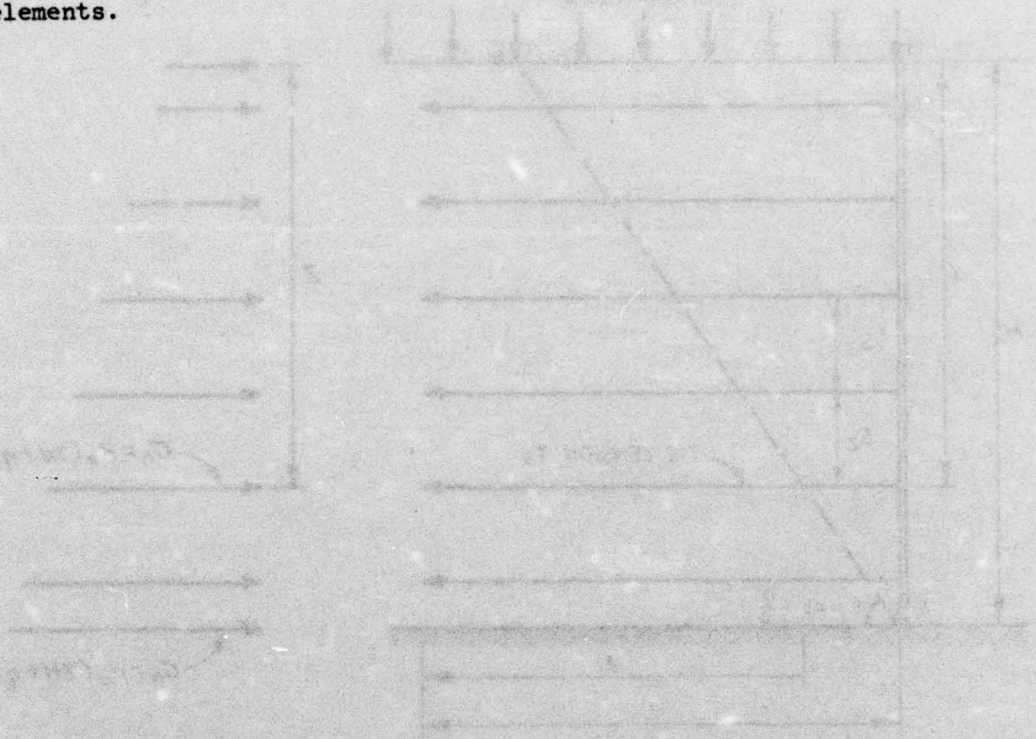

PART III: DEMONSTRATION TESTS AND CONSTRUCTION

Materials Used

47. The reinforced earth model test, like any other small-scale test, is not totally reliable since it is subject to unknown scale effect. Thus, in order to avoid scale effects, two full-scale demonstration tests were conducted at WES to determine the behavior of reinforced earth retaining walls during construction and at failure. Each wall (see Figure 5) was 12 ft high, 16 ft long, and 10 ft deep; the first one was reinforced with heavy-duty nylon fabric coated with rubber, and the other was reinforced with galvanized steel. For both walls, aluminum landing mat was used as skin element and commercial concrete sand was used as the backfill material.

Nylon fabric coated with rubber

48. The nylon base fabric was a single-ply weave, woven from an 840-denier continuous filament nylon yarn (polyamide of polyhexamethylene adipamide). The coating was a synthetic material made of compounded chloroprene synthetic rubber to impregnate and coat the nylon fabric. The membrane used was made of heavy-duty 4-ply nylon fabric coated with 5 oz of neoprene to the square yard and was cut into strips 4 in. wide and 10 ft long.

49. The stress-strain relation for the membrane was determined from tension tests conducted at WES. Various widths of membrane were tested using both the Webbing Capstan Grip Test[57] to obtain the ultimate strength and the Modified Grab Test[58] to obtain both the ultimate strength and the stress-strain curve. Figure 6 shows that the ultimate strength of the membrane increases rapidly with increasing width and becomes almost constant when the width exceeds 1/2 in. The average stress-strain curve shown in Figure 7 is concave upward with tangent modulus E_t increasing rapidly when the axial strain exceeded 15 percent. The ultimate strength of the membrane was equal to 14,500 psi at an axial strain of 25.3 percent.

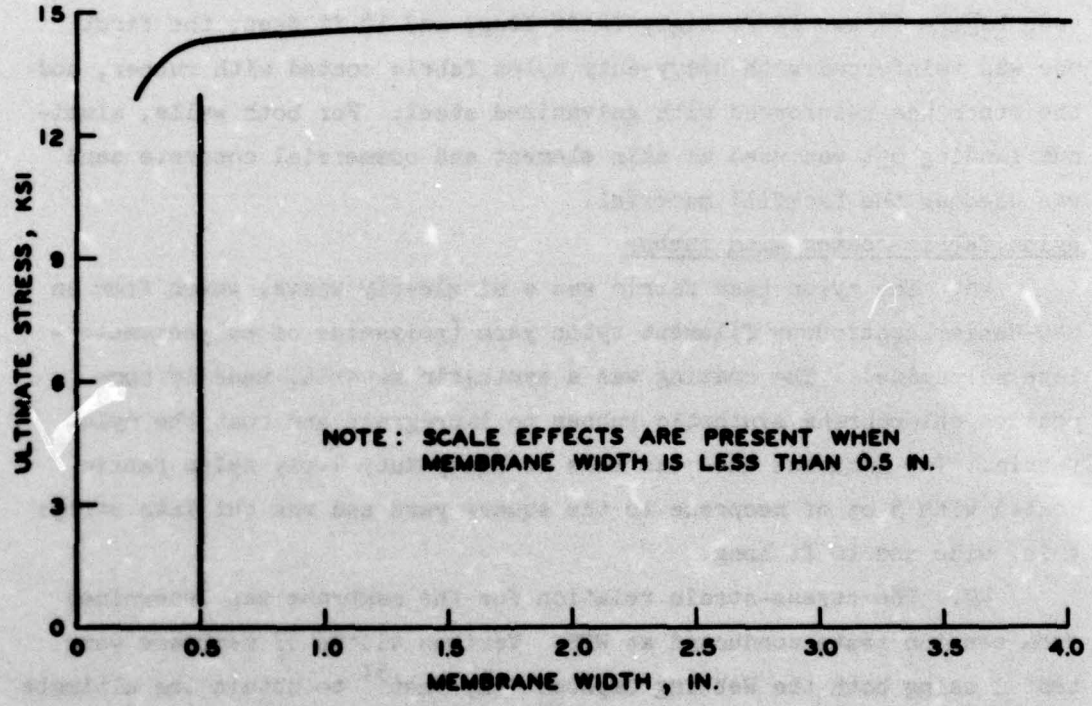

Figure 6. Variation of ultimate strength with width of membrane strip

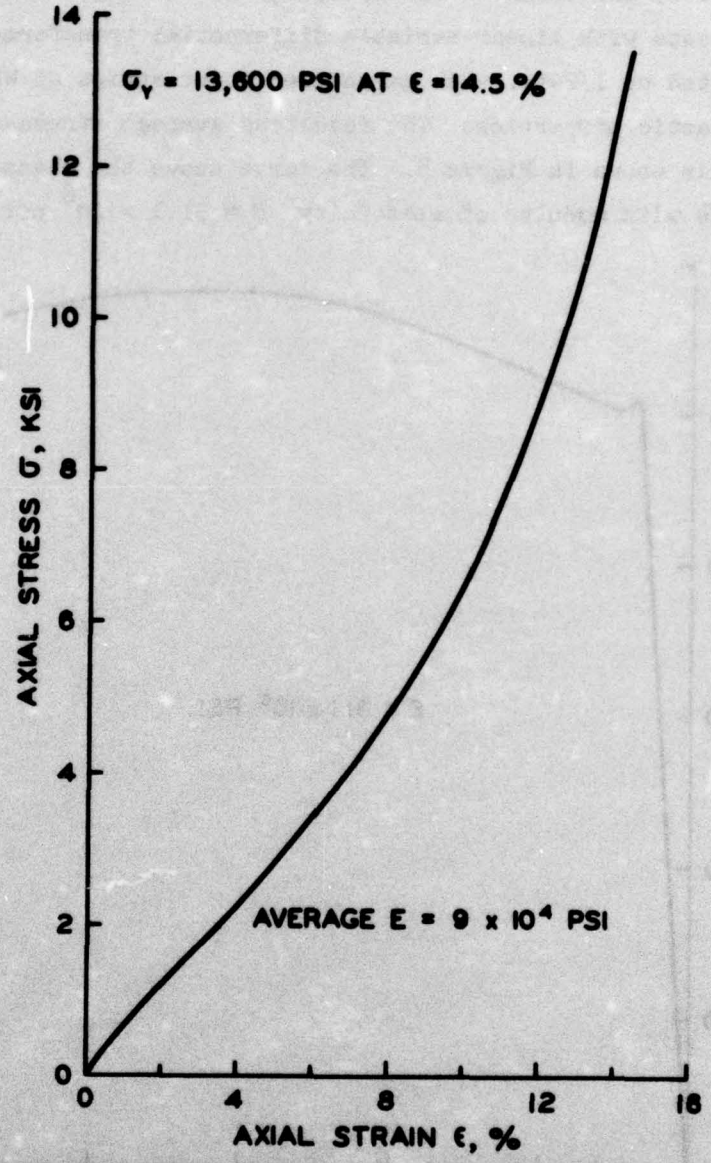

Figure 7. Stress-strain relationship for the membrane strips

Galvanized steel

50. The reinforcing steel strips used in the test program were made from galvanized zinc-coated, 24-gage, high-tensile steel. Each strip was 0.025 in. thick, 4 in. wide, and 10 ft long. Several modified grab tests with linear variable differential transformers (LVDT) were conducted on 1/2-in.-wide galvanized steel strips at WES to determine the elastic properties. The resulting average stress-strain relationship is shown in Figure 8. The curve shows the classical stress-strain curve with modulus of elasticity $E = 31.1 \times 10^6$ psi and

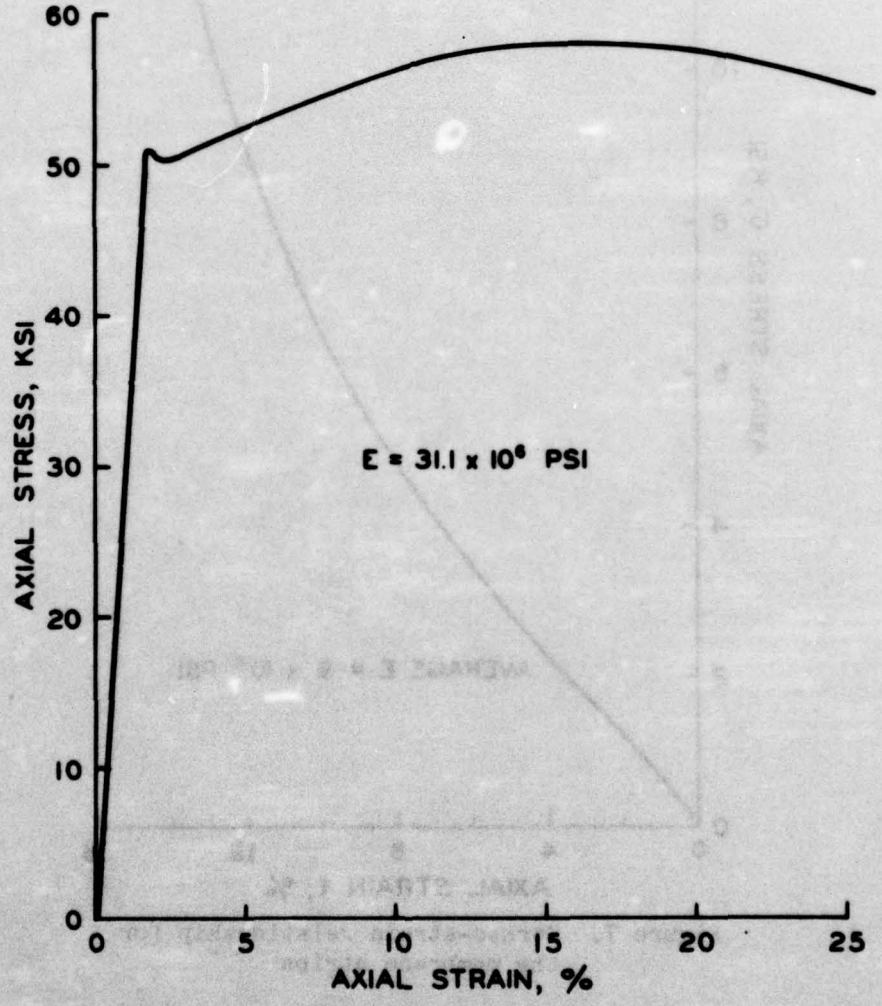

Figure 8. Average stress-strain relationship for the galvanized steel strips

tensile yield stress σ_y = 51.0 ksi.

Skin elements

51. The skin elements were made of Alcoa T11 high-strength aluminum landing mat panels such as are used in the expedient construction of airfields. Each panel is 2 ft wide, 12 ft long, and 1.6 in. thick and can be easily connected lengthwise to each other by a hinge-type connection. The panel, shown in Figure 9a, consists essentially of eight aluminum T sections, 1.5 in. high and placed equidistant from each other. The webs of the T sections are welded to a 0.1-in. plate (Figure 9b) made of high-strength alloy (7005) with yield strength of 46,000 psi. The total weight of the panel is 3.8 psf. A more detailed description of Alcoa T11 mat is presented by Carr.[59]

52. The reinforcing elements were fixed to the skin element through a connector as shown in Figure 10. The connector consisted of double angles; each was 1-1/2 by 3 by 1/4 in. and 12 in. long, and two 1/4-in. bolts were used to grip the reinforcing element. The connector was inserted inside the gap formed by two adjacent T sections of the aluminum panels that formed the skin element. This type of connection was simple to construct and proved to be satisfactory as long as the skin element exhibited very little or no bending deformations.

Backfill material

53. The backfill material used in the construction of the prototype reinforced earth retaining walls was clean concrete sand with particles ranging from subangular to angular and with grain-size distribution as shown in Figure 11. Other physical properties of the sand were as follows:

Specific gravity, G_s	= 2.66
Maximum dry unit weight, γ_{max}	= 117.7 pcf
Minimum dry unit weight, γ_{min}	= 98.2 pcf
Coefficient of uniformity, C_u	= 2
Mean diameter, D_{50}	= 0.5 mm

Laboratory Tests

54. Several laboratory tests were conducted at WES prior to the

a. Bottom of ribbed panel of Alcoa T11 mat

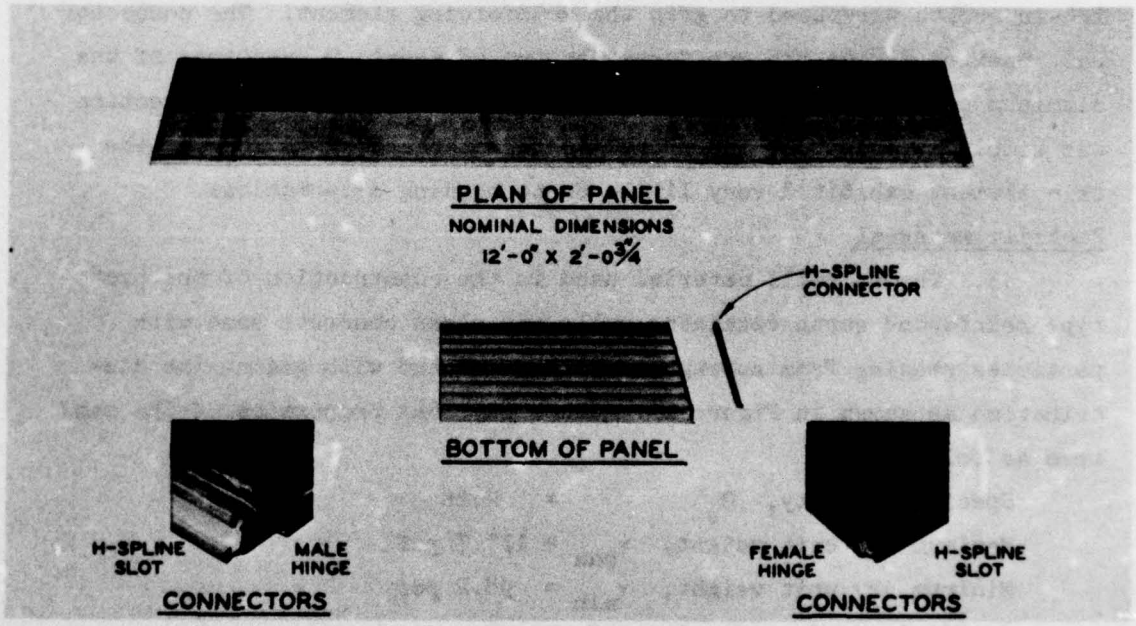

b. Composite view of Alcoa T11 mat

Figure 9. Details of the skin element

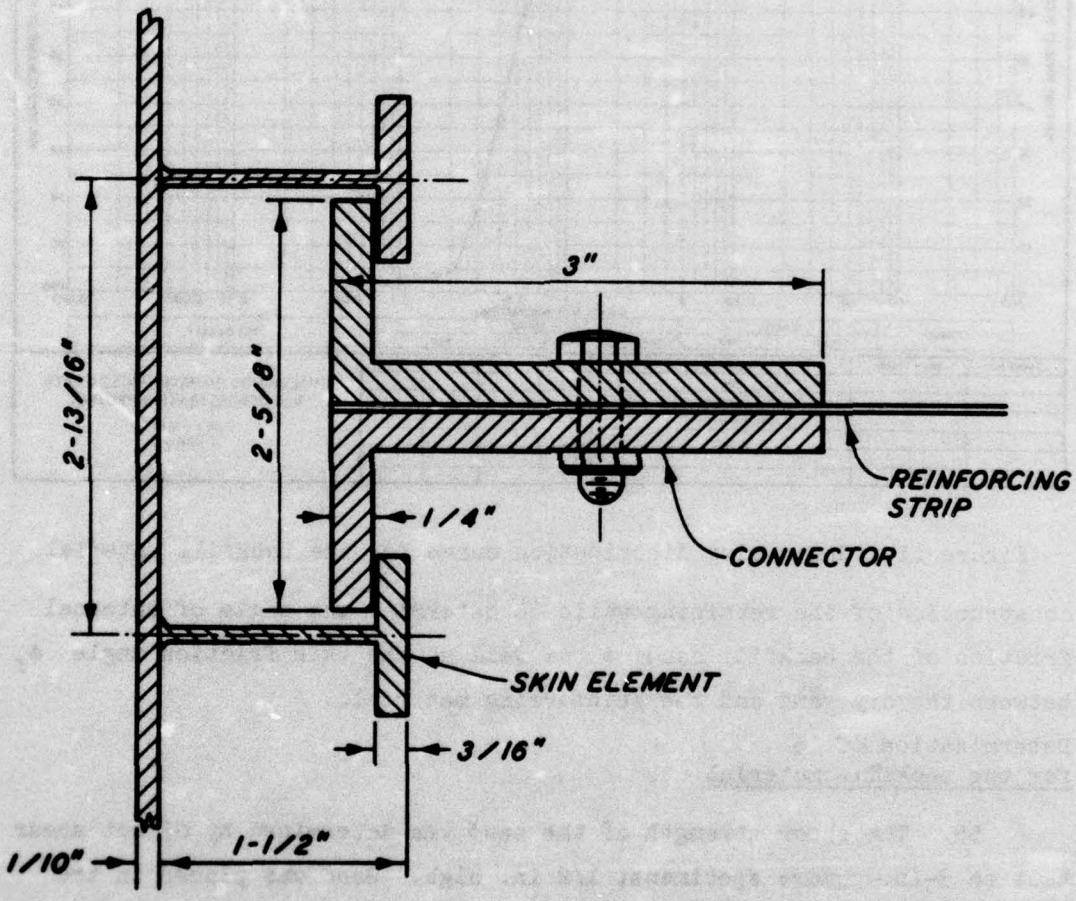

Figure 10. Details of the connector tieing the reinforcing strip to the skin element

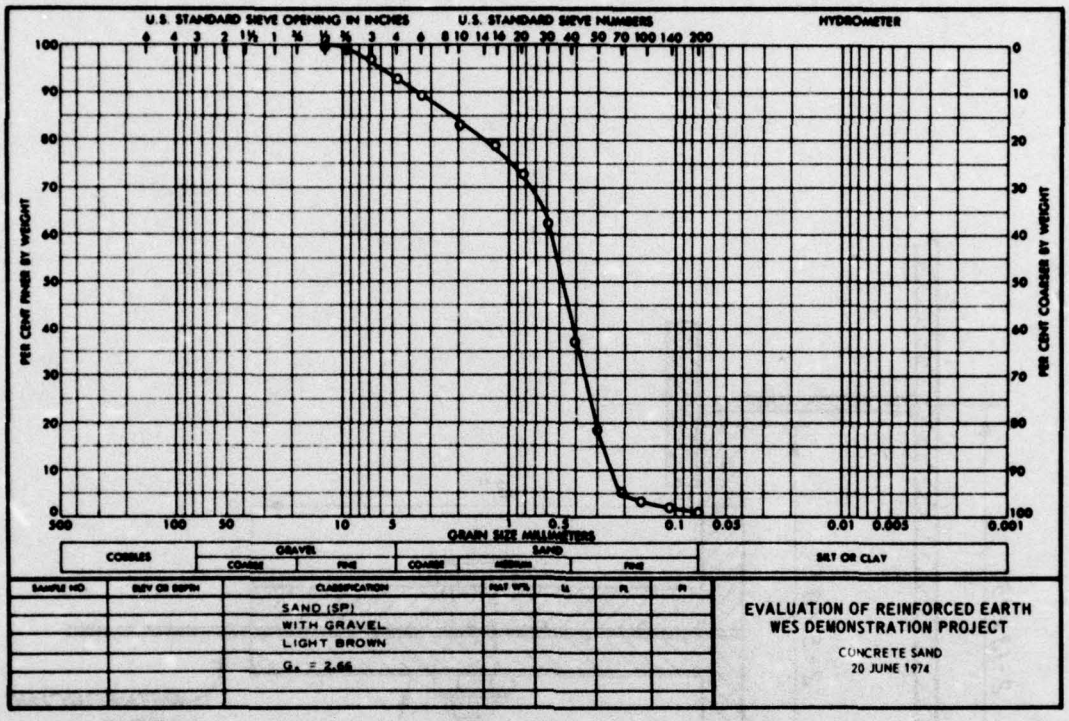

Figure 11. Grain-size distribution curve for the backfill material

construction of the retaining walls to determine the angle of internal friction of the backfill sand ϕ as well as the skin friction angle ϕ_f between the dry sand and the reinforcing material.

Determination of ϕ for the backfill material

55. The shear strength of the sand was determined by direct shear test on 3-in.-square specimens, 1/2 in. high. Sand was placed in the shear box and compacted to a dry density of 101.7 pcf. The in-place backfill material had an average water content of 4.5 percent and an average dry density of 97.5 pcf (see Table 1). The differences between these values and the laboratory dry density of 101.7 pcf are not believed to have significantly influenced the results obtained for ϕ or ϕ_f. Three direct shear tests were conducted with constant normal pressures of 50, 100, and 166 psi, respectively. The rate of shear

strain used was 0.5 in. per min. Results, shown in Figure 12, indicate a linear failure envelope passing through the origin with slope ϕ equal to 36 deg.

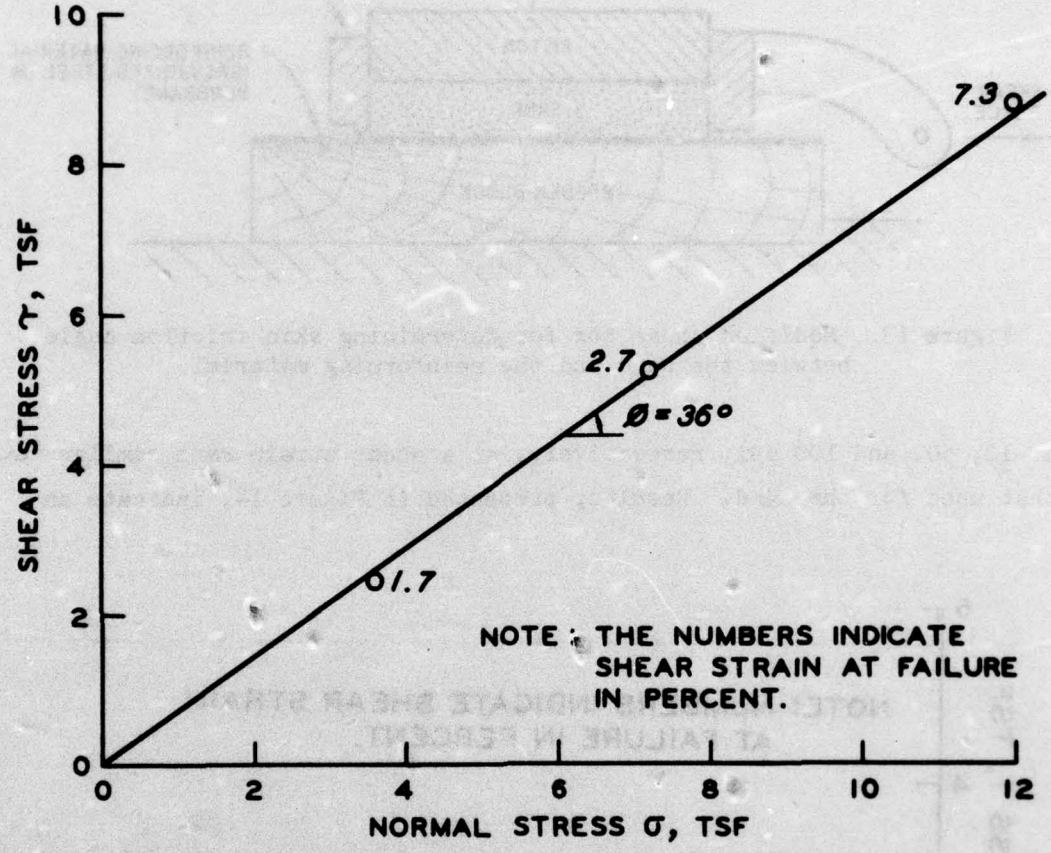

Figure 12. Direct shear test results for concrete sand (γ_d = 101.7 pcf)

Skin friction test

56. The angles of skin friction between the sand and the galvanized steel and the sand and the heavy-duty 4-ply nylon fabric coated membrane were determined using a specially designed shear box. The shear box is similar to the standard shear box[60] except that the lower frame was replaced by a sheet of the reinforcing material (i.e., galvanized steel or membrane) glued to a wooden block as shown in Figure 13.

57. Sand was compacted in the shear box to a dry density of 101.7 pcf. Three direct shear tests were conducted with normal stresses

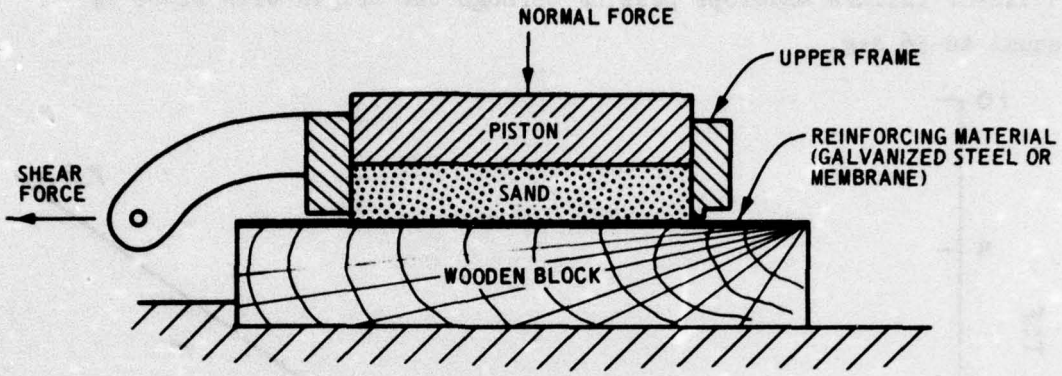

Figure 13. Modified shear box for determining skin friction angle between the sand and the reinforcing material

of 10, 50, and 100 psi, respectively, at a shear strain rate similar to that used for the sand. Results, presented in Figure 14, indicate an

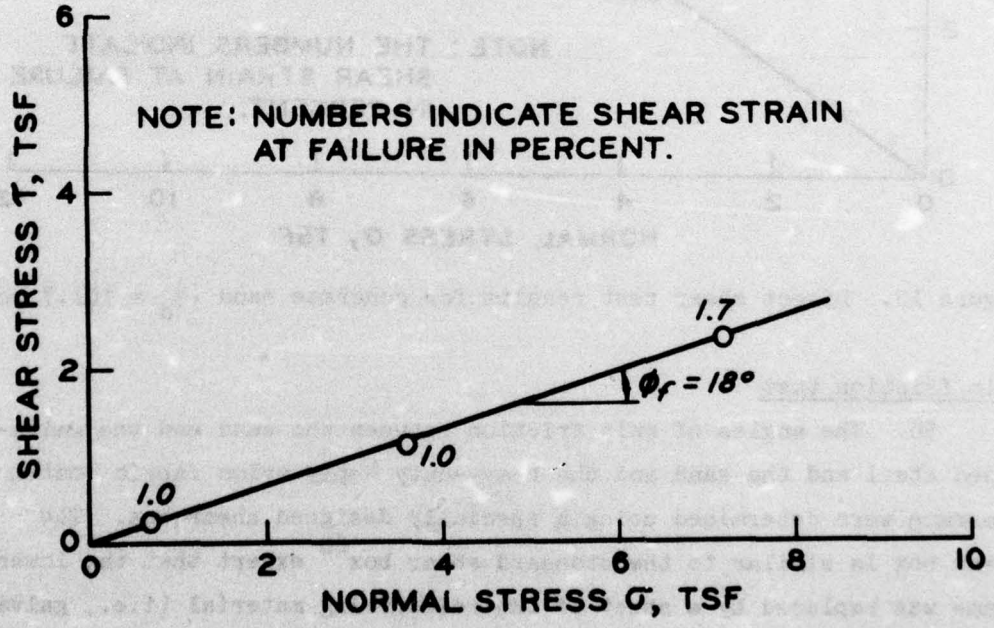

Figure 14. Skin friction tests between the concrete sand and the galvanized steel (γ_d = 101.7 pcf)

angle of skin friction ϕ_f of 18 deg between the sand and the galvanized steel. Similar tests revealed that the angle of skin friction between the membrane and the sand was 30 deg (Figure 15), which is much higher than that between the sand and the galvanized steel.

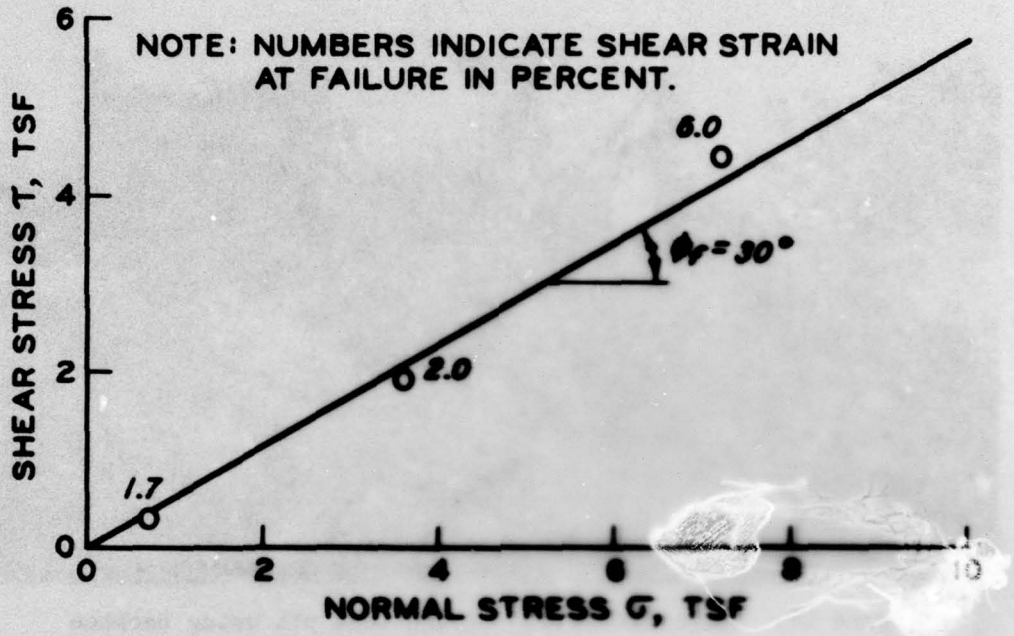

Figure 15. Skin friction tests between the concrete sand and the membrane (γ_d = 101.7 pcf)

Construction of the Retaining Walls

58. Two retaining walls, one reinforced with membrane and the other with galvanized steel, were constructed on the eastern edge of the WES grounds in a test area known locally as Miller's Ridge. The test area consisted of a sharply sloping bank of lean clay approximately 200 ft long and 10 ft high.

Excavation

59. The test area was cleared and excavation was begun during the latter part of May and completed on 14 June 1974. A backhoe was

used to excavate a rectangular hole 16 ft long, 12 ft deep, and 10 ft wide as shown in Figure 16 and the inside walls were then smoothed by

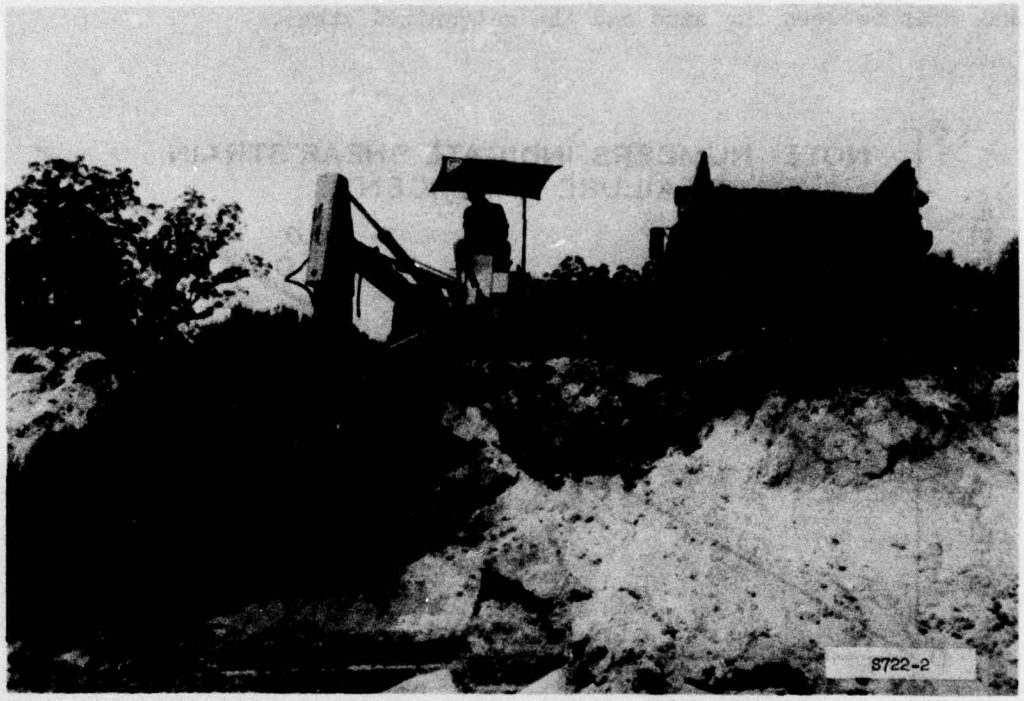

Figure 16. Rough excavation of the test pit using backhoe

an open-end loader as shown in Figure 17. While excavating the pit for the membrane-reinforced earth retaining wall, an old drainage pipe was uncovered on the north side of the pit. As the drainage pipe was removed, the wall sloughed off making the pit 17 ft long at the front face. In order to bring the length of the pit back to 16 ft, a strong panel of landing mat was placed vertically on end at the edge of the pit and anchored firmly by steel wire.

Construction procedure

60. Prior to placing the skin elements (i.e. Alcoa T11 landing mats), the sides of the excavated pits were covered with 6-mil-thick polyethylene sheets to reduce friction and possible arching between the sand and the pit. Two panels of the skin element, total height of 4 ft, were used to close the front of the pit with the bottom panel braced

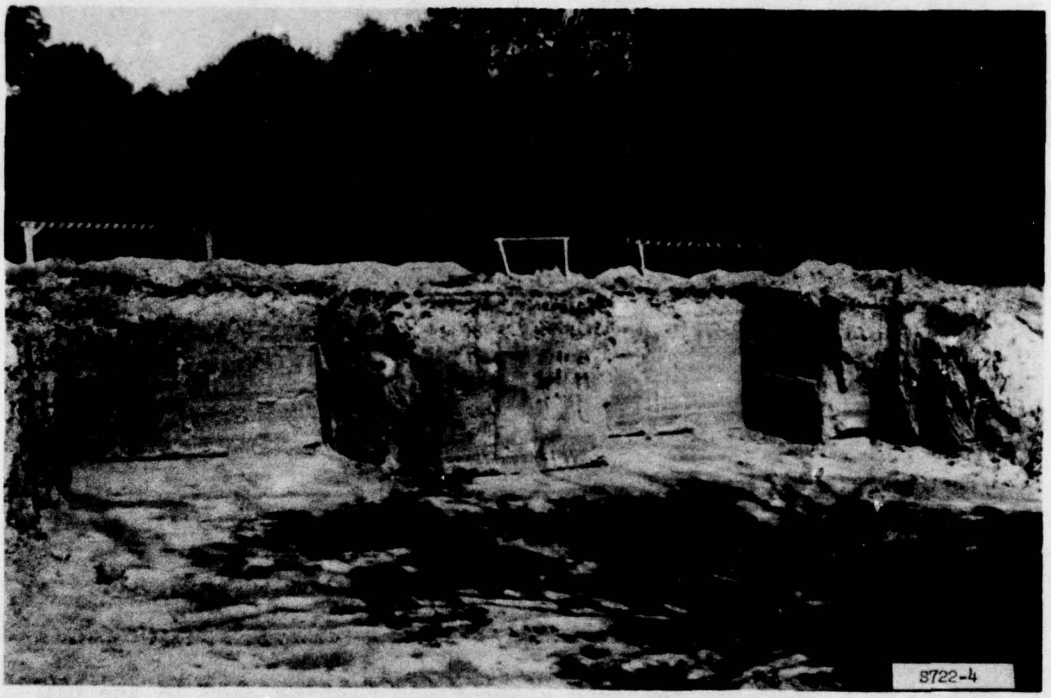

Figure 17. Test pits after walls were smoothed by front-end loader

firmly in a vertical position. The second panel was positioned vertically on the top of the first panel and held firmly to vertical panels placed on both edges of the pits using "c" clamps as shown in Figure 18. After securing the first two panels of the skin element, the sand was dumped in the test pit using a front-end loader.

61. The sand was placed in a manner to simulate expedient construction in the field. The sand was placed in the test pit in 1-ft lifts and spread evenly by hand without compaction. The reinforcing strips were connected to the double angle connectors which were anchored to the skin element, then stretched evenly and level on the surface of the sand as shown in Figure 19. Prior to placing the second lift of sand, the instrumented reinforcing ties were covered with sand to protect the strain gages. Pressure cells were carefully installed near the center line of the wall with one cell placed horizontally to measure the vertical stress and the other placed vertically to measure the

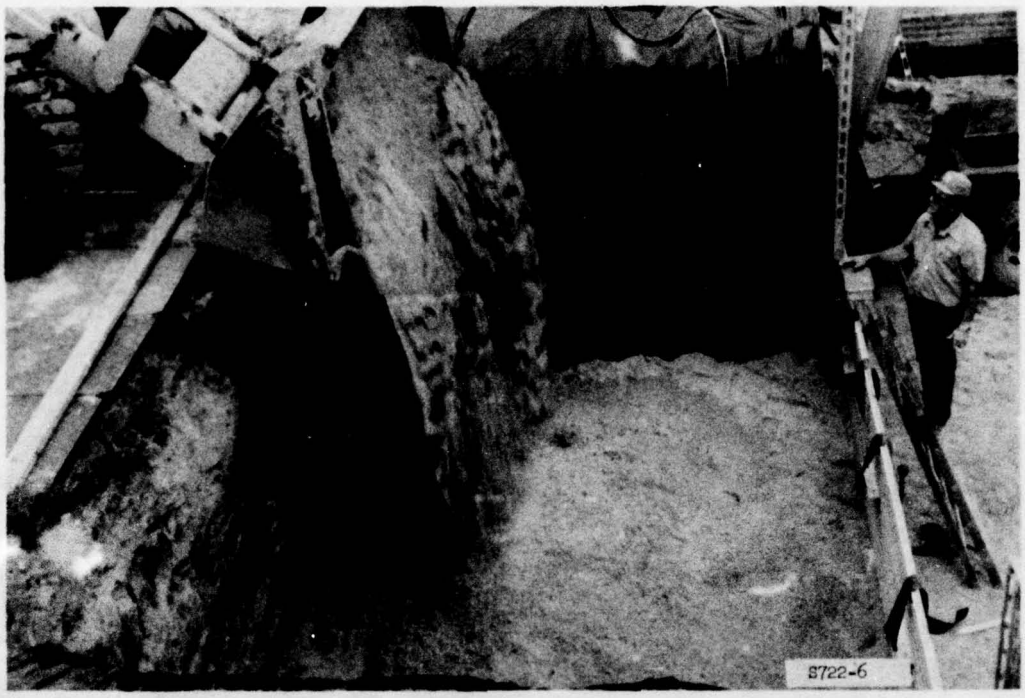

Figure 18. Securing the skin element and placing sand in the pit

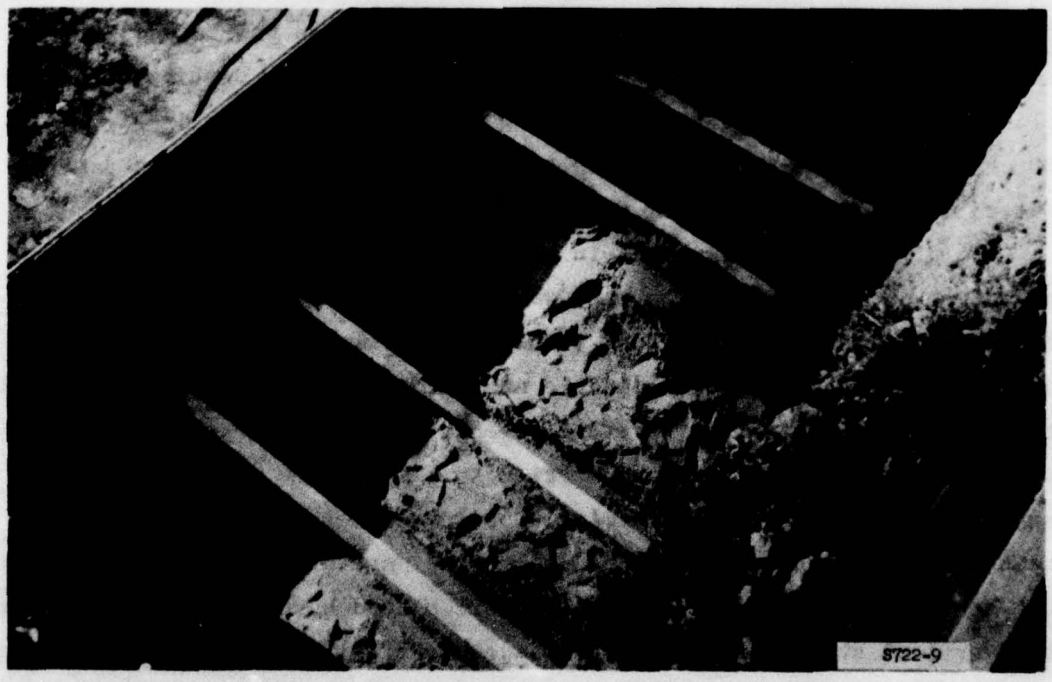

Figure 19. Reinforcing strips spread evenly on surface of sand

horizontal stress as shown in Figure 20. The pressure cells were checked

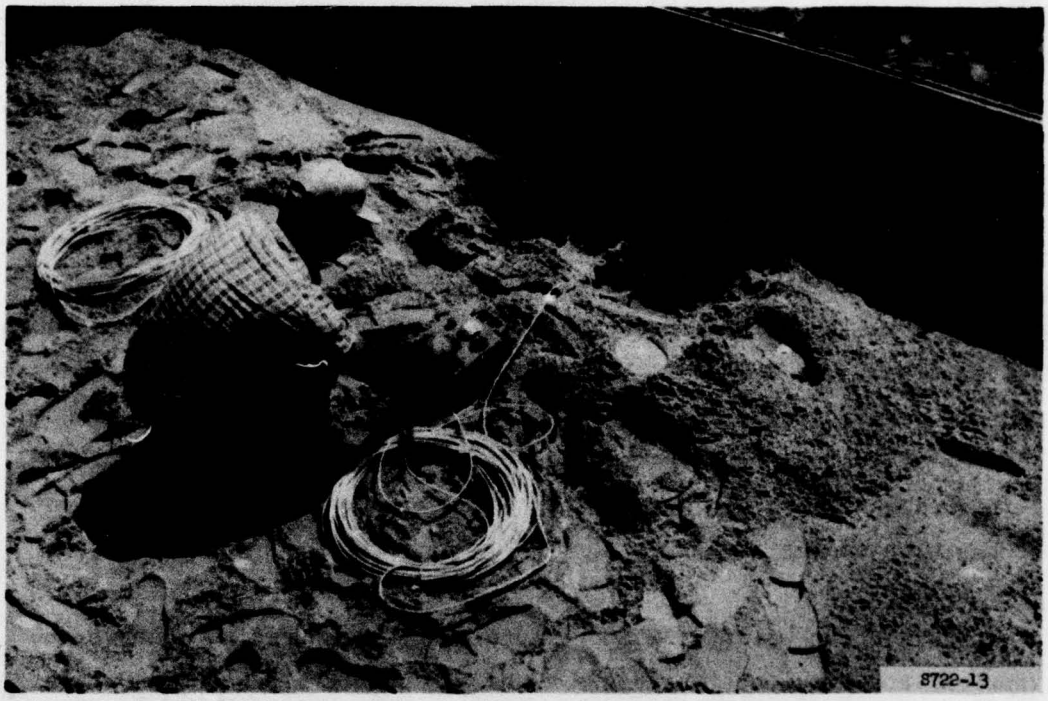

Figure 20. Installation and checking of pressure cell during construction

electrically to ensure proper performance and were covered with 1 ft of sand before placing the second lift of sand. The second lift of sand was placed and leveled by hand and the "c" clamps were removed from the vertical panels. This construction process was repeated for each lift until the retaining wall was 12 ft high.

Density and moisture control during construction

62. No serious attempt was made to control the density of the backfill sand during the construction of the retaining wall except that the surface of the sand was leveled between lifts. In order to determine the density and moisture distribution of the backfill material, three soil specimens were obtained from each lift using the Military Standard drive cylinder.[61] A summary of the average density and water content for each sand lift during the construction of the reinforced

earth retaining walls is presented in Table 1. The table shows that the overall average water content and density of the backfill sand were approximately the same in both retaining walls. The maximum deviation from the average value was 1.4 percent for the water content and 2.2 pcf for the density. This deviation was acceptable since no quality control procedure had been used during the construction of the two retaining walls.

Instrumentation

63. In order to determine the behavior of the reinforced earth retaining walls during construction and surcharge loading, an instrumentation scheme was devised. Instrumentation used in monitoring stresses and deformations consisted of pressure cells to measure vertical and lateral soil stresses, strain gages to measure tensile strains of the reinforcing strips, and gage points to determine the outward movement of the skin elements.

Pressure cells

64. Three pairs of WES pressure cells were used to measure the vertical and horizontal stresses along the center line of the wall at a distance of 1 ft from the skin element. The location of the pressure cells within the backfill material is shown schematically in Figure 21. The actual installation of the pressure cells in the sand is shown in Figure 20.

65. The basic components of the WES pressure cell are a mercury-filled chamber and a diaphragm instrumented with a full Wheatstone bridge circuit as shown in Figure 22. Both the mercury chamber and the instrumented diaphragm are hermetically sealed within a cell casing made of Ry cut 50 Hot Roll 4147-50 steel and covered by a steel plate which is screwed to the body of the cell as shown in Figure 23. The pressure applied to the cover plate is transmitted through the mercury chamber to the flexible diaphragm, causing it to deflect in proportion to the applied pressure. The strain in the diaphragm actuates the strain gages which produce change in the electric resistance proportional to the applied external pressure. The pressure cells were calibrated and checked prior to installation.

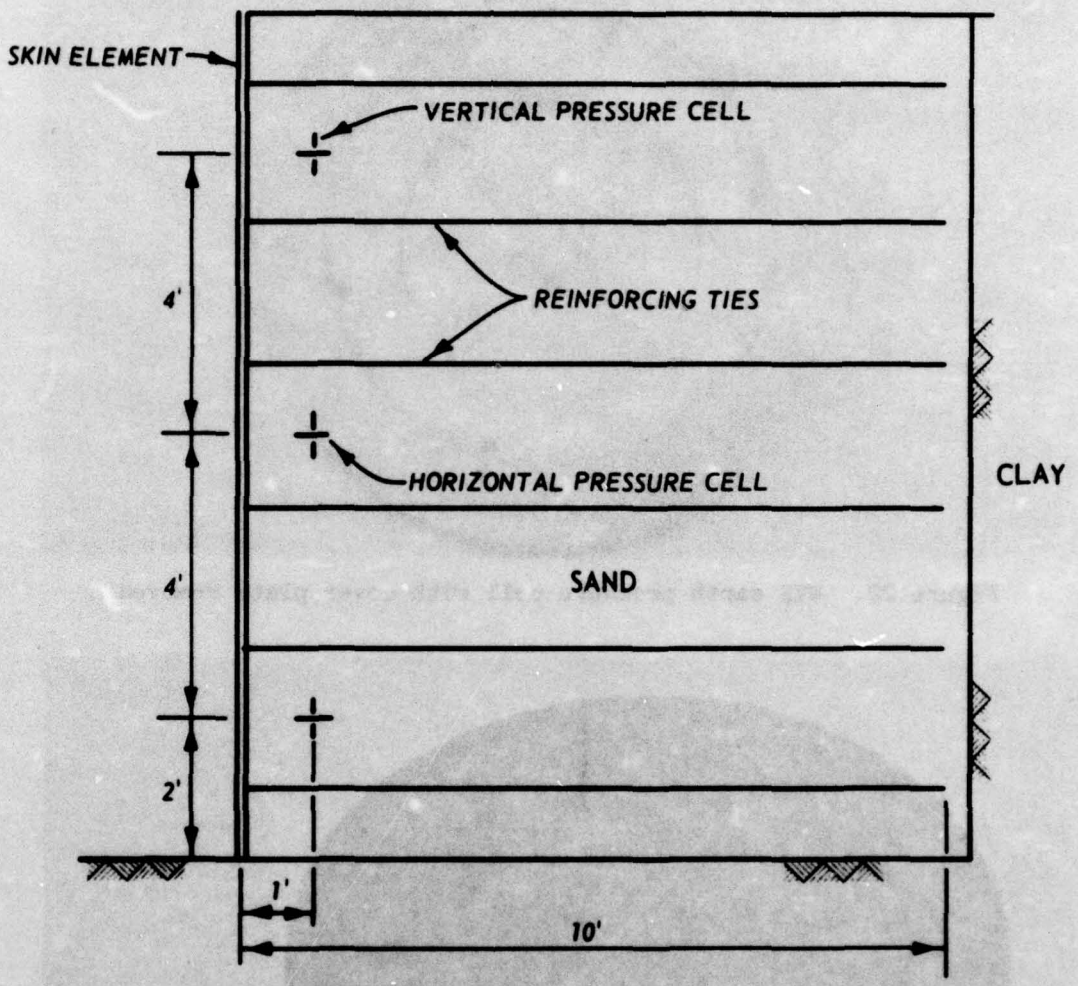

Figure 21. Schematic showing the location of the pressure cells along the center line of the wall

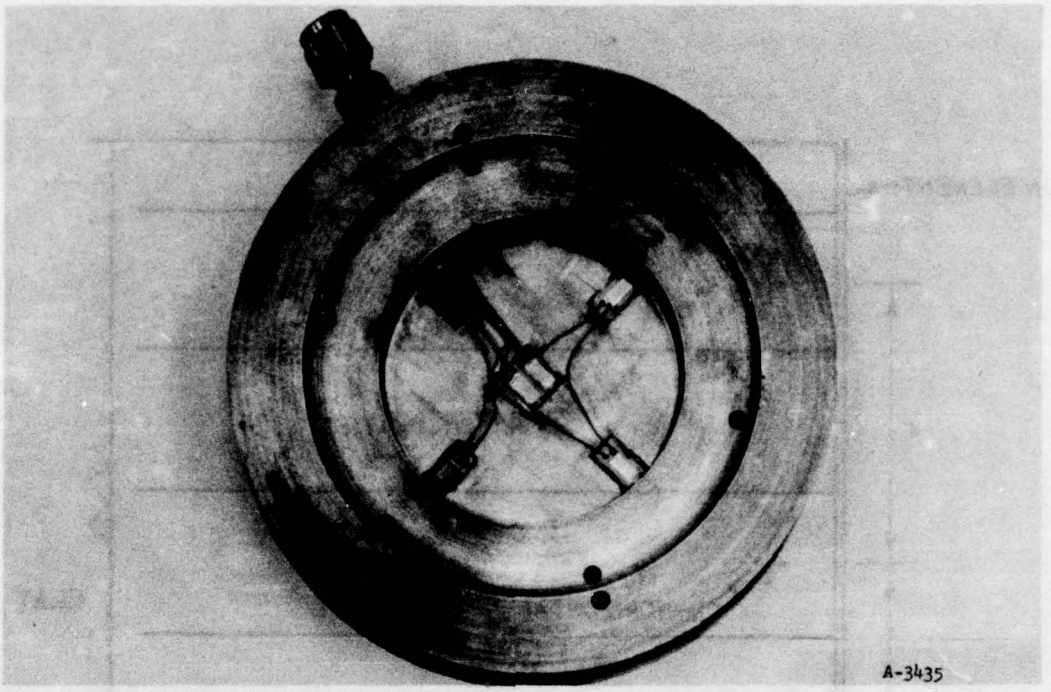

Figure 22. WES earth pressure cell with cover plate removed

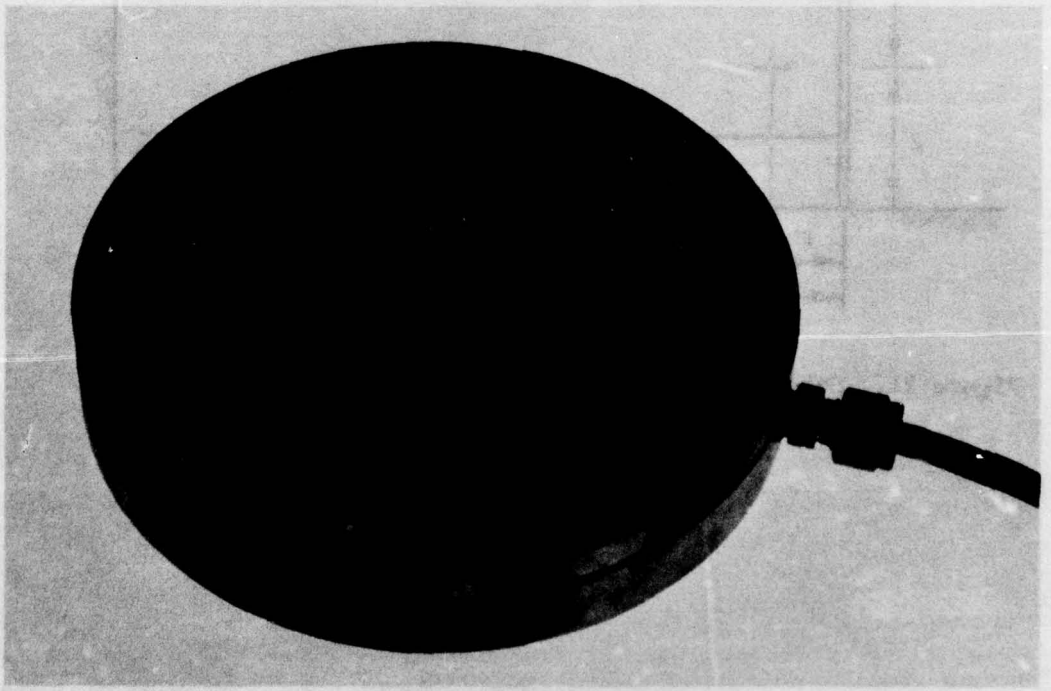

Figure 23. WES earth pressure cell with cover

Strain gages on reinforcing strips

66. Because of cost and time limitations, only three strips located along the center line of the retaining wall were instrumented. A schematic drawing showing the location of the strain gages along the instrumented strips is presented in Figure 24. The strain gages at each

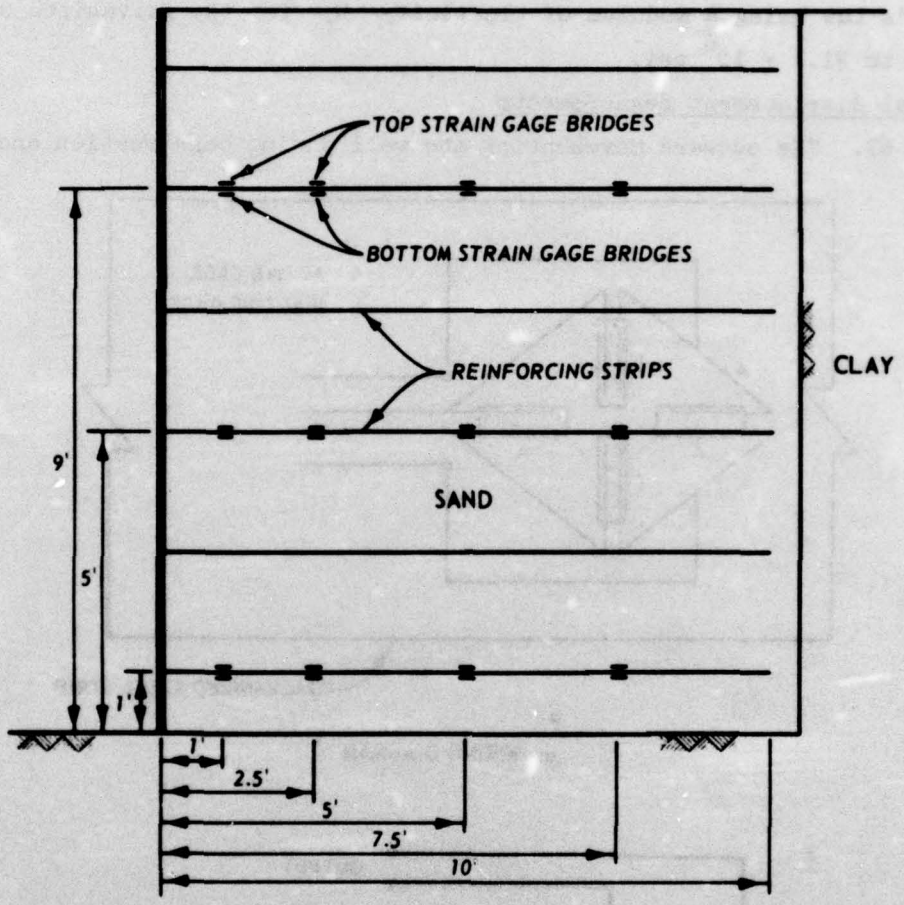

Figure 24. Schematic showing the location of the electric strain gage bridges along the center line of the retaining wall

location consisted of two complete Wheatstone bridges on both the top and bottom of the reinforcing strip. Such an arrangement enabled measurements of tensile strains due to direct tension as well as bending strains at that particular location. Each electric bridge consisted of four BLH strain gages with two active gages in the longitudinal direction and two dummy gages in the transverse direction of the reinforcing

strips. Figure 25 shows the circuit diagram of an individual electric bridge. All electric strain gage bridges were connected to an SR-4 strain indicator through a switching unit. Actual strains were calculated from the strain gage readings using a gage factor of 2.5. The tensile stresses were calculated from the measurements of strains and Hooke's Law using a modulus of elasticity E_t for the galvanized steel equal to 31.1×10^6 psi.

Lateral displacement measurements

67. The outward movement of the wall during construction and

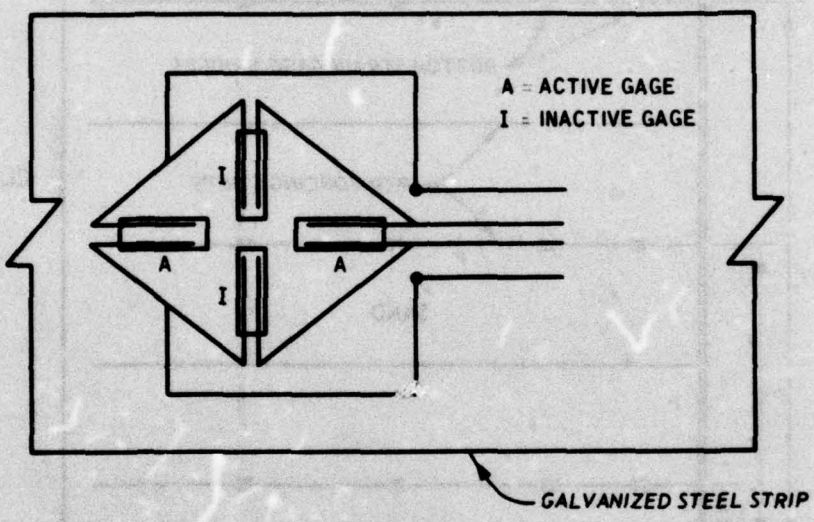

a. WIRING DIAGRAM

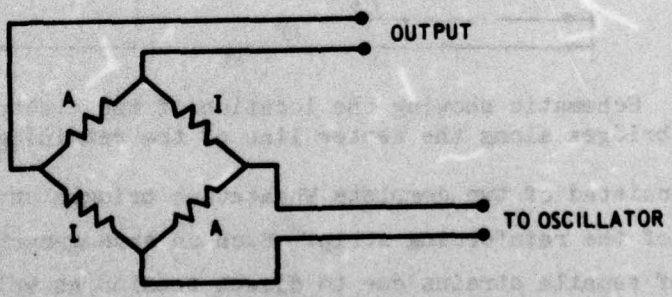

b. COMPLETE BRIDGE

Figure 25. Wiring and circuit diagram for the strain gages

surcharge loading was measured on the reinforced earth walls. Graduated rules were attached to the skin element along the center line of the wall at the same elevation of the reinforcing strips as shown in Figure 26. A transit located about 200 ft away was used to read changes in skin element deformation at every lift placement during construction and every two weeks during the period between the end of construction and surcharge loading. Figure 27 shows the wall with the graduated rules attached prior to surcharge loading.

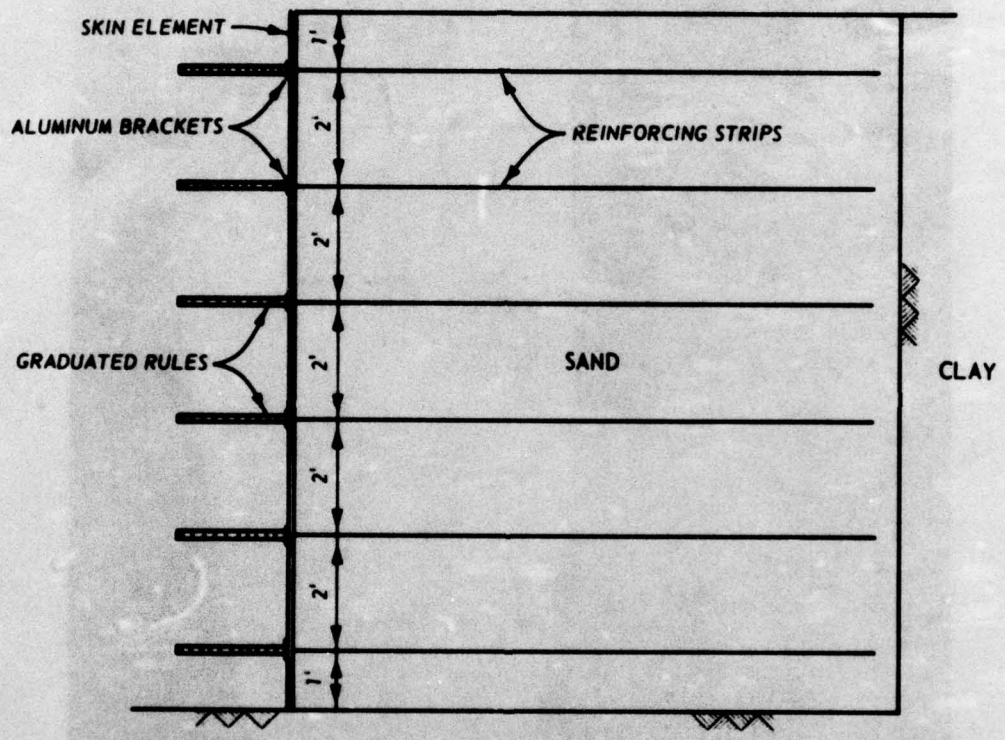

Figure 26. Schematic showing the graduated rules fixed to the skin elements along the center line of the wall

Figure 27. Reinforced earth retaining wall prior to surcharge loading

PART IV: SURCHARGE LOADING AND FAILURE

68. Two reinforced earth retaining walls were constructed at WES as a demonstration project. These two walls were identical except that one was reinforced with 0.08-in.-thick heavy-duty neoprene-coated membrane strips placed 4 ft apart in the horizontal direction, while 0.024-in. galvanized steel strips placed 2.5 ft apart were used for the other wall. The construction procedure was identical except that the retaining wall reinforced with membrane strips failed when the height reached 11 ft, while the wall reinforced with the galvanized strips did not fail when the full height (i.e. 12 ft) was reached.

Surcharge Loading

69. After the desired height of 12 ft was reached for the steel-reinforced wall, it was decided to surcharge load it to failure at some later date. The wall was covered with thin plastic membrane to protect it from weathering conditions, and it remained undisturbed for two months. When the plastic membrane was removed, it was observed that a crack extending the entire width of the wall had developed approximately 5-1/2 ft from the skin element (see Figure 28). Other surface cracks were noted around the perimeter of the backfill.

70. Prior to surcharge loading, landing mat sections (2 by 12 ft and 2 by 4 ft) were placed on the backfill surface to permit more uniform distribution of surcharge load. These mats were placed side by side parallel to the wall, but were not connected to each other in order to allow relative movements of the fill during loading. Surcharge loading was imposed on the wall by using 1-ton lead weights measuring 2 by 2 by 0.75 ft each. These weights were placed in a checkerboard fashion as shown in Figure 29. The first load increment consisted of placing weights 1 through 20, which was equivalent to 250 psf of surcharge pressure. After weight 20 was placed, readings of pressure cells, strain gages, and the lateral deformation along the center line of the skin elements were recorded. The second sequence of lead weights, which

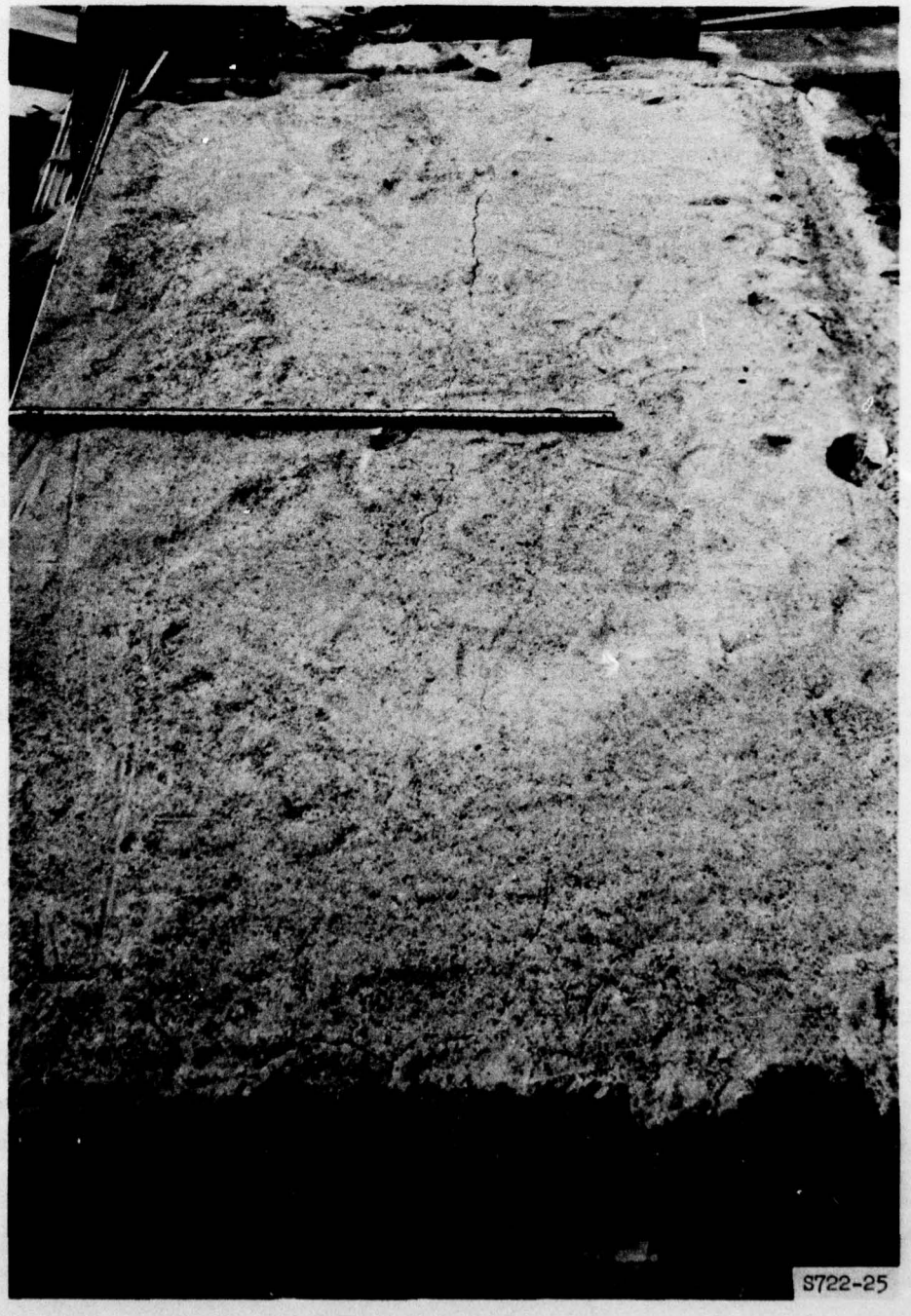

Figure 28. Development of surface cracks two months after the construction of the wall

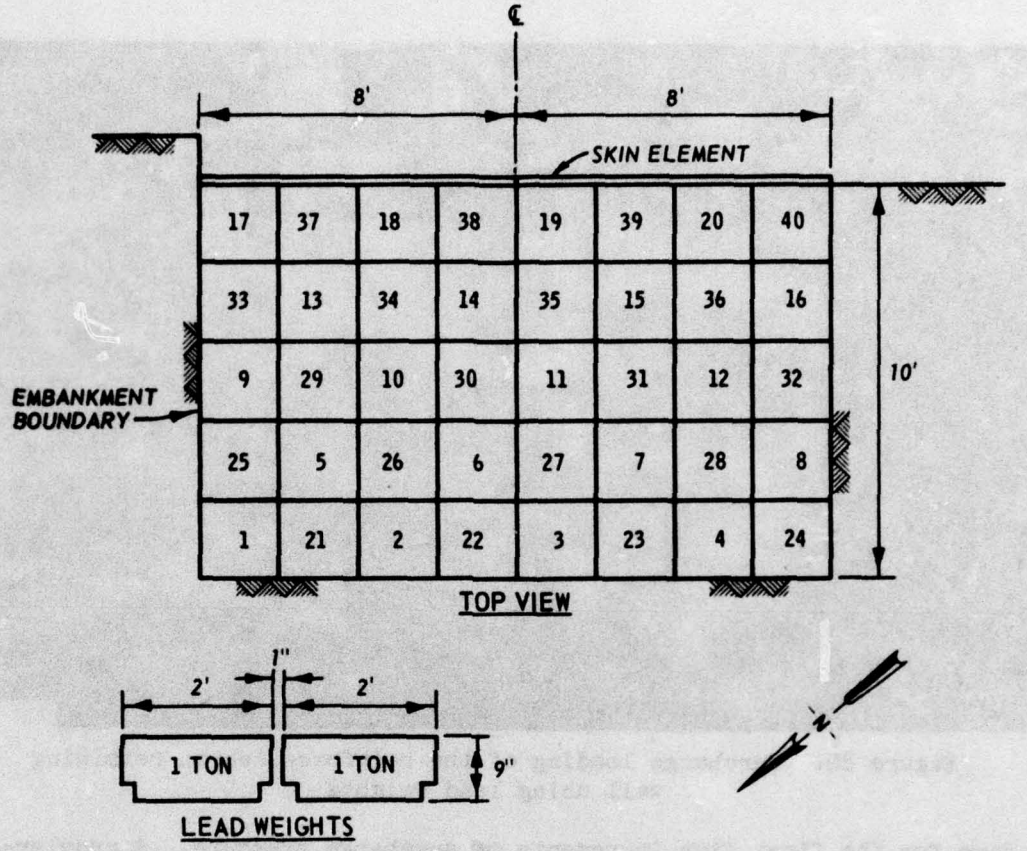

Figure 29. Sequence of placing lead weights for the first, second, and third layers of surcharge loading

included weights 21 through 40 as shown in Figure 29, were placed to fill the empty spaces of the checkerboard pattern and form a complete layer of weights. At this point the surcharge pressure was approximately equal to 500 psf and another set of instrumentation readings was recorded. The same procedure was followed for the succeeding layers of weights until the failure of the wall occurred at about 1500 psf of surcharge pressure. For safety purposes cables were wrapped around the second and third layers of weights, as shown in Figure 30, to keep them from toppling due to uneven settlement of the fill.

Loading Equipment and Wall Performance

71. The loading operation was accomplished using a telescoping

Figure 30. Surcharge loading of the reinforced earth retaining wall using lead weights

crane for the first five increments of surcharge pressure. A crawler-type crane was used for placing the sixth and seventh increments of surcharge load. For safety purposes a platform was constructed to fit on a forklift tractor from which a laborer could disconnect the cable supporting the lead weights once they were set in position. About 10 min after the third layer was completed, an audible sound of distress accompanied with 4-in. bulging in the skin element located between the first and second rows of the reinforcing strips from the bottom occurred. This lasted for about 1 to 2 sec, after which movements ceased. It was felt at this time that the wall was on the verge of collapse and could fail at any moment. Thus, the wall was left undisturbed for two days with nothing significant happening except that increased bulging in the skin element occurred at the northeast corner. It was decided to continue surcharge loading the wall until complete failure occurred.

72. Prior to continuation of loading, readings were made of the

pressure cells, strain gages, and the lateral deformation. The surcharge loading was continued using 2-ton basket weights since all the available 1-ton weights had been used in previous increments. The loading pattern followed is shown in Figure 31. After placement of basket weight 16, a

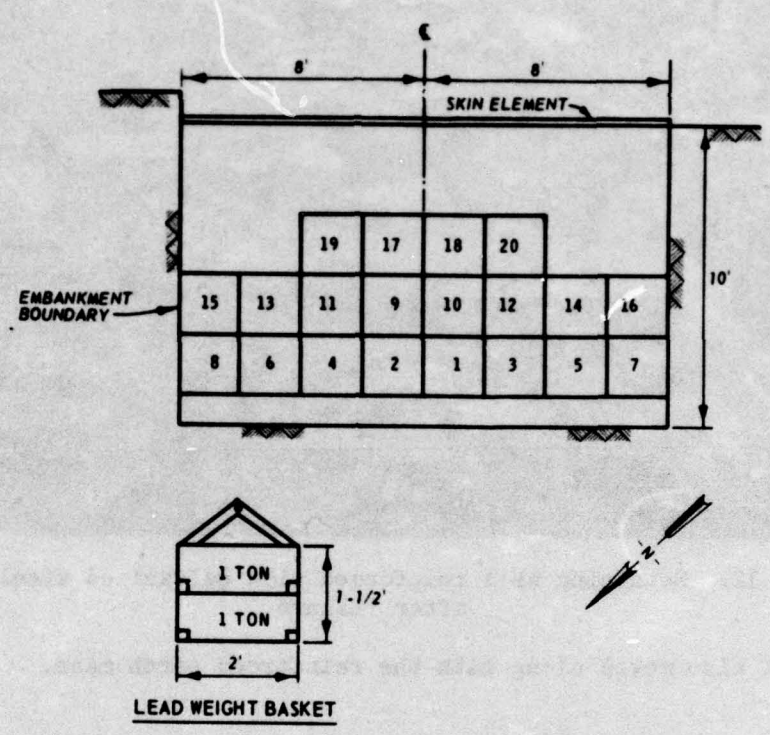

Figure 31. Sequence of placing the lead weight baskets for the fourth layer of surcharge loading

significant movement of the wall accompanied by a loud crushing noise was observed, and at this time another set of instrumentation readings was taken before adding the next basket weight. Surcharge loading was then continued until basket weight 20 was placed in position. At this moment the reinforced earth wall started to move and complete collapse took place in a short period of time (not more than 3 sec). The construction, instrumentation, surcharge loading, and failure of the wall were recorded on 16mm color movie footage which is available on loan from WES. Figure 32 shows the reinforced earth wall a few minutes after the catastrophic failure. Note that a large mass of the southeast

Figure 32. Retaining wall reinforced with galvanized steel strips *after failure*

embankment also moved along with the reinforced earth mass.

Assessment of Damage after Failure

73. After the failure of the reinforced earth wall, a general survey of the area was made in an effort to define some significant feature of the failure mechanism. It was hoped to locate the failure surface, but because of the severe damage inflicted by the tumbling lead weights, such hope disappeared quickly. Consequently, the survey was limited to taking elevations of the backfill material which are presented in contour form in Figure 33. Three cross sections of the fill material are presented in Figure 34, one along the center line of the wall and the other two along the sides. The average angle of fallen fill material was about 29 deg, which was approximately equal to the minimum angle of friction of the backfill sand. The uppermost landing

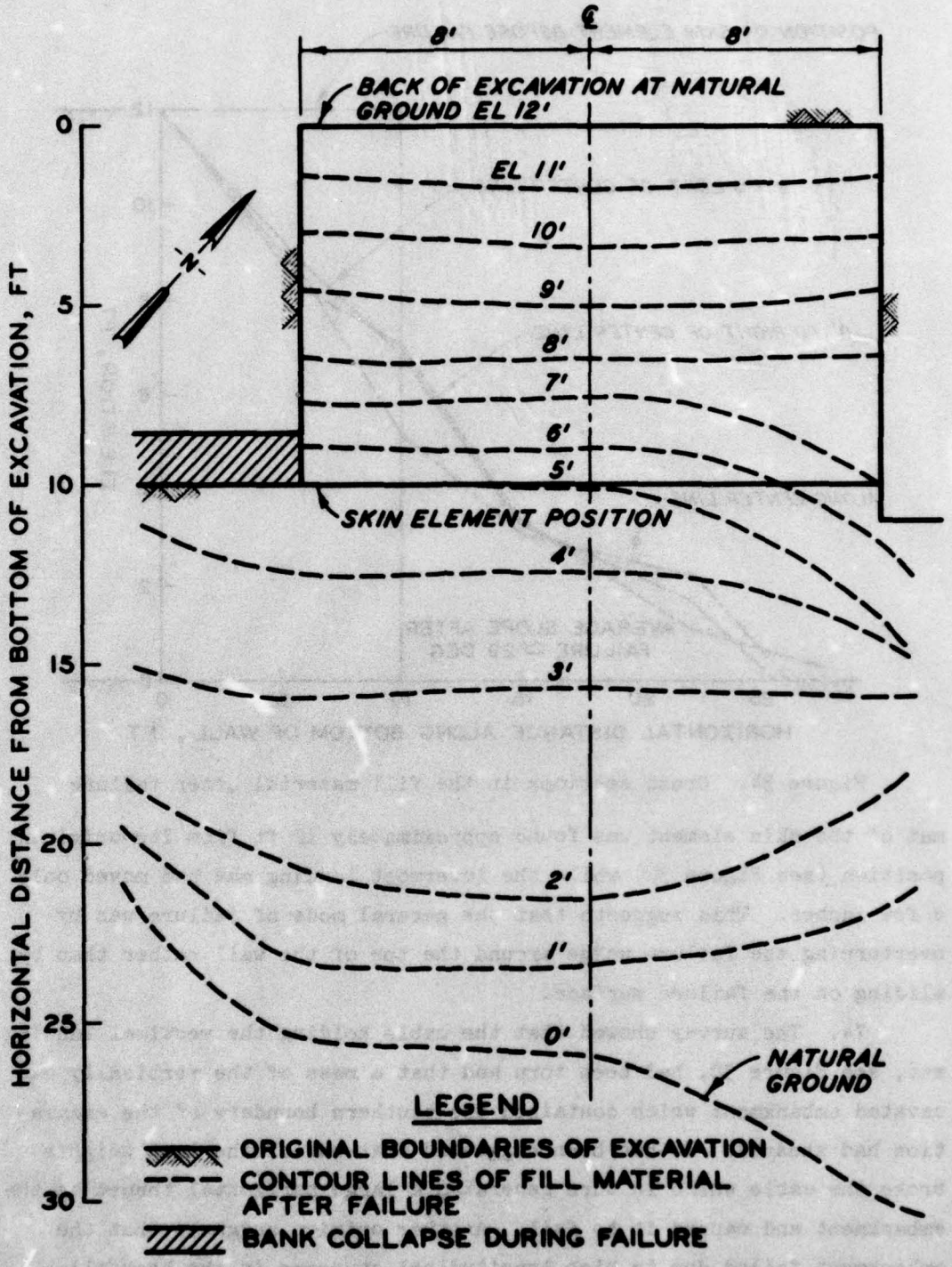

Figure 33. Contour lines for the fill material after the failure of the reinforced wall

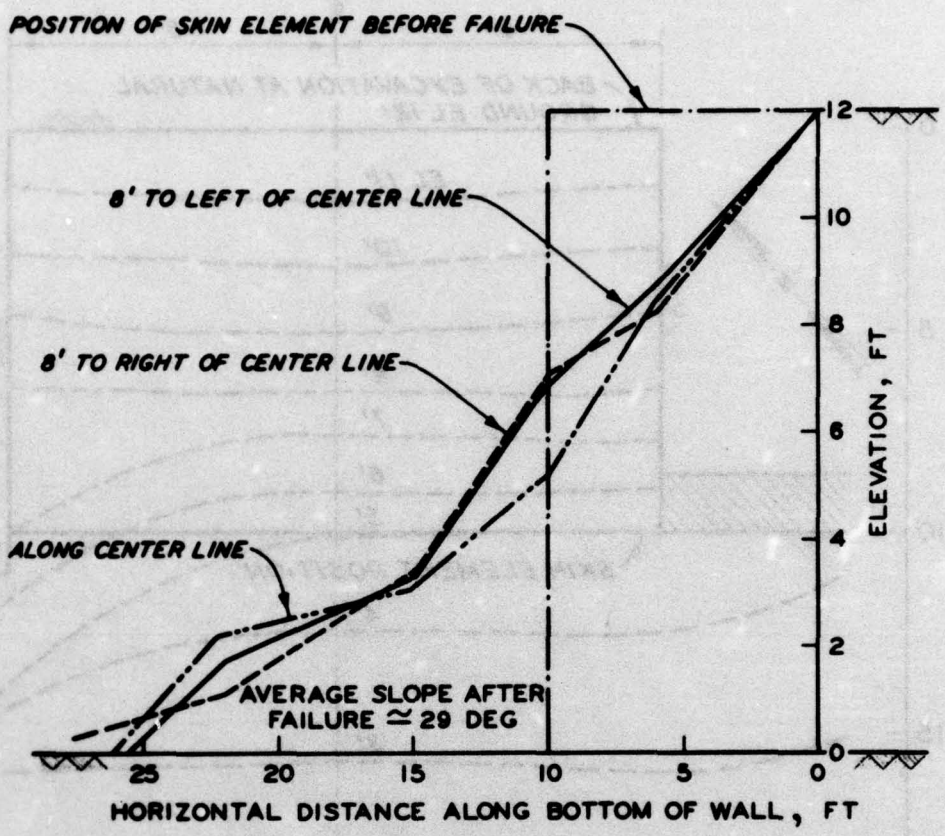

Figure 34. Cross sections in the fill material after failure

mat of the skin element was found approximately 12 ft from its original position (see Figure 32) while the lowermost landing mat had moved only a few inches. This suggests that the general mode of failure was by overturning the failure wedge around the toe of the wall rather than by sliding on the failure surface.

74. The survey showed that the cable holding the vertical landing mat, see Figure 30, had been torn and that a mass of the vertically excavated embankment which contained the southern boundary of the excavation had sheared. It has been suggested that one of the lead weights broke the cable which in turn generated a large horizontal thrust on the embankment and caused it to fail. Another opinion suggests that the embankment failed due to high longitudinal stresses in the backfill material which in turn caused the cable to fail. It is not significant

which failure occurred first, i.e., the cable or the embankment. What is significant, however, is that the wall might have been able to carry more surcharge load had the cable and the supporting embankment remained intact.

75. The mode of failure of the reinforcing elements and the relative displacement of each strip from its original position were examined and are summarized in Figure 35. Three types of failure were noted (see Figure 36), as follows:

a. Shear failure either across the full width of the

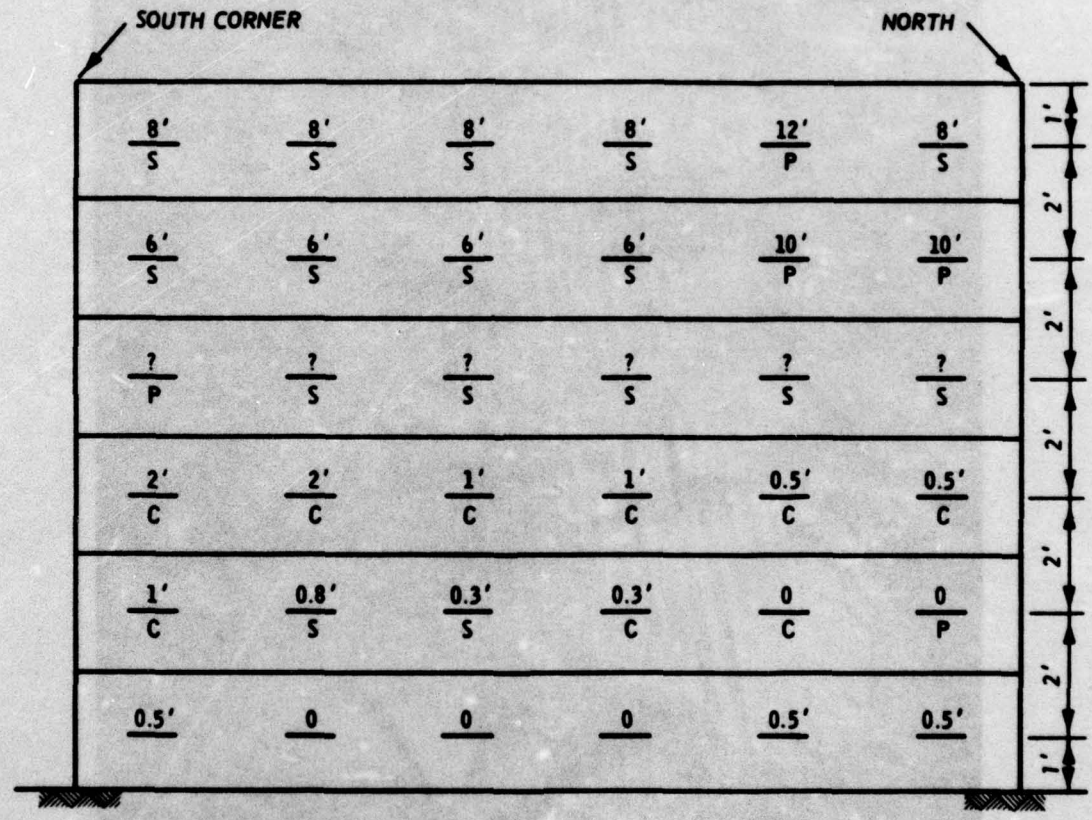

NOTE: S INDICATES SHEAR FAILURE IN THE STRIP
C INDICATES CONNECTION FAILURE
P INDICATES PULLOUT FAILURE
NUMBERS REPRESENT THE MOVEMENT OF THE STRIPS AFTER FAILURE FROM THEIR ORIGINAL POSITION

Figure 35. Mode of failure and the displacement of the galvanized steel strips after failure

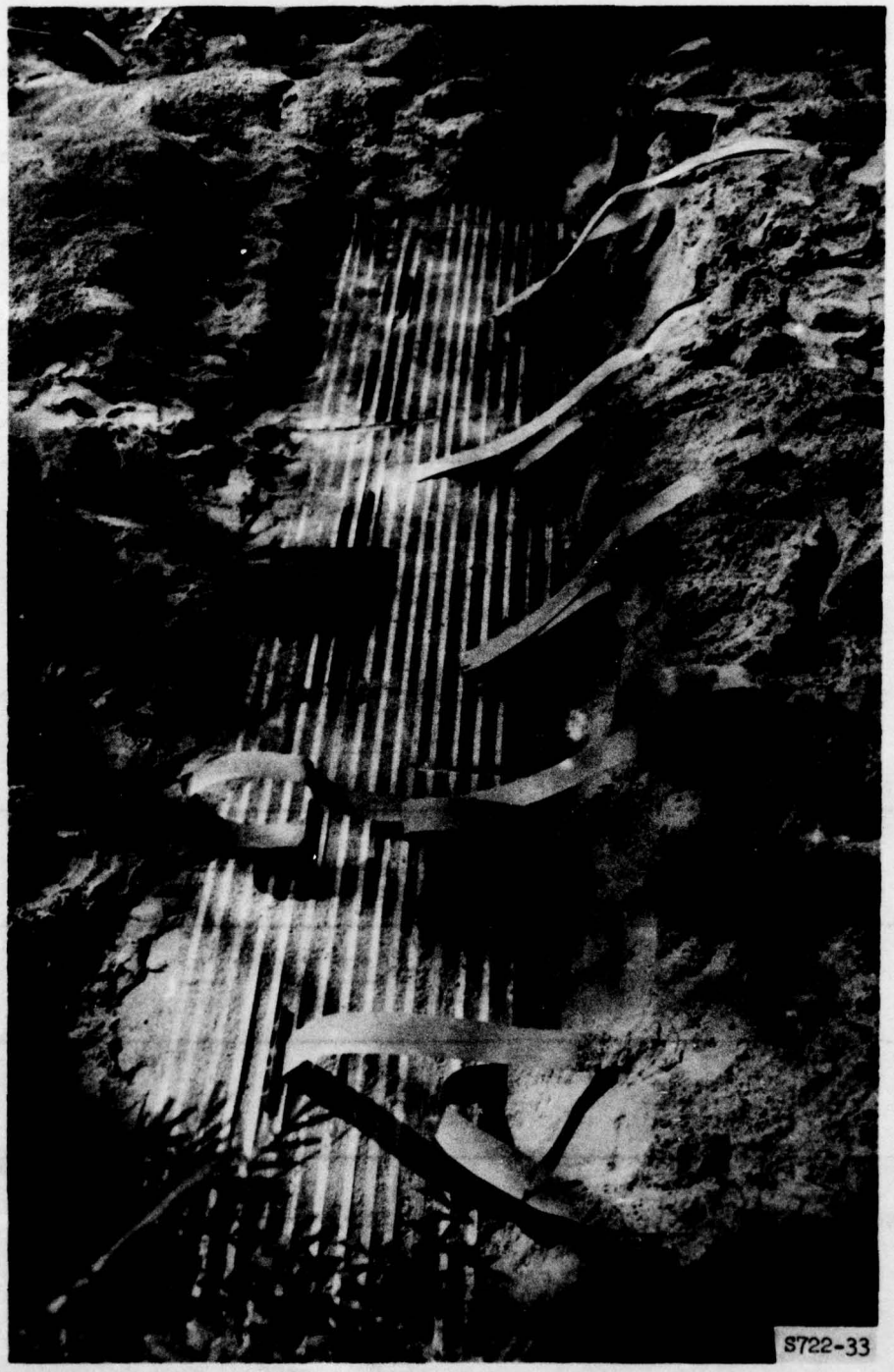

Figure 36. Modes of failure of the galvanized steel strips

reinforcing strip or around the bolts which connected the strip to the skin element.

b. Connection failure in which the two angles that fastened the reinforcing strip to the landing mat were detached due to the severe deformation of the skin element.

c. Pullout failure in which a substantial relative movement occurred between the reinforcing strips and the surrounding soil.

76. All reinforcing strips that broke did so at or very close to the brackets that connected them to the skin element. This may indicate that the highest tensile stress concentration at failure occurred at points along the strips close to the skin element. Failure was not limited to the reinforcing strips but also extended to the skin elements. It was observed that all vertical welding of joints connecting the landing mats had experienced severe deformation and buckling or horizontal shear along the joints as shown in Figures 37 and 38, respectively.

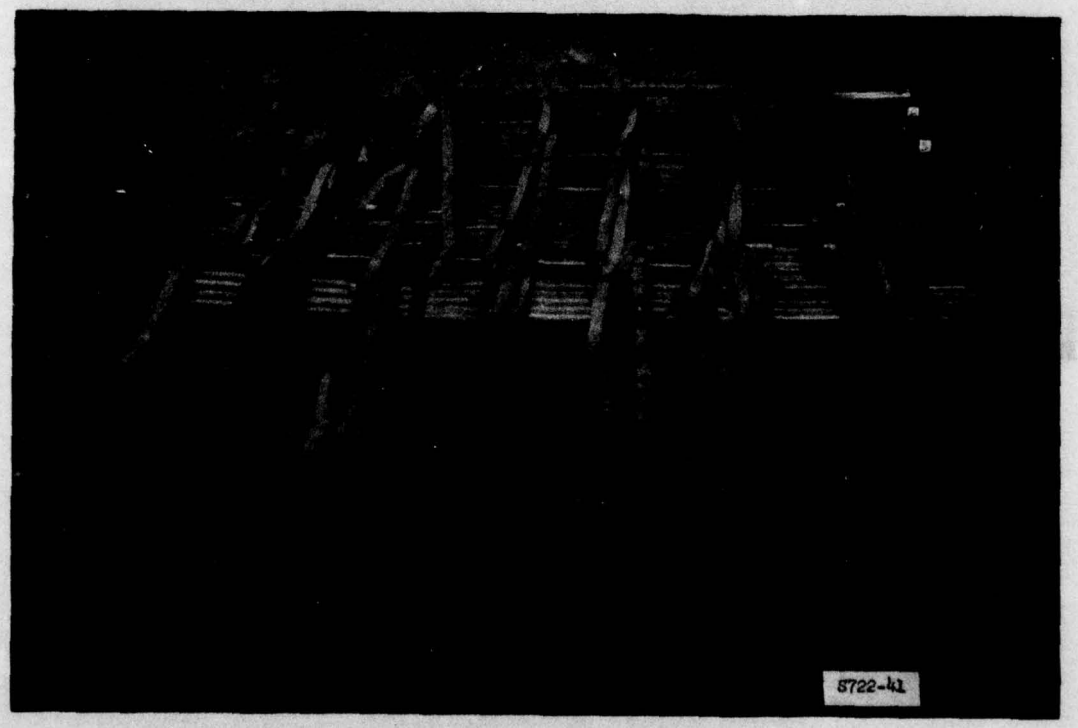

Figure 37. Deformation and buckling of landing mats composing the skin elements

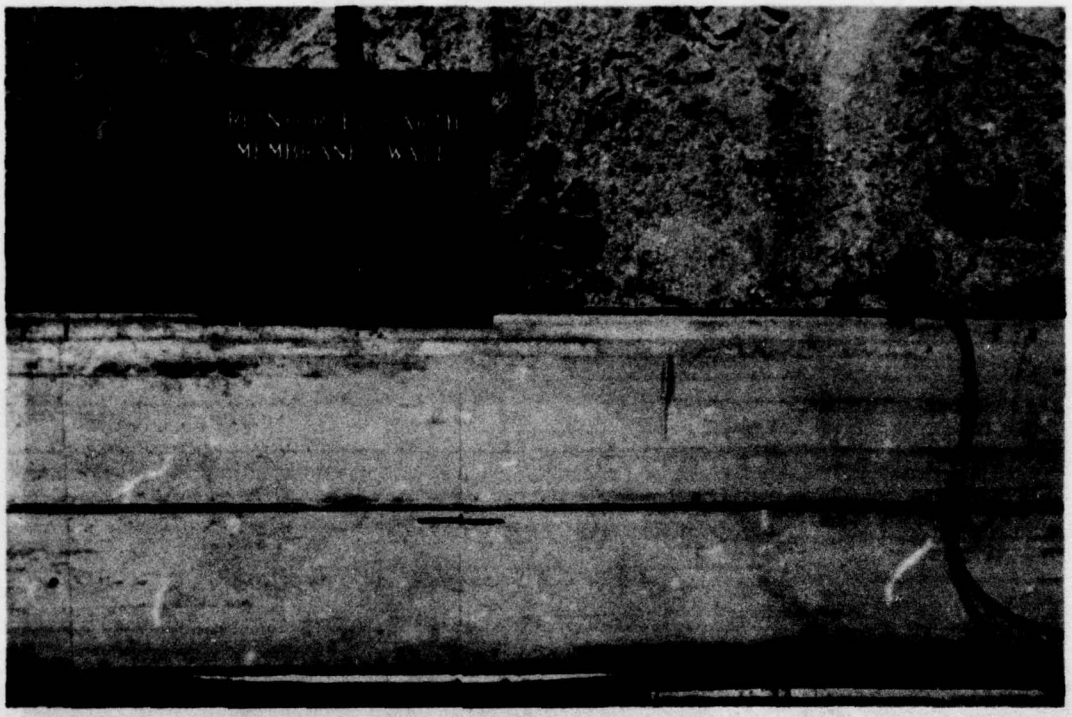

Figure 38. Shear failure of the skin element

PART V: INSTRUMENTATION MEASUREMENTS AND RESULTS

77. Three types of instrumentation were used in the test program for the measurement of stresses and deformation within the reinforced mass. The devices were pressure cells for measuring internal stresses within the soil, strain gages for measuring strains along the reinforcing strips, and wooden rules for measuring lateral deformation of the skin elements.

Stress Measurement Within the Backfill

78. Six WES pressure cells were used for each retaining wall, three placed horizontally to measure vertical stress at different levels, and three oriented vertically to measure the lateral stress as shown in Figure 21. These pressure cells were placed approximately 12 in. from the face of the wall and at elevations 1, 5, and 9 ft above the bottom of the wall.

Pressure cell measurement

79. The pressure cell readings were taken during construction of the wall reinforced with neoprene-coated membrane strips at every 1-ft lift, and the vertical and horizontal earth pressures calculated from these readings were compared with the theoretical overburden pressure above the pressure cell at the time of reading. The correlation between the vertical stress reading of the pressure cell and the calculated vertical pressure due to the depth of overburden is presented in Figure 39. As expected, the pressure cell reading increased with increase in the depth of overburden, but deviated slightly from the ideal condition. It appears that while the pressure cells overregistered at the early stages of loading, they underregistered when the wall approached failure. A similar correlation between the horizontal pressure cell reading and the overburden pressure for each lift is presented in Figure 40. The figure shows that although the correlation between σ_h and σ_v conforms with the active earth pressure relationship at low pressure, it deviates significantly at higher pressure indicating that most of the

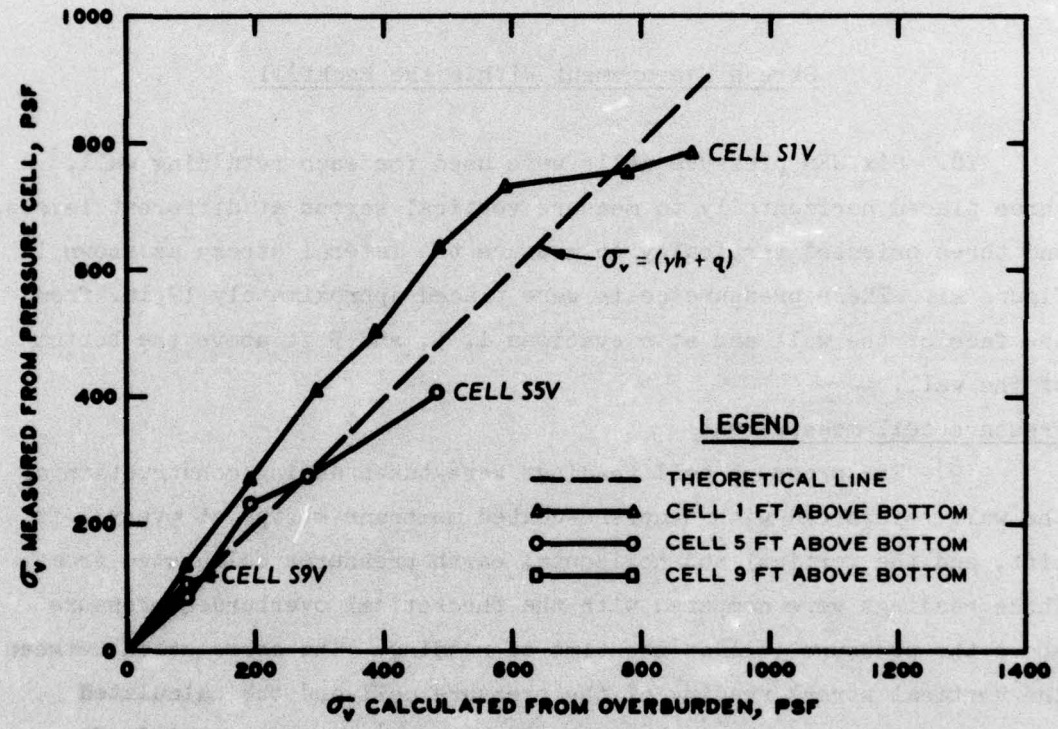

Figure 39. Correlation between measured and calculated vertical stresses for wall reinforced with rubber-coated strips

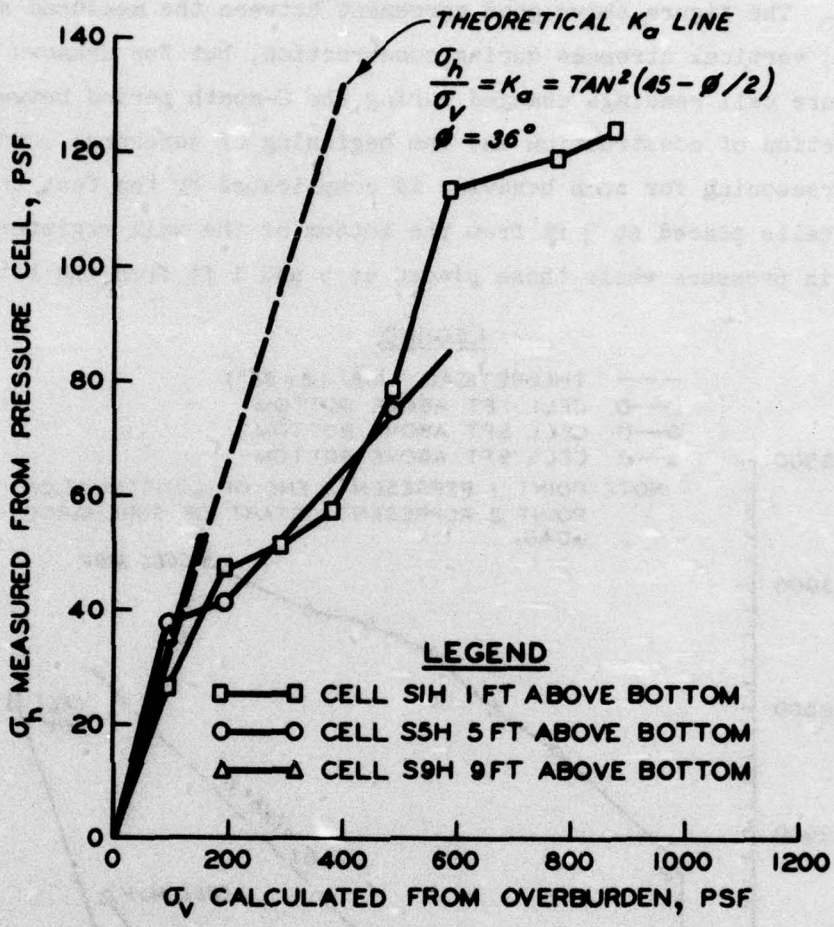

Figure 40. Comparison between the measured horizontal stress and the calculated vertical stress for wall reinforced with rubber-coated strips

horizontal stresses were carried by the reinforcing strips at the points where the pressure cells were placed.

80. A similar comparison between pressure cell readings and the pressure due to the depth of overburden plus the surcharge pressure was made for the wall reinforced with galvanized steel strips. Readings were taken not only at 1-ft lifts during construction, but also at each 250-psf increment of surcharge pressure. The relationship between the vertical pressure as measured by the pressure cells and that calculated from the depth of overburden plus the surcharge pressure is shown in

Figure 41. The figure shows good agreement between the measured and the calculated vertical stresses during construction, but for unknown reasons the pressure cell readings changed during the 2-month period between the completion of construction and the beginning of surcharge loading. Rational reasoning for such behavior is complicated by the fact that the pressure cells placed at 9 ft from the bottom of the wall registered an increase in pressure while those placed at 5 and 1 ft from the bottom

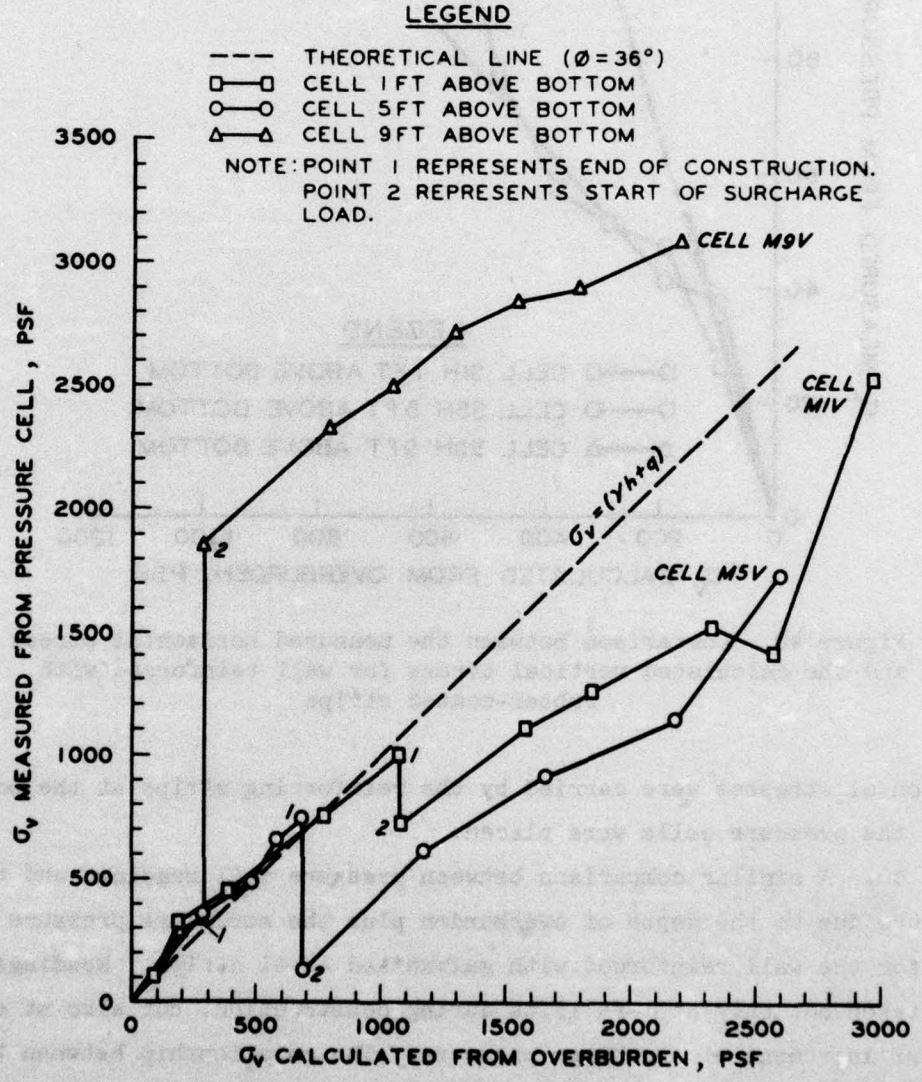

Figure 41. Comparison between measured and calculated vertical stresses for wall reinforced with galvanized steel strips

of the wall registered a decrease in pressure. It is possible that the zero reading was shifted after construction. During surcharge loading, however, the rate of increase in pressure cell readings was slightly less than the rate of increase in surcharge load, possibly due to arching of the sand.

81. The relationship between the lateral stress as measured by the pressure cells and the vertical stress due to the depth of overburden plus the surcharge load, for the wall reinforced with galvanized steel strips, is shown in Figure 42. This figure shows that the slope of σ_h versus σ_v is about half the value k_a during the construction and surcharge loading of the wall. The figure also shows that the measured lateral pressure increased during the 2-month period between the end of construction and the beginning of surcharge loading even though the vertical pressure was unchanged during that period. The reading for the pressure cell placed 1 ft above the bottom of the wall increased and at the end of the resting period the registered lateral pressure exceeded the vertical pressure. Again there is no satisfactory explanation for such unexpected behavior except the possibility of shift in the zero reading.

Strain measurement
of the reinforcing strips

82. Three galvanized steel strips along the center line of the wall were instrumented with strain gages to measure the tensile strains. These reinforcing strips were located at elevations of 1, 5, and 9 ft along the center line of the wall and instrumented with full SR4 bridges on both surfaces at points 1, 2.5, 5, and 7.5 ft from the face of the skin element, as shown in Figure 43. Strain gage readings were taken after the completion of every 1-ft lift and following the application of each increment of surcharge load. The readings were compared with the vertical stress computed using the overburden plus the surcharge pressures as shown in Figures 44, 45, and 46. These figures show that the strain gage readings increased with increasing vertical stress in a nonlinear fashion. It is of interest to note that the top and bottom strain gage bridges, in the majority of points, did not give the same

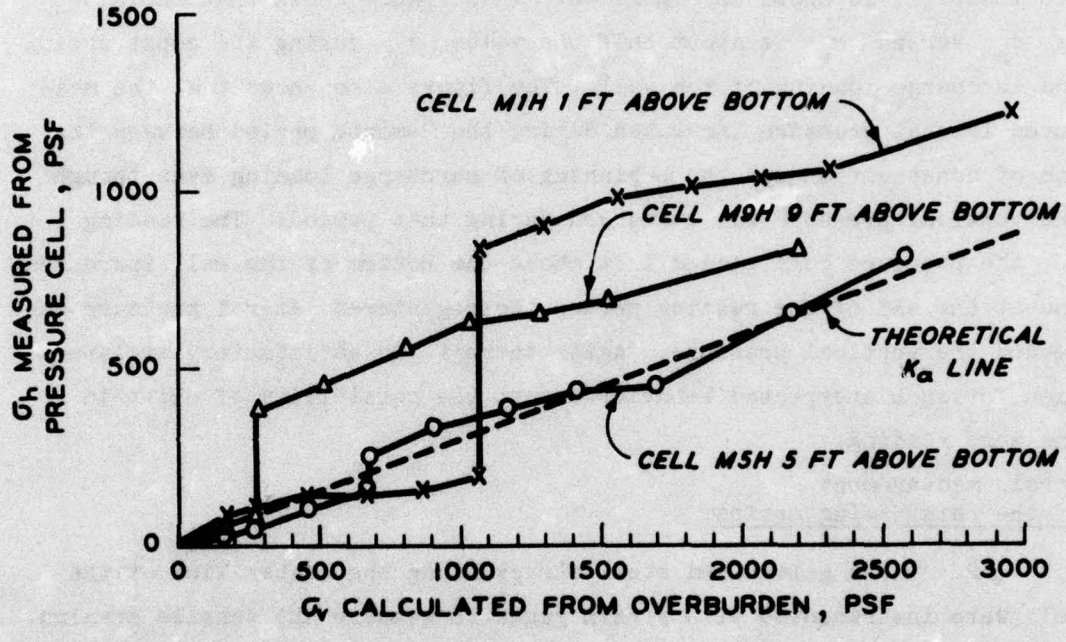

Figure 42. Comparison between the measured horizontal stress and the calculated vertical stress for wall reinforced with galvanized steel strips

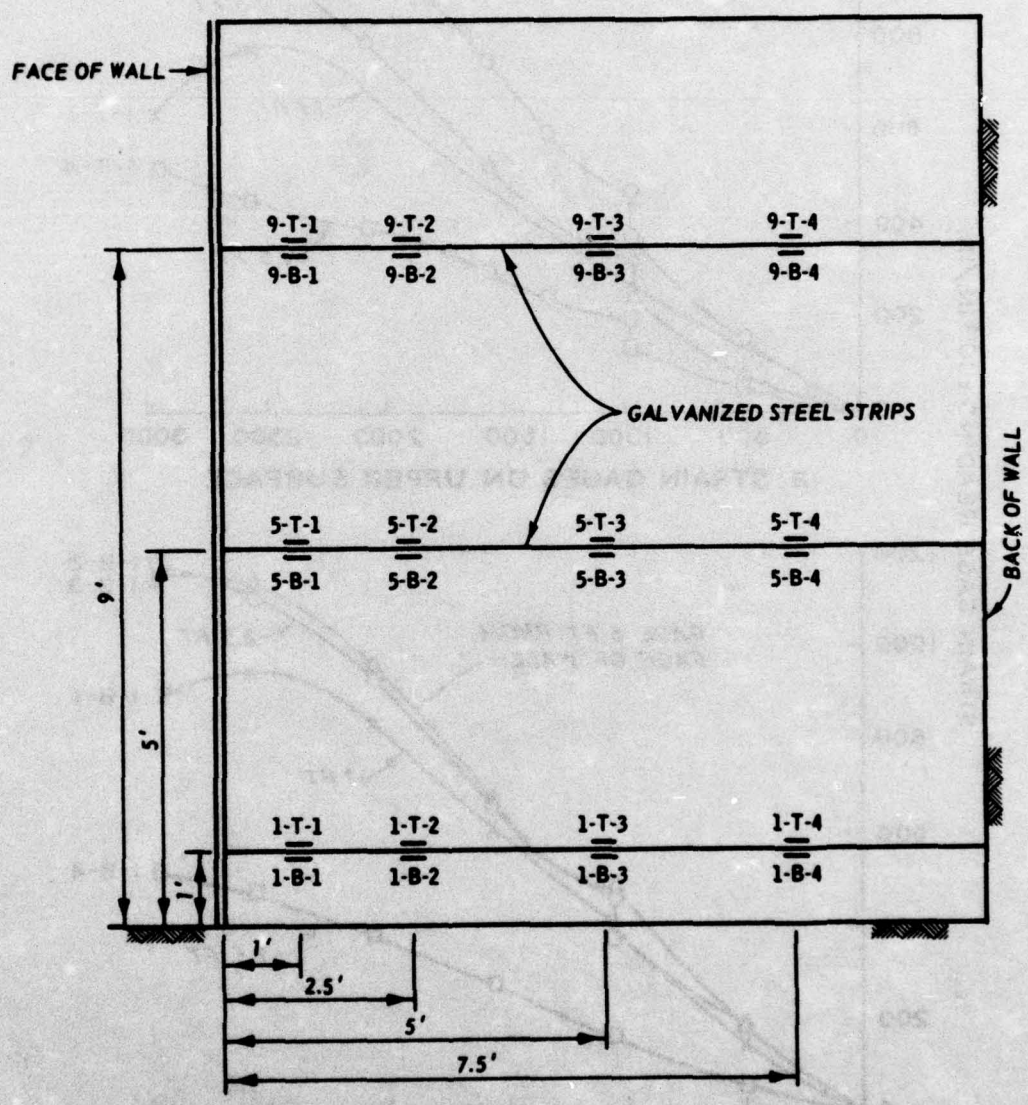

Figure 43. Layout of SR-4 strain gages on the galvanized steel strips along the center line of the reinforced earth wall

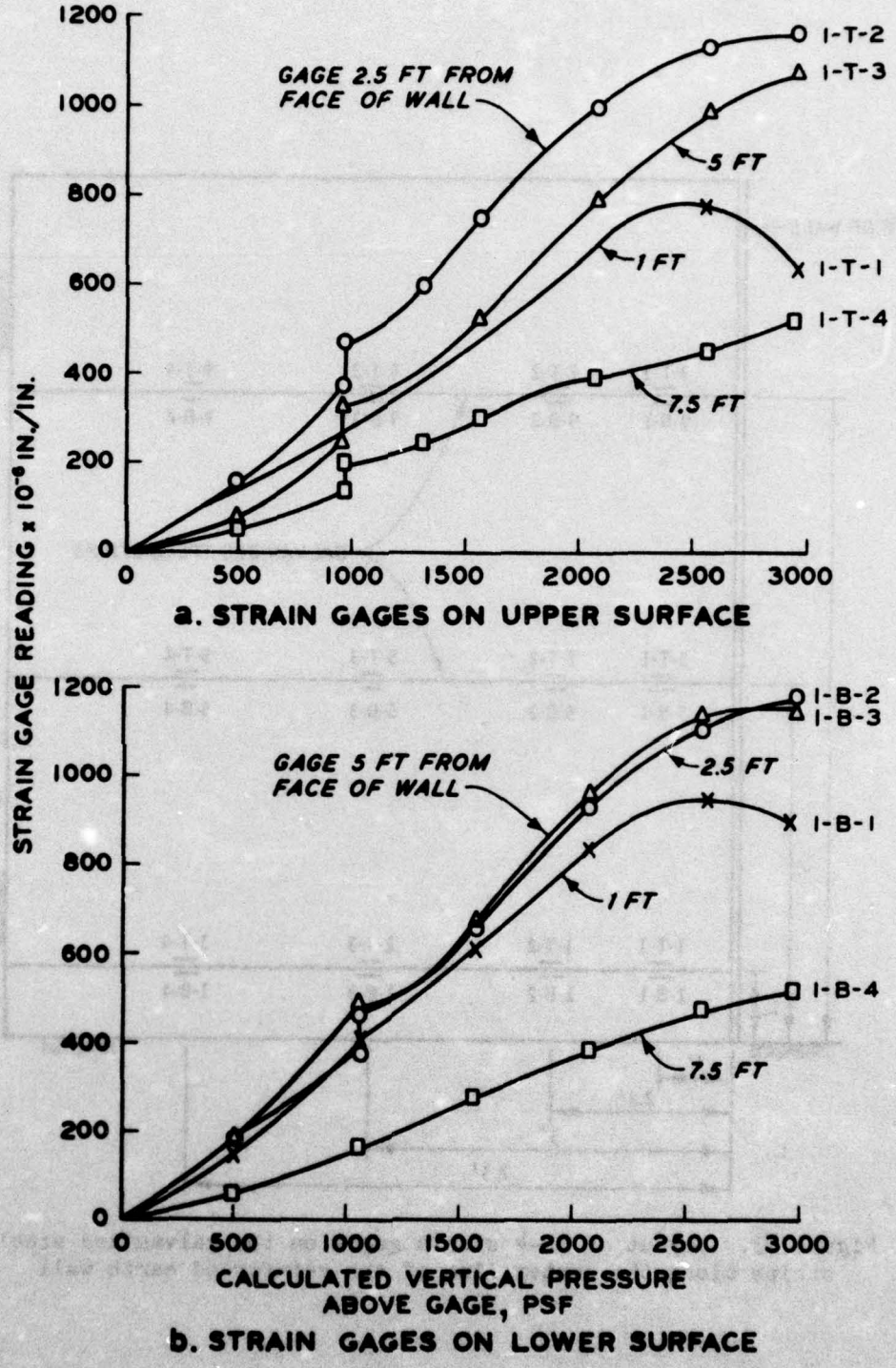

Figure 44. Strain gage readings versus vertical stress for the galvanized steel strip located 1 ft above bottom of wall

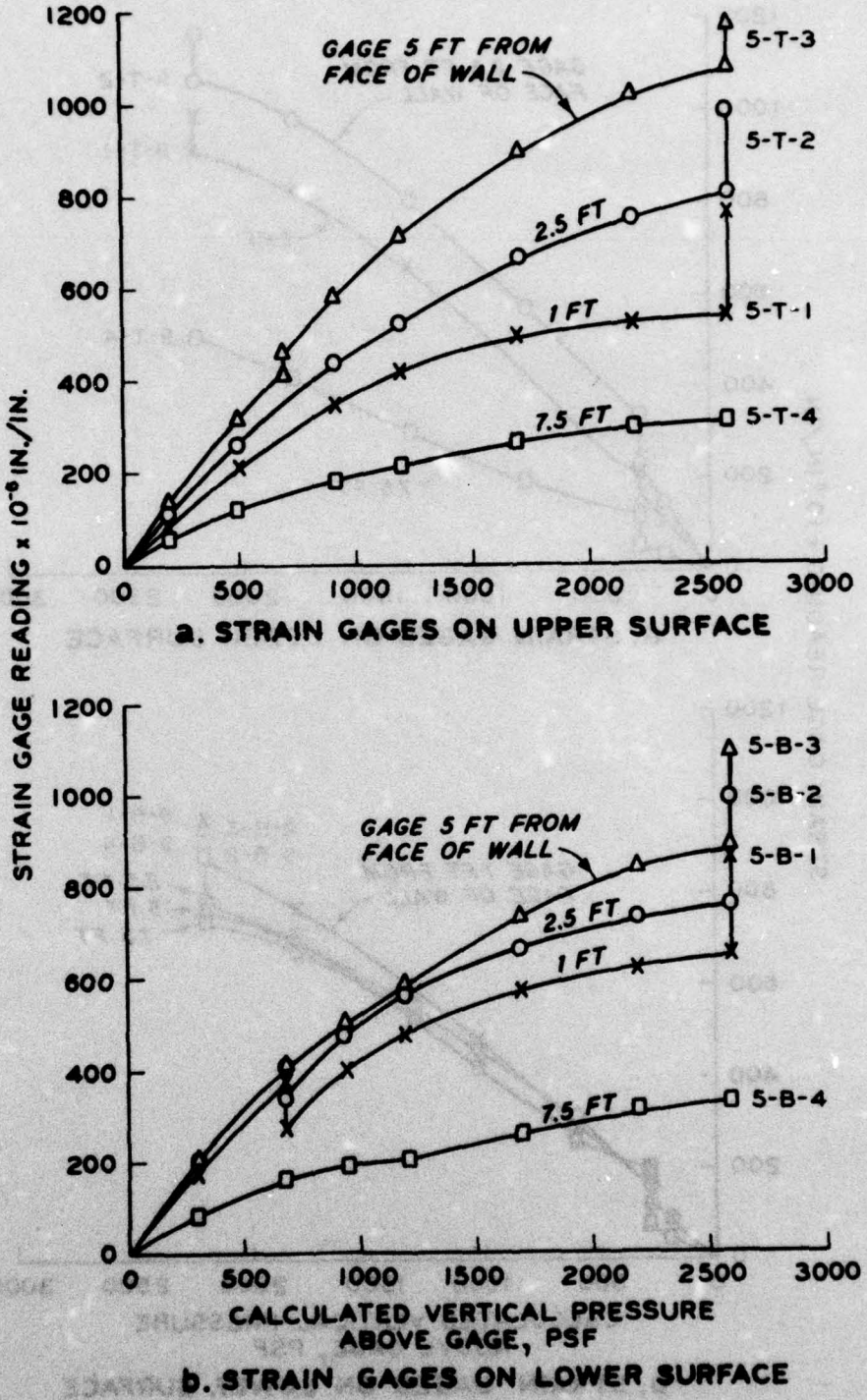

Figure 45. Strain gage readings versus vertical stress for the galvanized steel strip located 5 ft above bottom of wall

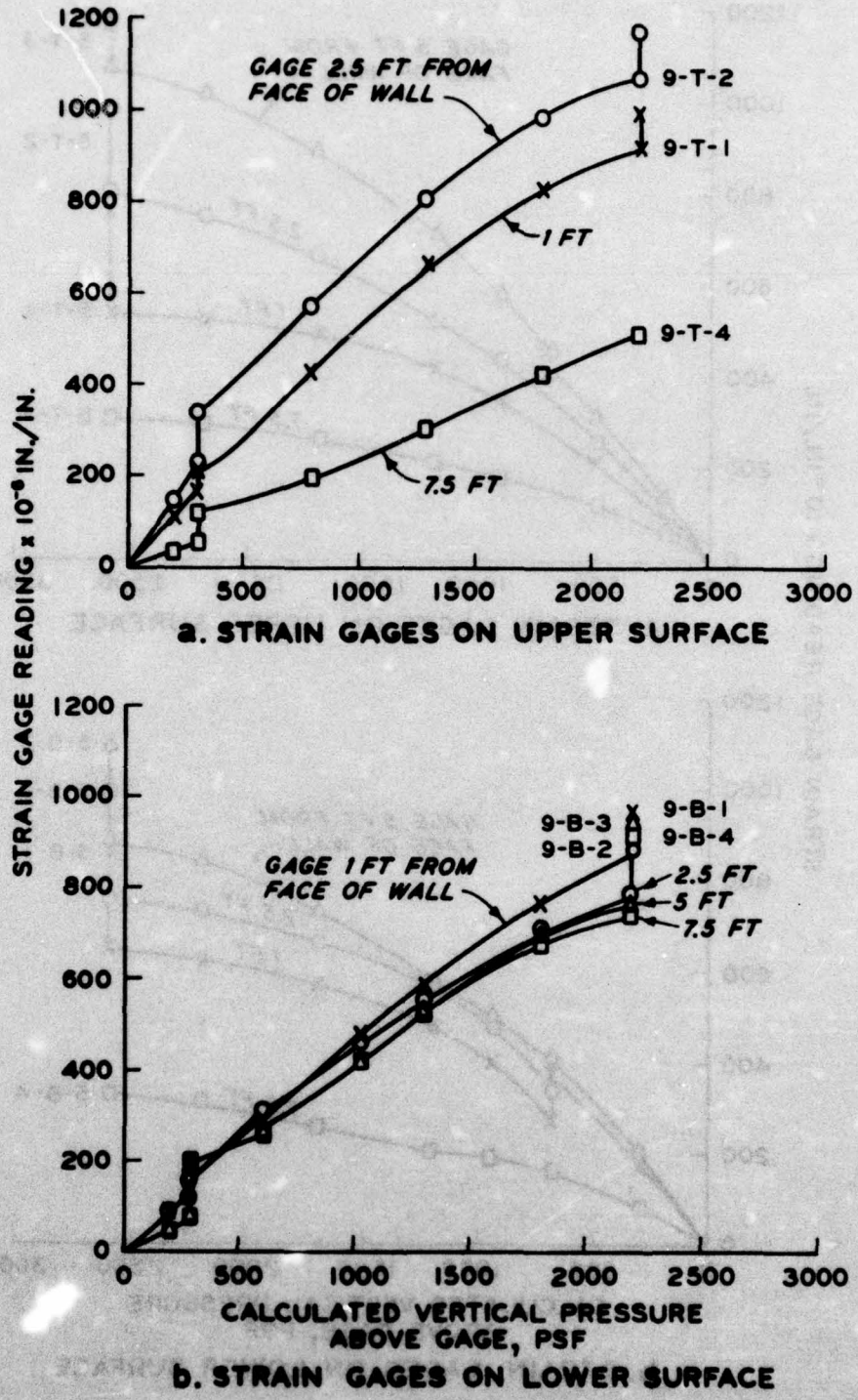

Figure 46. Strain gage readings versus vertical stress for the galvanized steel strip located 9 ft above bottom of wall

readings. This difference may be attributed partly to slight strain due to bending, to the difference in the characteristics of each bridge, and possibly to the effect of arching and other unknown factors. The figures also show that there was an increase in the strain gage readings during the 2-month period between the end of construction and beginning of surcharge loading, especially for the gages located at 1, 2.5, and 5 ft from the face of the wall. This may be attributed to the slow creep in the fill material and possibly to the settlement and readjustment of the soil particles within the reinforced mass.

83. Measured strains at the top and bottom of each instrumented point were averaged out to eliminate the effect of bending strains, and the resulting strain was used for tensile stress calculation. Knowing the modulus of elasticity of the galvanized steel, Figure 8, the tensile stress was calculated by multiplying the average strain by the modulus of elasticity for each loading increment. The relationships between the tensile stress, the tensile strain, and the superimposed vertical pressure for the reinforcing strips are shown in Figures 47, 48, and 49. It can be seen that the maximum tensile stress did not occur at the wall surface, but rather a few feet away from it. This point is illustrated more clearly in Figure 50, which shows the distribution of tensile stress along the instrumented reinforcing strips at the end of construction and prior to failure. As shown in Figure 50, the curve connecting the points where maximum tensile stress occurs in the reinforcing strips does not coincide with the theoretical Rankine failure surface.

Comparison between theoretical and experimental lateral earth pressures

84. In Rankine's theory it is assumed that the horizontal pressure on the wall increases linearly with depth. Consequently, one might expect the maximum lateral earth pressure to occur at the lowest point of the wall. Comparison between the Rankine earth-pressure theory, readings from earth-pressure cells, and also those stresses generated from the measured strains in the instrumented reinforcing strips within a segment of the wall ($S_x S_z$) surrounding the strip is presented in Figure 51. As shown in Figure 51a, the lateral pressure at the end of

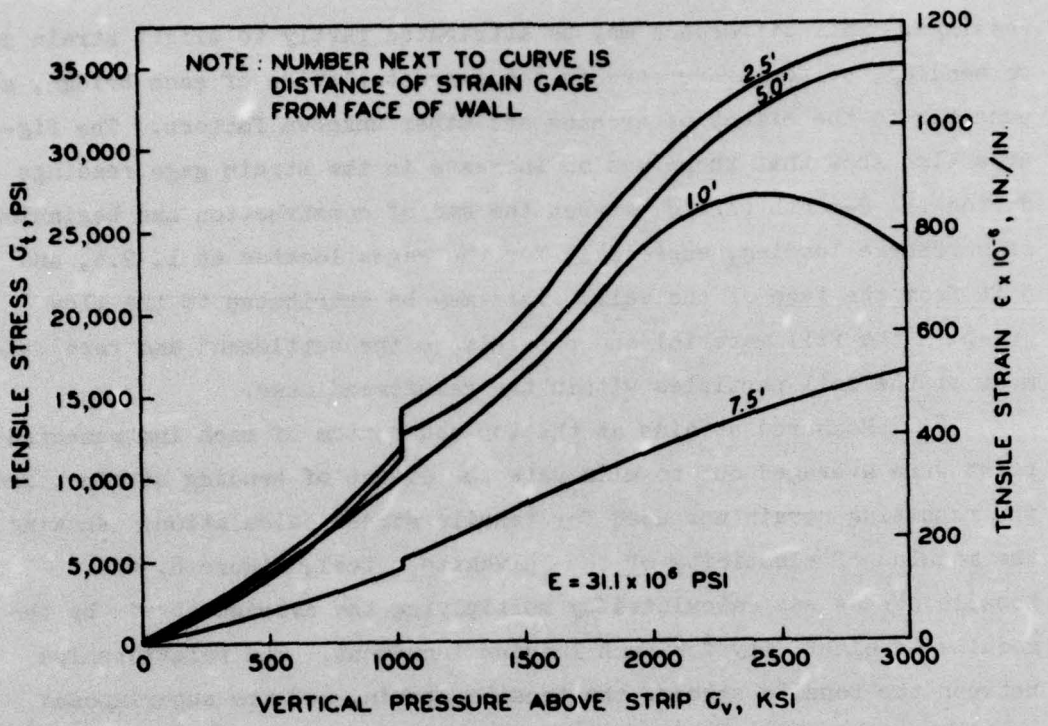

Figure 47. Relationship between tensile stress and vertical pressure for strips located 1 ft above the bottom of the wall

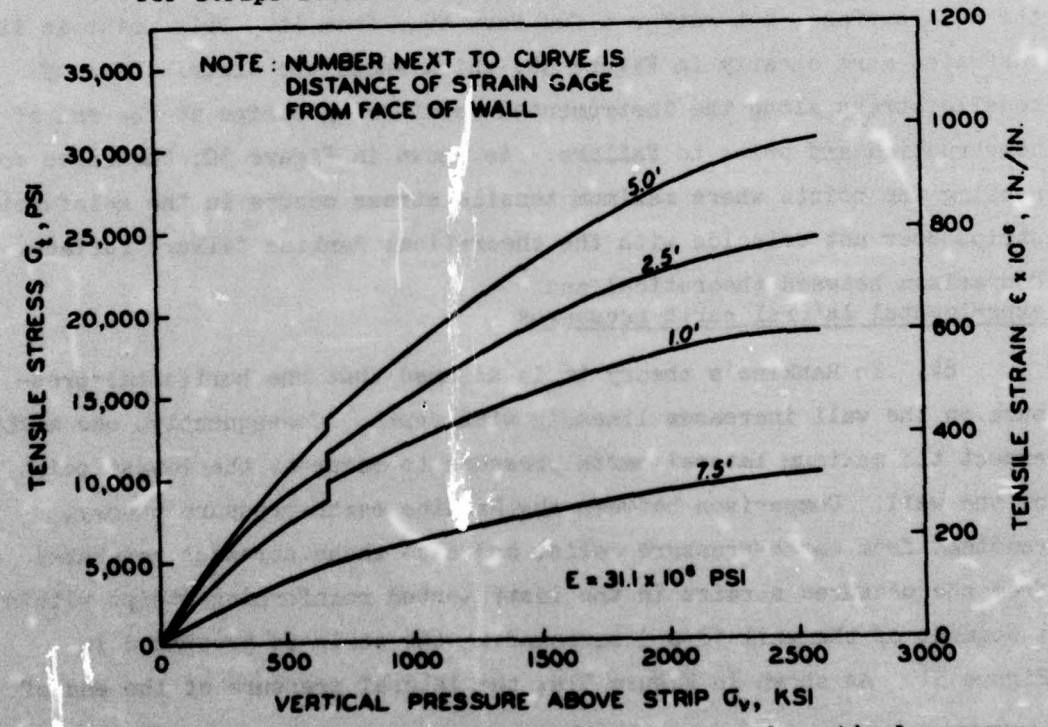

Figure 48. Relationship between tensile stress and vertical pressure for strips located 5 ft above the bottom of the wall

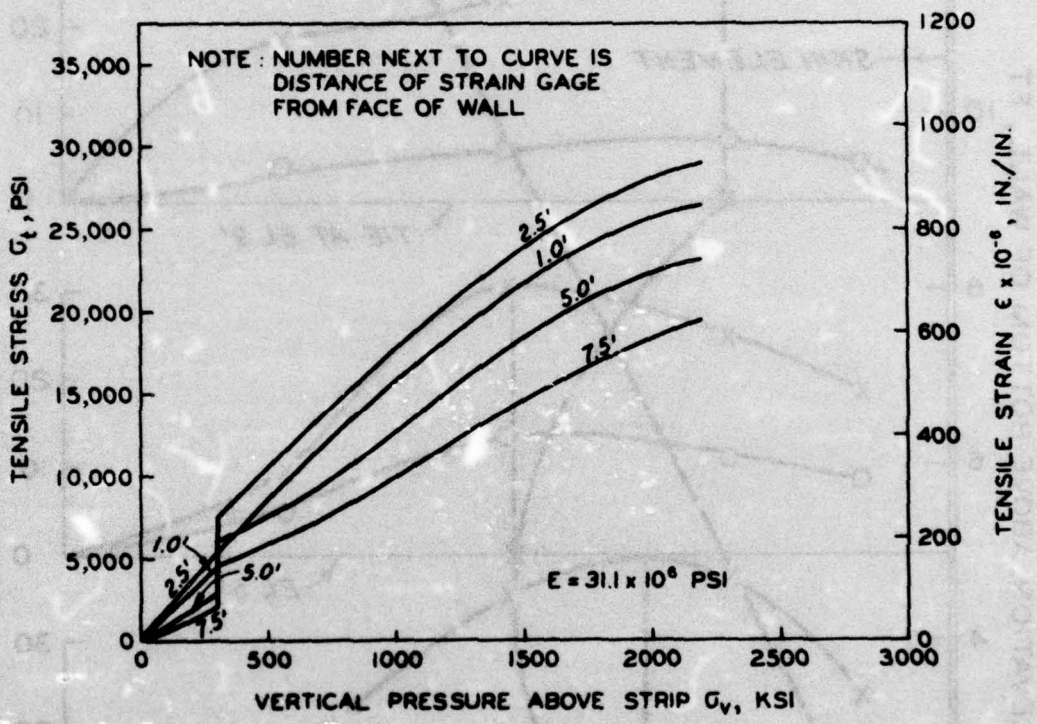

Figure 49. Relationship between tensile stress and vertical pressure for strips located 9 ft above the bottom of the wall

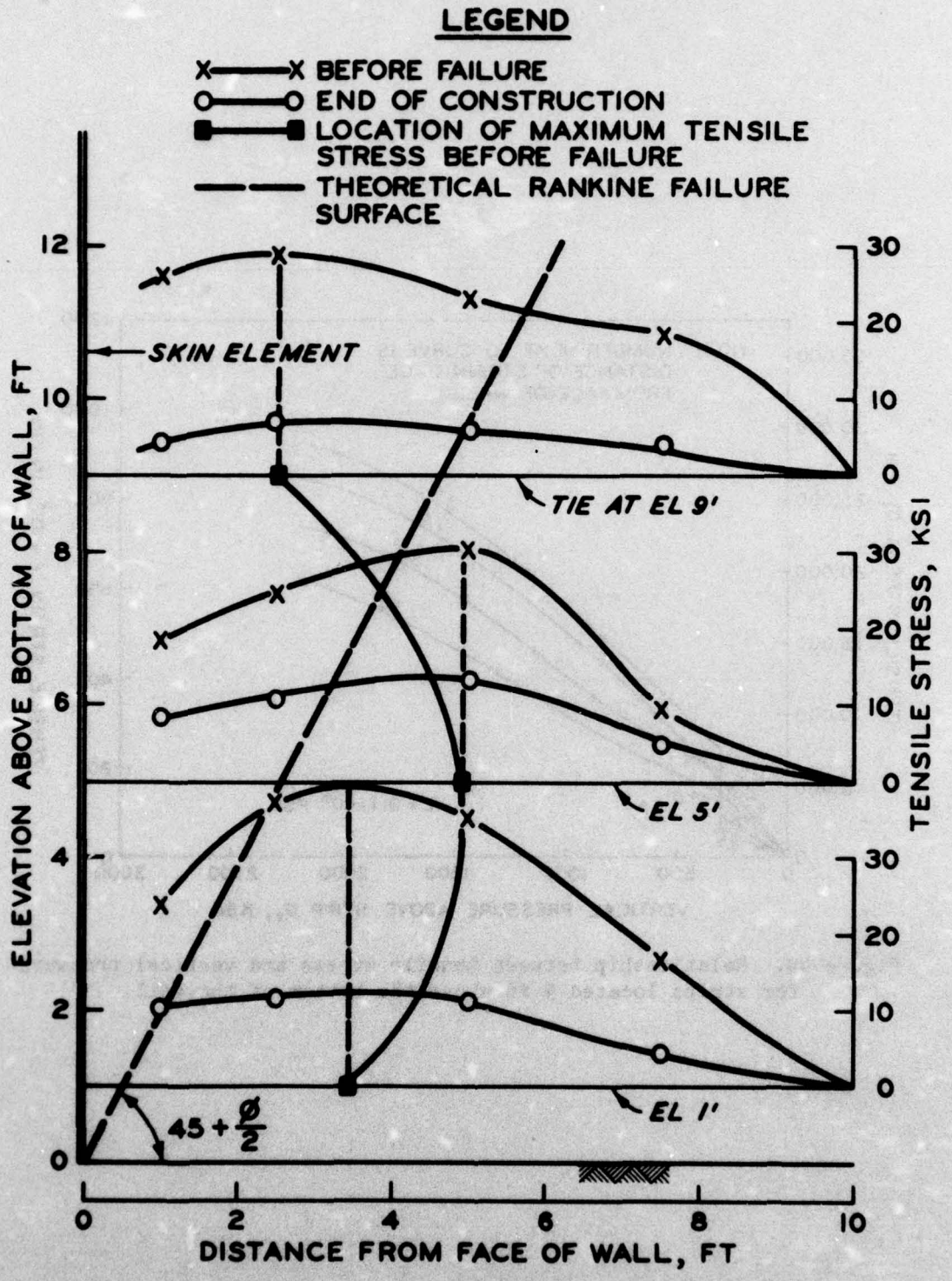

Figure 50. Tensile stress distribution along the instrumented reinforcing ties at the end of construction and before failure

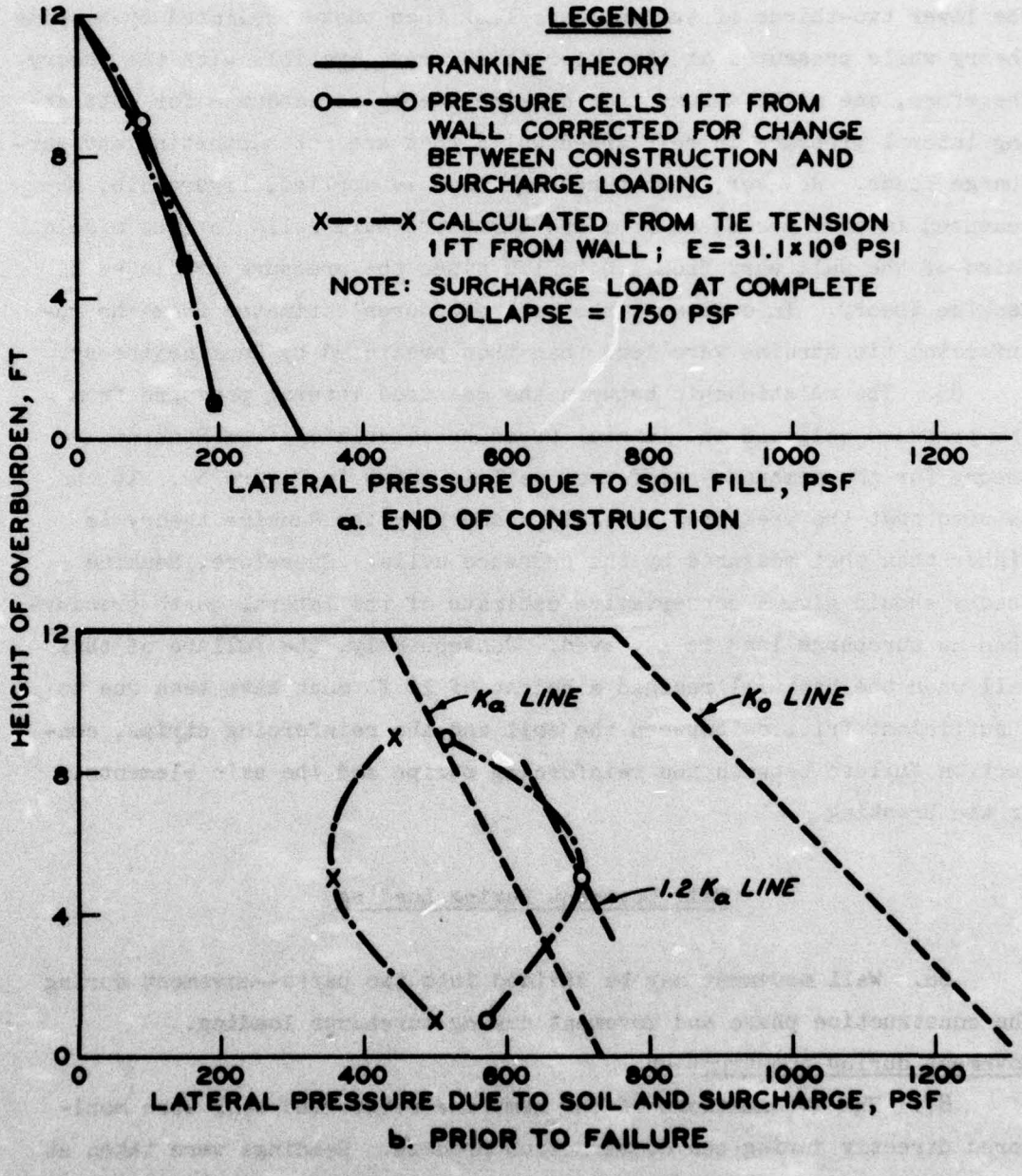

Figure 51. Comparison between theoretical and measured values of lateral pressures for the steel-reinforced wall

construction calculated from measured strains in the reinforcing strips, using modulus of elasticity $E = 31.1 \times 10^6$ psi, agrees with the pressure cell readings. In both cases the calculated lateral pressures on the lower two-thirds of the wall are less than those predicted by Rankine theory while pressures at the upper third are compatible with the theory. Therefore, one might assume that Rankine theory is adequate for estimating lateral pressure in reinforced walls that are not supporting any surcharge loads. However, when surcharge load is applied, Figure 51b, the measured lateral pressures from the earth pressure cells for the middle third of the wall vary from 1.0 to 1.2 times the pressure predicted by Rankine theory. In contrast, the wall pressures estimated from the reinforcing tie strains were less than that predicted by Rankine theory.

85. The relationship between the measured lateral pressure from the pressure cell and the lateral pressure calculated from Rankine theory for the membrane-reinforced wall is shown in Figure 52. It can be seen that the predicted lateral pressure by the Rankine theory is higher than that measured by the pressure cells. Therefore, Rankine theory should give a conservative estimate of the lateral earth pressure when no surcharge load is involved. Consequently, the failure of this wall when the backfill reached a height of 10 ft must have been due to insufficient friction between the soil and the reinforcing strips, connection failure between the reinforcing strips and the skin elements, or tie breaking.

Wall Movement During Loading

86. Wall movement may be divided into two parts--movement during the construction phase and movement during surcharge loading.

Movement during construction

87. The deformations of the membrane-reinforced wall were monitored directly during the construction process. Readings were taken at several points along the individual planks of the skin element after each 1-ft lift until the height of the wall reached 10 ft and the wall collapsed. The outward movement of the skin element during construction

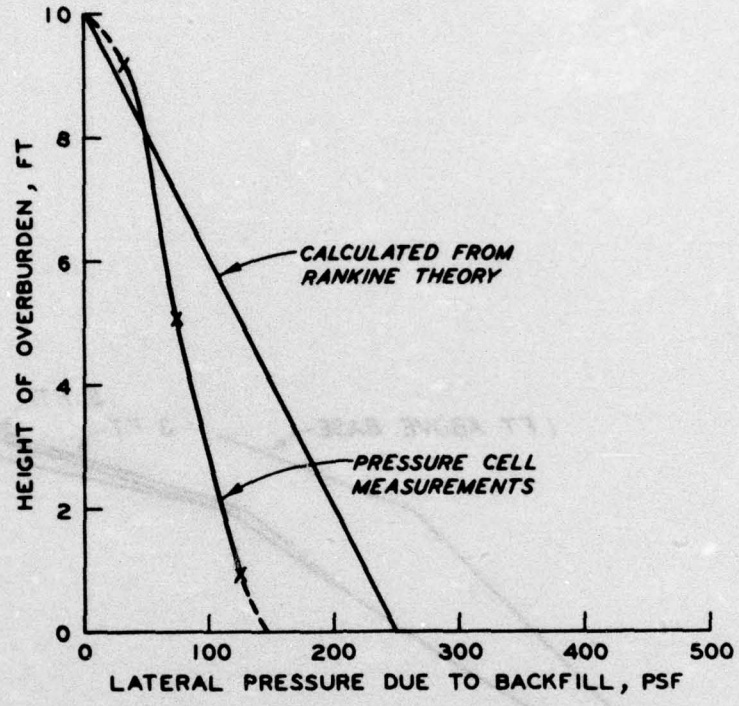

Figure 52. Comparison between theoretical and experimental values of lateral pressures acting on the membrane-reinforced wall

and prior to failure is shown in Figure 53. The figure shows that there was a steady outward movement as the height of fill increased with a minimum movement of 2.25 in. at the bottom and almost 6 in. at the top of the skin element prior to failure.

88. Examination of the skin element, connectors, and rubber membrane strips after failure (see Figure 54) showed no visible signs of defects, leading to the conclusion that the failure probably was entirely by pullout. However, laboratory direct shear tests indicated that the friction between the soil and the rubber was great enough to prevent pullout. The examination also showed that one connection at the lowermost row of landing mat came loose and that at three places a weld joint failed due to the great deformation of the skin element associated with the collapse of the wall. It may be possible, however, that the failure was caused by the large elongation of the membrane beyond that which was needed to create active failure in the soil mass.

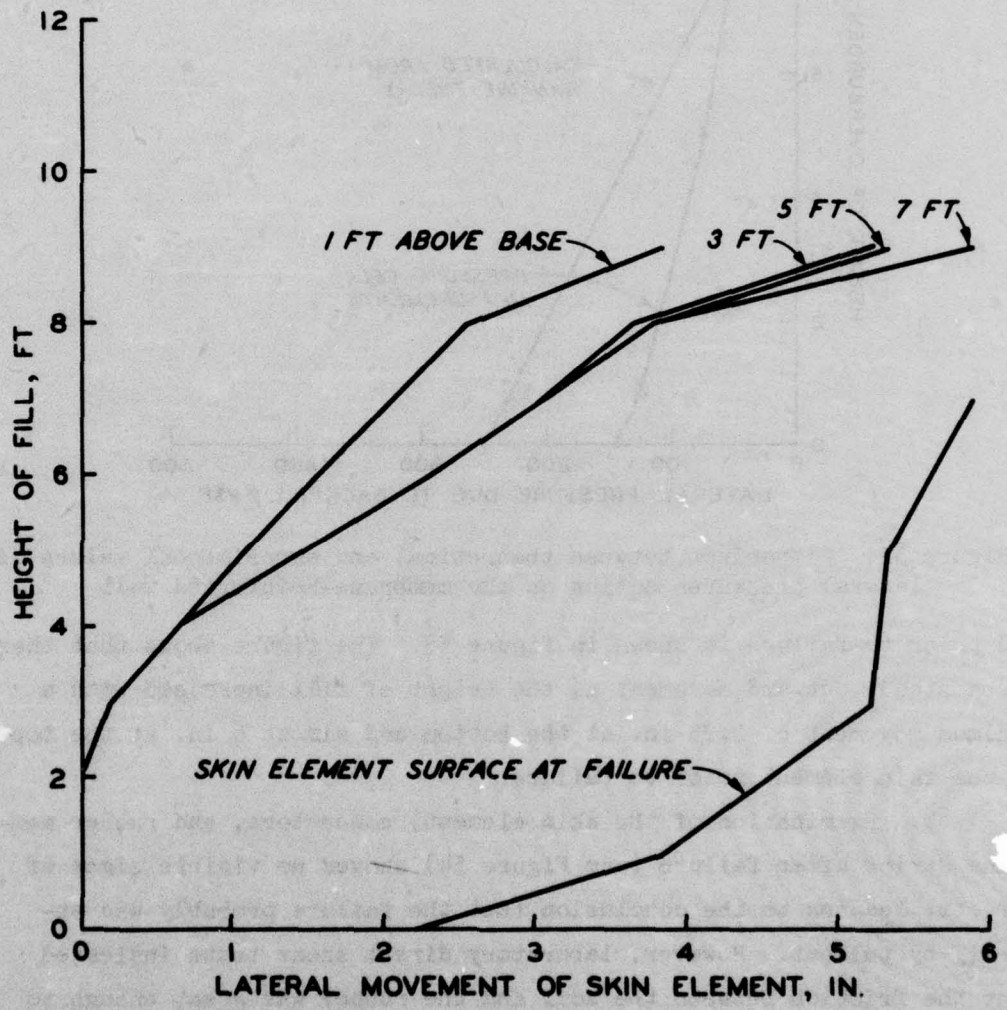

Figute 53. Lateral movement of skin element versus height of fill for the wall reinforced with rubber membrane

POSTFAILURE EXAMINATION:
ONE CONNECTOR CAME LOOSE AT THE FIRST ROW OF SKIN ELEMENTS.
WELD JOINT OF SKIN ELEMENT FAILED AT THREE PLACES.

Figure 54. Skin element for the rubber membrane-reinforced wall reassembled after failure

89. Measurement of the outward movement of the steel-reinforced wall was conducted in a manner similar to that used for the membrane-reinforced wall. The lateral deformations along the center line, however, were very small and were neglected.

Movement during surcharge loading

90. The deformation of the steel-reinforced wall was monitored during surcharge loading using wooden rules placed along the center line of the skin element at 2-ft intervals. The rules were read with every 250 psf of surcharge loading increment using a transit located about 200 ft from the wall. The lateral deformation of the skin element after each surcharge load increment is shown in Figure 55. This figure shows that the lateral deformation progressed slowly but uniformly until the surcharge pressure reached 1250 psf. However, beyond this surcharge pressure the deformation progressed very rapidly with load until failure

occurred very suddenly. The average ratio of lateral deformation to height was about 3 percent, which is much higher than that which might be expected during active failure for a conventional retaining wall of this height.

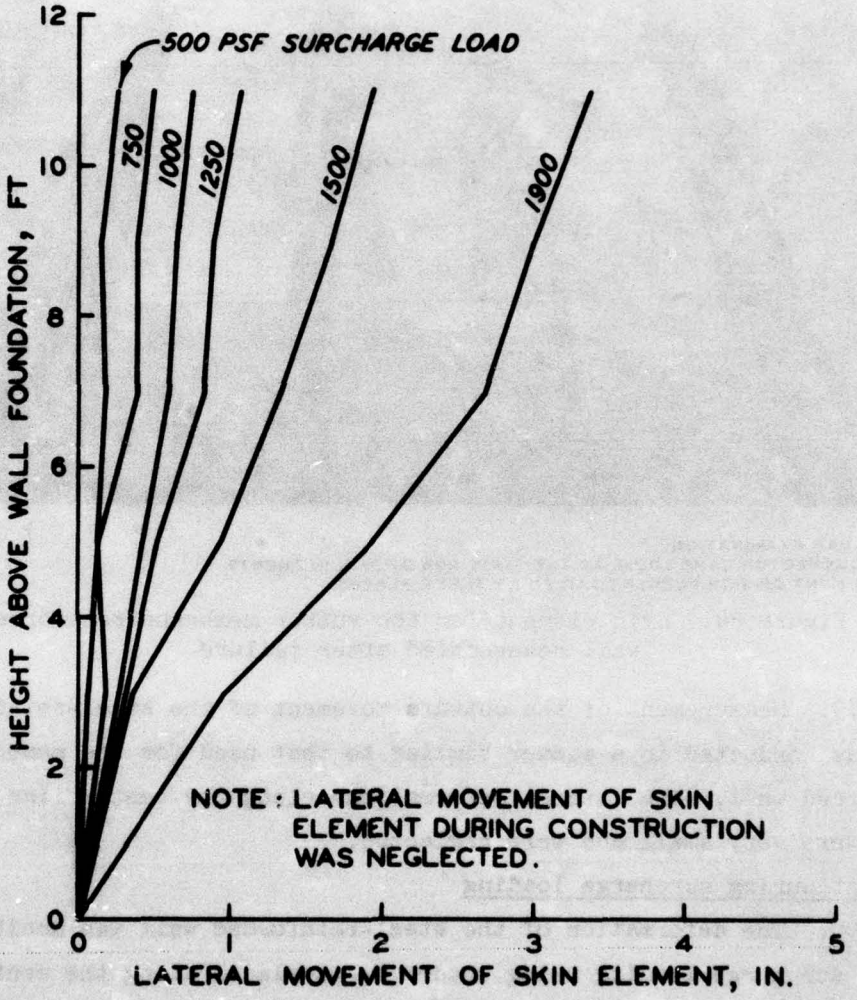

Figure 55. Skin element face deformation of the steel-reinforced wall due to surcharge load

PART VI: DESIGN CONSIDERATIONS

91. Three design criteria, which can be expressed in terms of safety factors, should be considered in designing reinforced earth structures similar to those described in this report. These criteria are related to tie breaking, tie pullout, and tie elongation.

Tie Breaking

92. The total horizontal force F_h induced by the weight of overburden acting on an area bounded by $S_x S_z$ (shown in Figure 2) may be expressed as:

$$F_h = k(q + \gamma d)S_x S_z \tag{22}$$

where k is the ratio of the horizontal to vertical pressure at any point along the skin element and q, γ, d, S_x, and S_z are as defined previously. The tie tension force F_t can be written as

$$F_t = \sigma_t wt \tag{23}$$

where σ_t is the average tensile stress in the reinforcing tie, and w and t are the width and thickness of the tie, respectively.

Factor of safety against tie breaking

93. The factor of safety against tie breaking FS_b may be defined as the ratio of the yield stress of the reinforcing tie σ_y to the expected maximum tensile stress σ_t. Thus

$$FS_b = \frac{\sigma_y}{\sigma_t} \tag{24}$$

Substituting Equation 24 into Equation 23 yields

$$F_t = wt \frac{\sigma_y}{FS_b} \tag{25}$$

Since F_t cannot exceed F_h, the maximum value of F_t is equal to

F_h . Therefore, by equating Equations 25 and 22, an expression for the factor of safety against tie breaking can be written as

$$FS_b = \frac{\sigma_y wt}{k(\gamma d + q)S_x S_z} \tag{26}$$

where k may vary between k_a and k_o as suggested in Figure 51. For this study the maximum k was found to be $1.2\ k_a$. While the maximum reinforcing tie tension is larger than values computed using estimated wall pressures (see Figure 50), the maximum measured tie tension values were not larger than those corresponding to $1.2\ k_a$.

Verification of FS_b

94. The properties of the reinforcing ties and the backfill material needed to calculate the factor of safety are presented in Table 2. Substituting the appropriate data from Table 2 in Equation 26, the factor of safety against breaking the most critical tie (lowest tie in the test walls) can be calculated.

a. Wall reinforced with neoprene-coated nylon membrane:

$$FS_b = \frac{\sigma_y wt}{k(\gamma d + q)S_x S_z} = \frac{14{,}500 \times 4 \times 0.08}{0.26(97.5 \times 8 + 0)4 \times 2} = 2.86$$

b. Wall reinforced with galvanized steel (no surcharge, $k = k_a$):

$$FS_b = \frac{\sigma_y wt}{k(q + \gamma d)S_x S_z} = \frac{55{,}000 \times 4 \times 0.024}{0.26(0 + 97.2 \times 11)2.5 \times 2} = 3.80$$

c. Wall reinforced with galvanized steel (with surcharge, $k = 1.2\ k_a$). Since the surcharge load at failure is not exactly known, one may ask what is the maximum surcharge load that the structure can carry at tie yield (i.e. $FS_b = 1$). Using Equation 26 yields

$$FS_b = \frac{\sigma_y wt}{k(q + \gamma d)S_x S_z} = \frac{55{,}000 \times 4 \times 0.024}{1.2 \times 0.26(q + 97.2 \times 11)2.5 \times 2} = 1$$

or $q = 2315$ psf, which is greater than the estimated surcharge load at failure (1500 psf for initial failure, about 1750 psf for complete collapse). This compares favorably with assessment of damage after collapse, which

indicated that all tie failures occurred near the connection brackets, probably due to high stress concentrations, and that no tie failures occurred within the backfill (see paragraph 76).

Tie Pullout

95. Because the frictional force is directly proportional to the relative movement between the tie and the surrounding soil mass and since soil movement is not known, it is not possible to directly determine the shear distribution along the tie. Lee, et al.[41] suggested in 1972 that only the length of reinforcing tie behind the Rankine failure surface, as shown in Figure 56, be used in calculating tie pullout. However, for this study, as shown in Figure 50, the curve connecting the points where maximum tensile stress occurs in the reinforcing ties does not coincide with the theoretical Rankine failure surface. Only the portion of the tie beyond the point of maximum tensile stress constitutes effective anchorage. Subsequent full-scale tests reported by Chang[26] and Lee[62] have also indicated that the curve connecting the points where maximum tensile stress occurs is not defined by the Rankine failure surface. However, as noted by Lee,[62] the information from full-scale field tests has not at present been used to develop an improved method of defining the effective tie length in computing tie pullout. Therefore, it can be assumed that the shear stress distribution at incipient active failure is as shown in Figure 56. If the frictional stress distribution along bc (see Figure 56) is approximated by a parabola, then the total effective frictional force along the reinforcing tie T_e is

$$T_e = 2w\left(\frac{2}{3}\tau_m \ell\right) = \frac{4}{3}\tau_m \ell w \qquad (27)$$

where τ_m is the maximum frictional stress along the tie and ℓ is the effective length of the tie.

Factor of safety against tie pullout

96. The factor of safety against pullout failure, FS_p, can be defined as follows:

$$FS_p = \frac{\tau_{ult}}{\tau_m} \qquad (28)$$

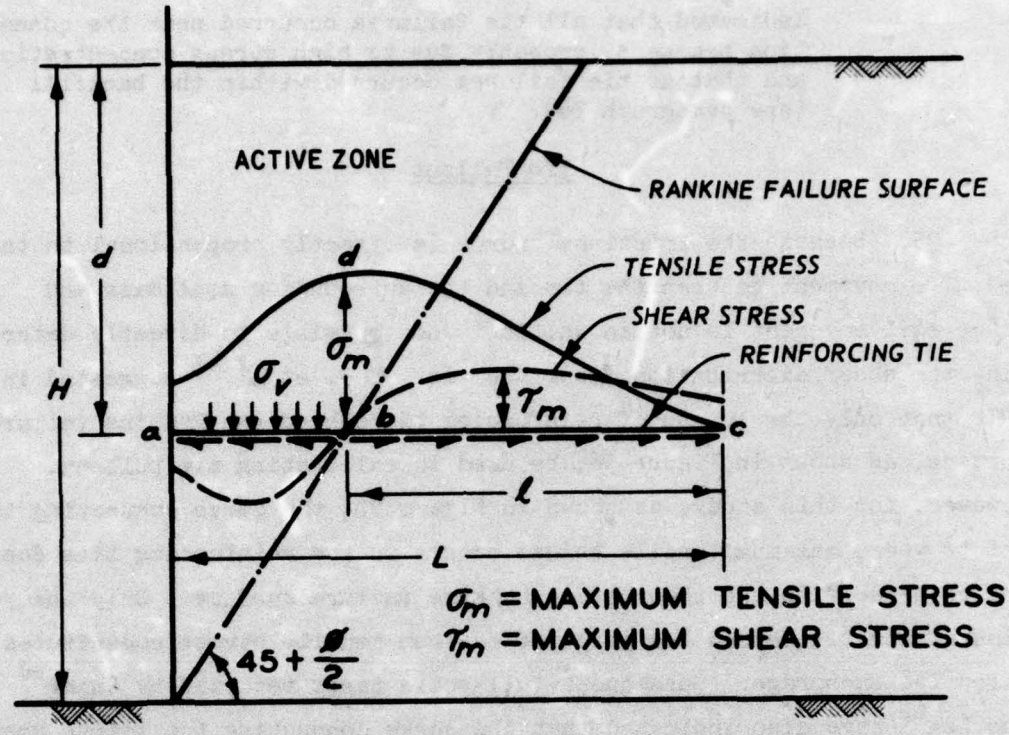

Figure 56. Hypothetical stress distribution along reinforcing tie

where τ_{ult} and τ_m are the ultimate and the maximum shear stresses between the reinforcing tie and the surrounding soil, respectively. The maximum mobilized τ_{ult} can be expressed in terms of the applied vertical stress on the tie as

$$\tau_{ult} = (q + \gamma d) \tan \phi_f \tag{29}$$

where ϕ_f is the angle of friction between the reinforcing tie and the surrounding soil as obtained by the direct shear tests and q, γ, and d are as defined previously. Substituting Equations 29 and 28 into Equation 27 and arranging terms, the following expression may be obtained:

$$T_e = \frac{4}{3} w\ell(q + \gamma d) \frac{\tan \phi_f}{FS_p} \tag{30}$$

97. If the friction force acting on the portion of the lowest tie within the Rankine zone is small and can be ignored, the effective friction force T_e should be equal to the horizontal force F_h as expressed by Equation 22. Therefore by equating Equations 30 and 22, an expression for the factor of safety against tie pullout FS_p can be obtained as

$$FS_p = \frac{4w\ell \tan \phi_f}{3kS_xS_z} \tag{31}$$

where k, depending on the loading conditions, may vary between k_a and k_o. For this study the maximum k was found to be $1.2\ k_a$.

Verification of FS_p

98. The factor of safety against pullout can be calculated from Equation 31 in conjunction with Tables 2 and 3 for the reinforced earth walls at the lowest tie. In general, the effective length ℓ may be expressed as

$$\ell = L - (H - d) \tan \left(45 - \frac{\phi}{2}\right) \tag{32}$$

where $(H - d)$ is the elevation of the tie above the floor, ϕ is the angle of internal friction of the fill, and L is the total length of the tie.

a. Neoprene-coated nylon fabric ties:

$$FS_p = \frac{4}{3} \frac{w\ell \tan \phi_f}{k_a S_x S_z} = \frac{4 \times 0.333 \times 9.49 \times 0.58}{3 \times 0.26 \times 4 \times 2} = 1.17$$

b. Galvanized steel ties at end of construction:

$$FS_p = \frac{4}{3} \frac{w\ell \tan \phi_f}{k_a S_x S_z} = \frac{4 \times 0.333 \times 9.49 \times 0.32}{3 \times 0.26 \times 2.5 \times 2} = 1.04$$

c. Galvanized steel ties prior to failure:

$$FS_p = \frac{4}{3}\frac{w\ell \tan \phi_f}{1.2\, k_a S_x S_z} = \frac{4 \times 0.333 \times 9.49 \times 0.32}{3 \times 1.2 \times 0.26 \times 2.5 \times 2} = 0.86$$

99. From the above calculations, it appears that the steel-reinforced wall was on the verge of pullout failure at the end of construction and should have failed in the early stages of surcharge loading. However, this did not occur, illustrating that assuming the effective length of reinforcing tie to be the length of tie behind the Rankine failure surface in calculating tie pullout can give erroneous results. An improved method of defining the effective tie length, compatible with full-scale field test results, to be used in computing tie pullout is needed. Pending development of an improved method for determining the portion of the tie that is effective for pullout resistance, Figure 50 could be used as an empirical guide.

Tie Deformation

100. Although it is not possible to obtain the exact total deformation in a reinforcing tie, it may be approximated from the measurement of strains. The strain distribution along the lowest galvanized steel tie is presented in Figure 57 as a function of the applied vertical load. The total deformation was obtained by multiplying the mean strain* under the applied load by the length of the tie; the results are summarized in Table 3.

101. Another indirect method, based on the elastic properties of the tie material and the total horizontal thrust, can be used to estimate the total tie deformation. From elementary strength of materials, the change in length ΔL in an elastic bar is

$$\Delta L = \frac{\sigma_t L}{E} \qquad (33)$$

---

* The mean strain was obtained by dividing the tie into ten equal segments (Figure 57) and then averaging the sum of strains corresponding to the midpoint of each segment.

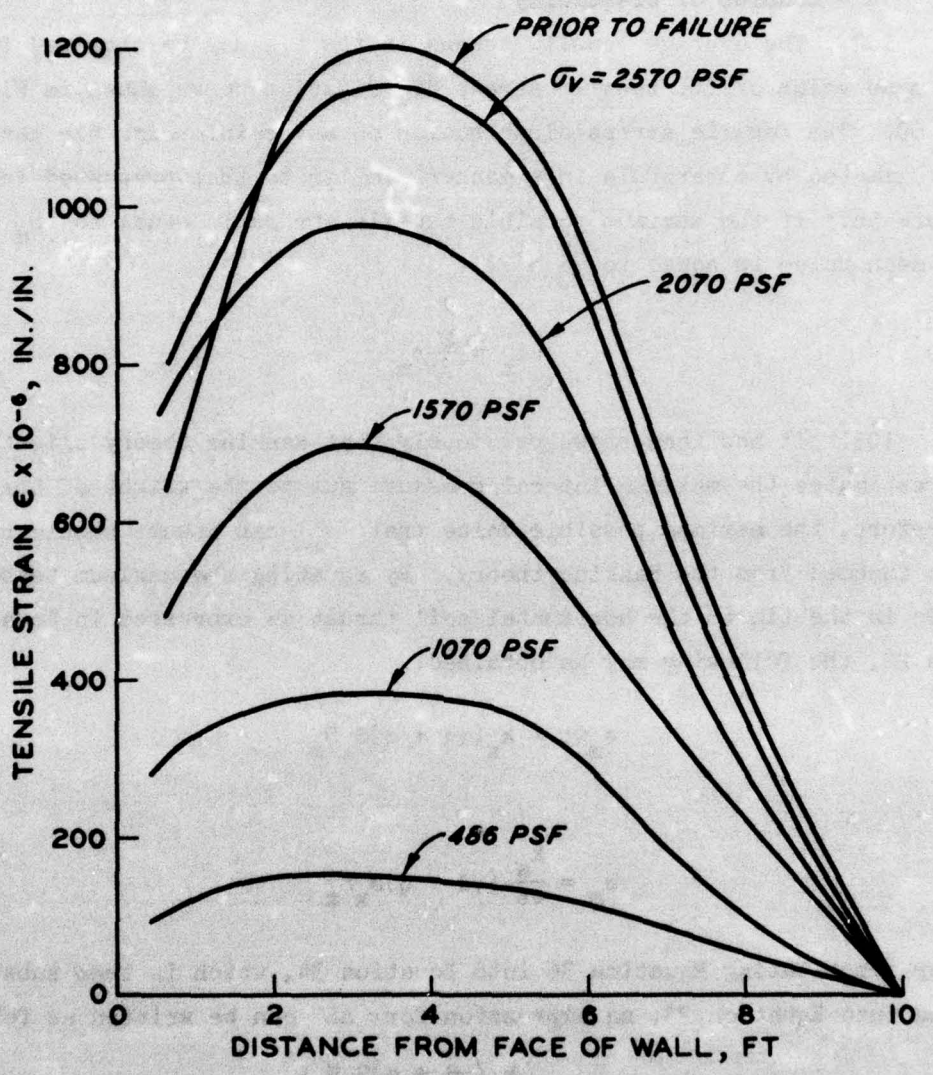

Figure 57. Variation of strain with respect to the applied vertical load for the lowest galvanized steel tie

where

σ_t = average tensile stress

L = initial length of the bar

E = modulus of elasticity

102. The average tensile stress in the tie may be obtained from the mean value of the tensile stress distribution curve shown in Figure 50. The tensile stress distribution on any reinforcing tie can be approximated by a parabola in a manner similar to that presented in Figure 56. If the maximum possible tensile stress is equal to σ_m and the mean value is equal to $\frac{2}{3}\sigma_m$,

$$\sigma_t = \frac{2}{3}\sigma_m \tag{34}$$

103. It has been shown previously that Rankine theory slightly overestimates the maximum lateral pressure due to the weight of the fill. Therefore, the maximum possible value that σ_m can assume should be that induced from the Rankine theory. By equating the maximum tensile force in the tie to the horizontal soil thrust as expressed in Equation 22, the following may be obtained.

$$\sigma_m wt = k_a(\gamma d + q)S_x S_z \tag{35}$$

or

$$\sigma_m = \frac{k_a}{wt}(\gamma d + q)S_x S_z \tag{36}$$

After substituting Equation 36 into Equation 34, which is then substituted into Equation 33, an expression for ΔL can be written as follows:

$$\Delta L = \frac{2}{3}\frac{k_a(\gamma d + q)S_x S_z L}{wtE} \tag{37}$$

Deformation of galvanized steel tie

104. The properties of the galvanized steel and the backfill material presented in Table 3 were substituted in Equation 37 to obtain the total deformation in the reinforcing ties. The lowermost tie was

selected for comparison, and the calculation of the total deformation is presented in Table 4.

105. Comparison between the total deformations obtained from strain measurements (Table 3) and those calculated from Equation 37 (Table 4), as presented in Figure 58, shows a close agreement between the two methods of prediction. Therefore, it appears that Equation 37 provides a reasonable means for obtaining the total deformation of the reinforcing tie under a given applied load.

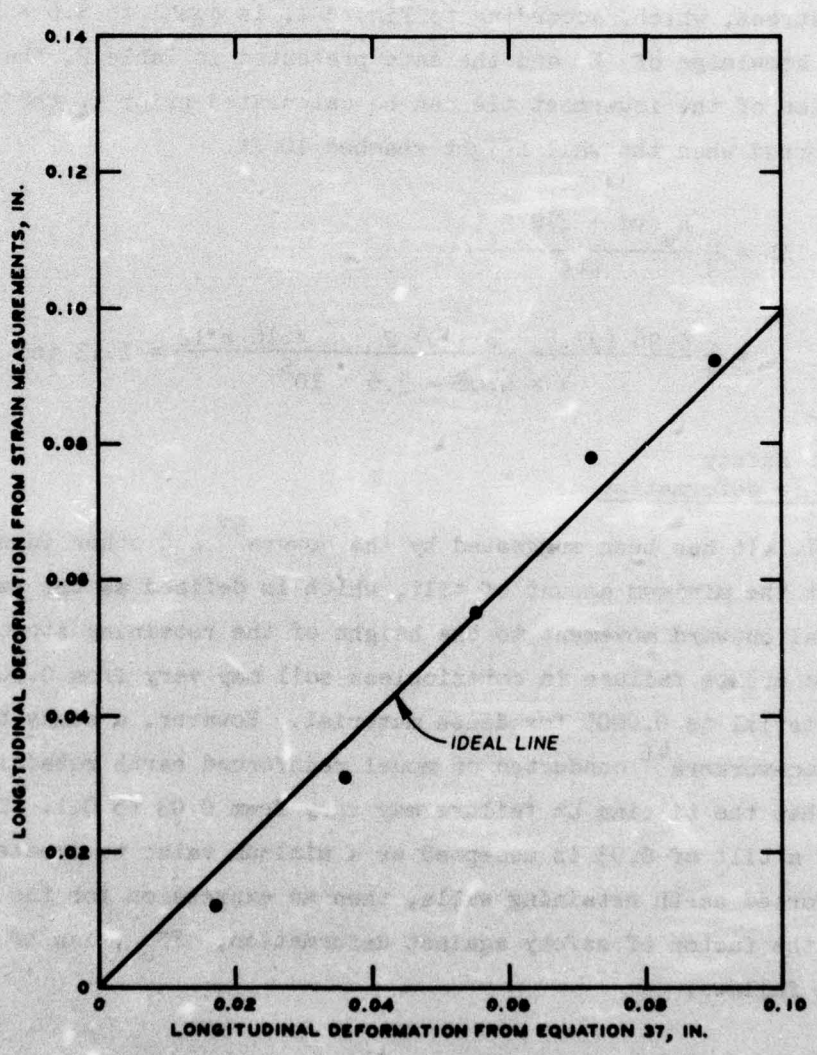

Figure 58. Comparison between measured and calculated deformations

Deformation of
neoprene-coated nylon fabric tie

106. Since the neoprene-coated nylon fabric ties were not instrumented with strain-measuring devices, the indirect method was used to estimate the total deformation. Unlike the galvanized steel ties, the modulus of elasticity of the neoprene-coated nylon fabric is not constant. Therefore, the modulus of elasticity used in the calculation is the secant modulus that corresponds to the stress equal to half the failure stress, which, according to Figure 7, is equal to 3.6×10^5 psi. From the knowledge of E and the data presented in Table 2, the total deformation of the lowermost tie can be calculated prior to the failure that occurred when the wall height reached 10 ft.

$$\Delta L = \frac{2}{3} \frac{k_a(\gamma d + q)S_x S_z L}{wtE}$$

$$= \frac{2}{3} \frac{0.26\ (97.5 \times 8 + 0)\ 2 \times 4 \times 10 \times 12}{4 \times 0.08 \times 3.6 \times 10^5} = 1.13 \text{ in.}$$

Factor of safety
against tie deformation

107. It has been suggested by the Sowers[63] and other investigators that the minimum amount of tilt, which is defined as the ratio of horizontal outward movement to the height of the retaining structure, needed to create failure in cohesionless soil may vary from 0.002 for loose material to 0.0005 for dense material. However, a study by Lee and his co-workers[41] conducted on model reinforced earth retaining walls showed that the tilting at failure may vary from 0.03 to 0.1. Therefore, if a tilt of 0.03 is accepted as a minimum value to create failure in reinforced earth retaining walls, then an expression for the tilt, θ, and the factor of safety against deformation, FS_d, can be formulated as follows:

$$\theta = \frac{\Delta L}{(H - d)} \tag{38}$$

$$FS_d = \frac{0.03}{\theta} = \frac{0.03\ (H - d)}{\Delta L} \qquad (39)$$

108. Equation 39 was applied to the lowest ties of the field tested walls to obtain the following factors of safety against failure due to tie deformations.

a. Neoprene-coated nylon fabric tie (ΔL = 1.13 in.):

$$FS_d = \frac{0.03\ (H - d)}{\Delta L} = \frac{0.03\ (9 - 8) \times 12}{1.13} = 0.32$$

b. Galvanized steel tie at end of construction (ΔL = 0.037 in.):

$$FS_d = \frac{0.03\ (H - d)}{\Delta L} = \frac{0.03\ (12 - 11) \times 12}{0.037} = 9.73$$

c. Galvanized steel tie prior to failure (ΔL = 0.090 in.):

$$FS_d = \frac{0.03\ (H - d)}{\Delta L} = \frac{0.03\ (12 - 11) \times 12}{0.090} = 4.0$$

109. From the above calculations, it can be seen that the factor of safety against tie deformation of the neoprene-coated nylon fabric reinforced wall is less than one, which may explain why it failed when it reached a height of 10 ft at a time when all calculations showed that it was safe against tie breaking and pullout.

PART VII: CONCLUSIONS AND RECOMMENDATIONS

Conclusions

110. A field test was conducted at WES on two instrumented reinforced earth retaining walls to investigate the feasibility of using reinforced earth as a viable construction material. Each wall was 16 ft long, 10 ft deep, and intended to be 12 ft high, with the first wall reinforced with neoprene-coated nylon fabric (membrane) and the second reinforced with galvanized steel strips. Although the membrane-reinforced wall failed when the height reached 10 ft, the steel-reinforced wall was built to a height of 12 ft and was able to carry a uniform surcharge load in excess of 1500 psf before collapse. Based on the data collected from the instrumentation of the wall, the following conclusions are offered.

Membrane-reinforced wall

a. The lateral earth pressure measured by pressure cells was found to be slightly lower than that predicted by the active Rankine earth-pressure theory.

b. There were no visible striations or defects in the ties which would have been present if pullout failure had occurred.

c. The average tilting of the skin element during construction was about 5 percent. This tilt, which is in excess of that needed to create active failure, was attributed to tie deformation and not to pullout due to the lack of friction between the tie and the surrounding soil.

Steel-reinforced wall

a. The pressure cells used to measure vertical pressure registered slightly higher than the actual overburden pressure up to 850 psf and registered slightly lower thereafter. The same trend occurred in measuring the lateral pressure.

b. The lateral earth pressure at the end of construction of the wall as measured by the pressure cells was found to be approximately equal to that predicted by the Rankine theory for the active condition.

c. The measured earth pressure along the skin element prior to failure was maximum at the middle third of the wall

AD-A036 120 ARMY ENGINEER WATERWAYS EXPERIMENT STATION VICKSBURG MISS F/G 8/13
EFFECT OF HORIZONTAL REINFORCEMENT ON STABILITY OF EARTH MASSES--ETC(U)
SEP 76 M M AL-HUSSAINI, E B PERRY

UNCLASSIFIED WES-TR-S-76-11 NL

2 OF 2
AD
A036120

END

DATE
FILMED
3-77

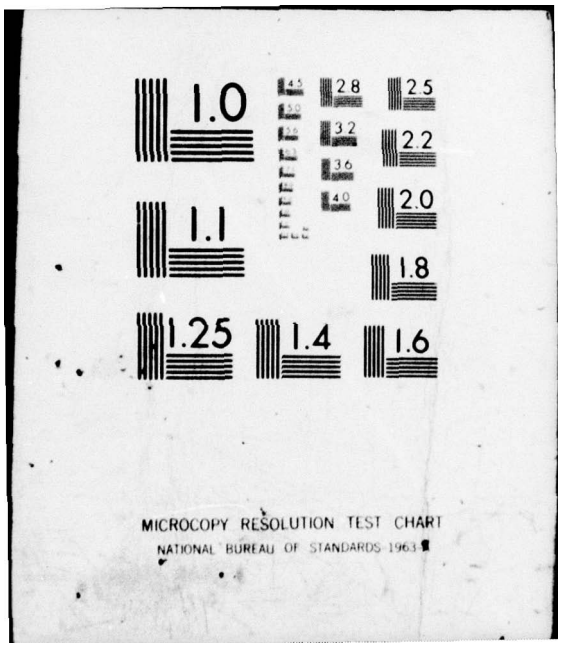
1.0
1.1
1.25
1.4
1.6
2.8
3.2
3.6
4.0
2.5
2.2
2.0
1.8
MICROCOPY RESOLUTION TEST CHART
NATIONAL BUREAU OF STANDARDS 1963

and varied from 1.0 to 1.2 times the earth pressure predicted by the Rankine theory for the active case.

d. The curve connecting the points where maximum tensile stress occurred in the reinforcing ties did not coincide with the theoretical Rankine failure surface.

e. The collapse of the wall was very quick (less than 3 sec) and the mode of failure was complex, but the general trend was overturning of the reinforced wedge about the toe. The average slope angle of the fallen fill was approximately equal to $(45 - \phi/2)$.

f. The reinforcing tie failure cannot be attributed to a single factor but rather to a combination of several factors, namely: connection failure at the junction between the tie and the skin element; tearing of the tie around the bolt joining the tie to the connector; tension failure across the tie at the junction with the skin element; pullout failure due to loss of skin friction; deformation, buckling, and shear failure in several parts of the skin element.

111. The field tests, especially the steel-reinforced wall test, indicate that the reinforced earth method of construction offers another alternative for constructing both temporary and permanent structures relating to problems of retaining earth masses. In some situations, the concept of reinforced earth can provide an economical, easy, and quick method of construction.

112. Current reinforced earth research activity at the WES includes the following:

a. Verifying the findings of this study with small-scale model tests using the same construction materials. The validity of the scale model tests should then be extended by varying the geometry and spacing of the various components of the reinforced earth wall.

b. Development of a finite element computer program with appropriate constitutive equations for the reinforced earth mass and performance of a parametric study for the system.

Recommendations

113. Based on the findings of this research, it is recommended that the study be expanded to:

a. Develop an improved method of defining the effective length of reinforcing tie, compatible with full-scale field test results, to be used in computing tie pullout.

b. Investigate the feasibility of using reinforced earth to improve the bearing capacity of pavements, footings, and other earth supporting structures.

c. Study the feasibility of using reinforced earth in zones of high tensile stresses in earth and rock-fill dams.

d. Investigate the feasibility of using reinforced earth for temporary flood protection systems over levees, dikes, and similar structures.

e. Study the feasibility of using reinforcement to improve the engineering behavior of soils with high silt and sand contents.

REFERENCES

1. "French Build Vertical Earth Retaining Walls," Engineering News-Record, Vol 182, 3 Apr 1969, pp 26-28.
2. "Reinforced Earth," Technical Information Note, Apr 1973, Central Laboratory of Ponts et Chaussees, Paris, France.
3. "Concrete Units Reduce Earth Wall Cost," Engineering News-Record, Vol 191, 8 Nov 1973, p 26.
4. Baguelin, F. and Bustamante, M., "Conception et etude de la Stabilite des Ouvrages en Terre Armée," Bulletin de liaison des Laboratoires des Ponts et Chaussees, Special R., pp 101-114, Dec 1971, Paris, France.
5. Consedine, R. L., ed., "Cost-Cutting Techniques Succeed on Quebec City Autoroute," Engineering and Contract Record, Vol 6, Jun 1973, pp 48-50.
6. Darbin, M., "The Reinforced Earth for the Construction of Roads and Motor Roads," Revue Generale des Routes et Aerodromes, No. 457, Sep 1970, pp 118-127. (Translation distributed by the Reinforced Earth Company, Washington, D. C.)
7. Kratochvil, L., "New Trends in Improving Physical Qualities of Rocks," International Civil Engineering, Vol 2, No. 6, 1971-1972, pp 241-258.
8. Legrande, J. and Baguelin, F., "La Terre Armée: Principes-Exemples d'Ouvrages de Soutènement," Proceedings, Seventh International Conference on Soil Mechanics and Foundation Engineering, Speciality Session Nos. 14 and 15, 1969, pp 206-211.
9. Sanglerat, G., "Massifs de Terre Armée," Revue Technica, Jul-Sep 1971.
10. Schlosser, F., "Reinforced Earth," Bulletin No. 62, pp 79-92, 1972, Central Laboratory of Ponts et Chaussees, Paris, France.
11. _____, "Reinforced Earth in Sete Interchange," Bulletin No. 63, pp 149-151, 1973, Central Laboratory of Ponts et Chaussees, Paris, France.
12. Schlosser, F. and Long, N. T., "Behavior of Reinforced Earth for Retaining Structures," Proceedings, Fifth European Conference on Soil Mechanics and Foundation Engineering, Vol 1, Apr 1972, pp 299-306.
13. Schlosser, F., Long, N. T., and Sevestre, F., "Reinforced Earth Structures on Loose Soils," Proceedings, Eighth International Conference on Soil Mechanics and Foundation Engineering, Vol 2.2, 1973, pp 201-205.
14. Schlosser, F. and Vidal, H., "Reinforced Soil," Bulletin No. 41, pp 101-144, Nov 1969, Central Laboratory of Ponts et Chaussees,

Paris, France. (Translation distributed by the Reinforced Earth Company, Washington, D. C.)

15. Vidal, H., "Reinforced Earth (A New Material for Public Works)," Annales, de l'Institut Technique du Bâtiment et des Travaux Publics, Vol 19, Nos. 223-224, Series: Materials (30), Jul-Aug 1966, pp 888-938. (Also published as Translation No. 67-12, Dec 1967, U. S. Army Engineer Waterways Experiment Station, CE, Vicksburg, Miss.)

16. _____, "The Principle of Reinforced Earth," Soil Theories: Reinforced Earth, Displacements, Bearing, and Seepage, Highway Research Board Record No. 282, 1969, pp 1-16, National Academy of Sciences - National Academy of Engineering, Washington, D. C.

17. _____, "Reinforced Earth, Recent Applications," Annales, de l'Institut Technique du Bâtiment et des Travaux Publics, Nos. 259-260, Series: Materials (38), Jul-Aug 1969, pp 1099-1155. (Translation distributed by the Reinforced Earth Company, Washington, D. C.)

18. _____, "Reinforced Earth Steel Retaining Wall Used on High, Steep Side Slope in France," Civil Engineering, Vol 40, No. 2, Feb 1970, pp 72-73.

19. "Metal Strips Reinforce 70-ft-High Roadbed," Engineering News-Record, Vol 188, No. 8, 24 Feb 1972, p 13.

20. "First Reinforced Earth Jobs in U. S. Completed," Roads and Streets, Vol 116, No. 2, Feb 1973, pp 94-95.

21. "Cuts and Fills Reconstructed on Unstable Mountain Highways," Engineering News-Record, Vol 190, 31 May 1973, p 15.

22. "Earth Laced with Metal Strips to Support Load," Engineering News-Record, Vol 191, No. 3, 19 Jul 1973, p 15.

23. Chang, J. C., Forsyth, R. A., and Beaton, J. L., "Performance of a Reinforced Earth Fill," Research Report CA-DOT-TL-2115-1-74-04, Jan 1974, California Department of Transportation, Division of Highways, Transportation Laboratory, Sacramento, Calif. (Paper presented at the Highway Research Board Annual Meeting, Jan 1974.)

24. _____, "Design and Field Behavior of the Reinforced Earth Embankment - Road 39," California Department of Transportation, Division of Highways, Transportation Laboratory, Sacramento, Calif. (Paper presented at the American Society of Civil Engineers National Water Resources Engineering Meeting, Los Angeles, Jan 1974.)

25. Chang, J., Forsyth, R., and Smith, T., "Reinforced Earth Highway Embankment - Road 39," Highway Focus, Vol 4, No. 1, Jan 1972, pp 15-35.

26. Chang, J. C., "Earthwork Reinforcement Techniques," Research Report CA-DOT-TL-2115-9-74-37, Oct 1974, California Department of Transportation, Division of Highways, Transportation Laboratory, Sacramento, Calif.

27. Gedney, D. S., "Reinforced Earth as a Highway Structure," Proceedings, Tenth Annual Engineering Geology and Soils Engineering Symposium, Apr 1972, pp 165-172.

28. _____, "Reinforced Earth as a Highway Structure," Landslide - The Slope Stability Review, Vol 1, No. 1, 1973, pp 11-14.

29. The Reinforced Earth Company, "Progress Report," Dec 1972, Washington, D. C.

30. _____, "Progress Report," Aug 1973, Washington, D. C.

31. _____, "RE/EARTH Wall Under Construction in Marine Environment," 9 May 1974, Washington, D. C.

32. Lindberg, H. A., "Reinforced Earth - Termination of an Experimental Feature of Construction," FHWA Notice N 5080.26, 22 Nov 1974, Federal Highway Administration, U. S. Department of Transportation, Arlington, Va.

33. Walkinshaw, J. L., "Reinforced Earth Construction," Report FHWA-DP-18, Apr 1975, Region 15, Federal Highway Administration, U. S. Department of Transportation, Arlington, Va.

34. Munoz, A., Jr., "Use of Reinforced Earth to Correct the Heart O' the Hills Slide," Proceedings, Twelfth Annual Engineering Geology and Soils Engineering Symposium, Apr 1974.

35. Royster, D. L., "Construction of Reinforced Earth Fill Along Interstate 40 in Tennessee," 25th Annual Highway Geology Symposium, Raleigh, N. C., May 1974.

36. Scott, C. P., "Construction of Reinforced Earth Fill in Tennessee," Highway Focus, Vol 6, No. 3, Jul 1973.

37. Binquet, J. and Lee, K. L., "Bearing Capacity of Strip Footings on Reinforced Earth Slabs," Report to National Science Foundation, Grant No. G1 38983, May 1975, Washington, D. C.

38. Guégan, Y. and Legeay, G., "Étude en Laboratoire de la Terre Armée en modèles réduits bidimensionnels," Rapport non Public Laboratoires des Ponts et Chaussees, Jan 1969.

39. Long, N. T. et al., "Étude des murs en Terre Armée sur modèles réduits bidimensionnels," Research Report No. 30, Dec 1973, Central Laboratory of Ponts et Chaussees, Paris, France.

40. Schlosser, F. and Long, N. T., "Recent Results in French Research on Reinforced Earth," Nov 1973, Central Laboratory of Ponts et Chaussees, Paris, France.

41. Lee, K. L., Adams, B. D., and Vagneron, J. J., "Reinforced Earth Walls," UCLA-ENG-7233, Apr 1972, University of California, Los Angeles, Calif.

42. Schlosser, F., "Recent Results in French Research on Reinforced Earth," Nov 1973, Central Laboratory of Ponts et Chaussees, Paris, France. (Paper presented at the American Society of Civil Engineers

National Water Resources Engineering Meeting, Los Angeles, Calif., Jan 1974.)

43. Long, N. T., Guégan, Y., and Legeay, G., "Study of Reinforced Soil Using the Triaxial Test Apparatus," Research Report No. 17, Jul 1972, Central Laboratory of Ponts et Chaussees, Paris, France.

44. Behnia, C., Étude des Voutes en Terre Armée, Doctor-Engineer Dissertation, University of Paris, Paris, France, Feb 1972.

45. Pratap, V., Stress Distribution in Reinforced-Earth, M. S. Dissertation, University of Cincinnati, Cincinnati, Ohio, 1970.

46. Lee, K. L., Adams, B. D., and Vagneron, J. J., "Reinforced Earth Retaining Walls," Journal, Soil Mechanics and Foundations Engineering Division, American Society of Civil Engineers, Vol 99, No. SM10, Oct 1973, pp 745-764.

47. Richardson, G. N., The Response of Reinforced Earth Walls to Vibratory Loading, M. S. Dissertation, University of California, Los Angeles, Calif., 1973.

48. Richardson, G. N. and Lee, K. L., "Response of Model Reinforced Earth Walls to Seismic Loading Conditions," UCLA-ENG-74-12, Feb 1974, University of California, Los Angeles, Calif.

49. Vagneron, J. J., Reinforced Earth Walls, M. S. Dissertation, University of California, Los Angeles, Calif., 1972.

50. Yang, Z., Strength and Deformation Characteristics of Reinforced Sand, Ph. D. Dissertation, University of California, Los Angeles, Calif., 1972.

51. Yang, Z. and Singh, A., "Strength and Deformation Characteristics of Reinforced Sand," paper presented at the American Society of Civil Engineers National Water Resources Engineering Meeting, Los Angeles, Jan 1974.

52. Richardson, G. N. and Lee, K. L., "Seismic Design of Reinforced Earth Walls," paper presented at the American Society of Civil Engineers National Water Resources Engineering Meeting, Los Angeles, Calif., Jan 1974.

53. Bell, J. R., Stilley, A. N., and Vandre, B., "Fabric Retained Earth Walls," Proceedings, Thirteenth Annual Engineering Geology and Soils Engineering Symposium, Apr 1974.

54. Yamanouchi, T., "Experimental Study on the Improvement of the Bearing Capacity of Soft Ground by Laying a Resinous Net," Proceedings, Symposium on Foundations on Interbedded Sands, 1970, pp 144-150.

55. Taylor, D. W., Fundamentals of Soil Mechanics, Wiley, New York, 1948.

56. Terzaghi, K., "A Fundamental Fallacy in Earth Pressure Computations," Engineering Publication No. 182, Soil Mechanics Series No. 3, 1936, Harvard University, Cambridge, Mass.

57. Instron Corporation, "Instruments and Equipment," Catalog 1-1, 1966, Canton, Mass.

58. American Society for Testing and Materials, "Standard Methods of Test for Breaking Load and Elongation of Textile Fabrics; Modified Grab Test, MG," Designation: D 1682, 1975 Book of ASTM Standards, Part 32, 1975, Philadelphia, Pa., p 309.

59. Carr, G. L., "Evaluation of Modified T11, Dow, U. S. Steel, Alcoa T11, and Fenestra Landing Mats," Miscellaneous Paper S-69-17, May 1969, U. S. Army Engineer Waterways Experiment Station, CE, Vicksburg, Miss.

60. Office, Chief of Engineers, Department of the Army, "Laboratory Soils Testing," Engineer Manual EM 1110-2-1906, 30 Nov 1970, Washington, D. C.

61. Department of Defense, "Military Standard for Pavement, Subgrade, Subbase, and Base-Course Materials," Military Standard MIL-STD-621A, Method 102, 22 Dec 1964, Washington, D. C.

62. Lee, K. L., "Reinforced Earth--An Old Idea in a New Setting," paper submitted to the 1976 International Symposium on New Horizons in Construction Materials, Bethlehem, Pa., Nov 1976.

63. Sowers, B. G. and Sowers, G. F., Introductory Soil Mechanics and Foundations, 3rd ed., Macmillan, New York, 1970.

Table 1

Summary of Water Content and Density of Soil During Construction of Reinforced Earth Walls

Elevation ft	Heavy-Duty Membrane		Galvanized Steel	
	Water Content %	Dry Density pcf	Water Content %	Dry Density pcf
1	4.7	98.1	4.8	98.8
2	5.2	97.9	4.7	97.7
3	4.9	96.0	5.1	97.9
4	4.8	97.1	5.0	97.8
5	5.0	96.3	5.0	98.0
6	4.5	97.3	4.8	95.5
7	4.5	97.3	5.3	96.0
8	4.4	99.4	4.9	95.7
9	3.6	98.0	3.7	98.1
10	3.4	97.1	4.3	98.6
11	--	--	3.2	95.0
12	--	--	--	--
Average	4.5	97.5	4.6	97.2

Table 2

Properties of Materials Used in Reinforced Earth Walls

Variable	Wall with Galvanized Steel	Wall with Neoprene-Coated Membrane
S_x	2.5 ft	4.0 ft
S_z	2.0 ft	2.0 ft
w	4.0 in.	4.0 in.
t	0.024 in.	0.08 in.
σ_y	55,000 psi	14,500 psi
E	31.1×10^6 psi	(Nonlinear)
γ	97.2 pcf	97.5 pcf
ϕ	36 deg	36 deg
ϕ_f	18 deg	30 deg
k_a	0.26	0.26
k_o	0.41	0.41
q	1500 psf	none
d	11 ft	8 ft

Table 3

Total Deformation at Lowest Galvanized Steel Tie

Using Strain Distribution Curve

d ft	γ_d psf	q psf	q + γ_d psf	ΔL in.
5	486	0	486	0.012
11	1070	0	1070	0.031
11	1070	500	1570	0.055
11	1070	1000	2070	0.078
11	1070	1500	2570	0.092
11	1070	1900	Prior to failure	0.094

Table 4

Total Deformation at Lowest Galvanized Steel Tie

Using Equation 37

d ft	q psf	γ_d + q psf	$k_a(\gamma_d + q)S_xS_z$ lb	$\frac{2}{3}\frac{L}{wtE}$ in./lb	ΔL in.
5	0	486	632	0.0263×10^{-3}	0.017
11	0	1070	1390		0.037
11	500	1570	2041		0.055
11	750	1820	2366		0.063
11	1000	2070	2691		0.072
11	1250	2320	3016		0.081
11	1500	2570	3341		0.090

APPENDIX A: NOTATION

C_u	Coefficient of uniformity of sand
d	Vertical distance from top of retaining wall (L)
D_{50}	Mean diameter of sand grains (L)
E_t	Tangent modulus (F/L^2)
F	Resultant of gravity force (F)
F'	Resultant force acting at angle ϕ to the normal of the failure plane (F)
F_h	Horizontal thrust acting on area $S_x S_z$ (F)
F_t	Tie tension force (F)
FS_b	Factor of safety against reinforcing element breaking
FS_d	Factor of safety against deformation
FS_p	Factor of safety against reinforcing element pulling out
G_s	Specific gravity
h	Distance from backfill surface to point in soil mass (L)
H	Height of retaining wall (L)
i	Angle between earth fill and horizontal
k	Coefficient of earth pressure = σ_h/σ_v ; ratio of horizontal to vertical pressure at any point along reinforcing element
k_a	Coefficient of active earth pressure
k_o	Coefficient of earth pressure at rest
K'	Constant defined in terms of ϕ , α , δ , and i
K"	Constant defined in terms of ϕ and δ
ℓ	Effective length of reinforcing element (L)
L	Length of reinforcing element (L)
p	Pressure at a point (F)
P	Resultant of total pressure acting on vertical plane (F)
P'	Resultant force acting at angle δ to retaining wall (F)
q	Retaining wall surcharge pressure (F/L^2)
Q	Resultant of retaining wall surcharge (F)
S_x	Horizontal distance between reinforcing elements (L)
S_z	Vertical distance between reinforcing elements (L)
t	Thickness of reinforcing element (L)

T_d	Tensile force in reinforcing element (F)
T_e	Total effective frictional force along reinforcing element (F)
T_{max}	Maximum tensile force in reinforcing element (F)
w	Width of reinforcing element (L)
W	Resultant of gravity force (F)
W'	Sum of the resultant forces W and Q (F)
α	Angle between contact surface of retaining wall and vertical
γ	Unit weight of backfill (F/L^3)
γ'	Composite unit weight of soil and surcharge (F/L^3)
γ_d	Dry unit weight of soil (F/L^3)
γ_{max}	Maximum unit weight of soil (F/L^3)
γ_{min}	Minimum unit weight of soil (F/L^3)
δ	Angle between thrust for P' and the normal to the retaining wall
ΔL	Change in length of reinforcing element
ε	Axial strain
ε_h	Horizontal strain
θ	Angle between any failure plane in the backfill and the horizontal
σ	Axial or normal stress (F/L^2)
σ_h	Horizontal stress (F/L^2)
σ_m	Maximum possible tensile stress (F/L^2)
σ_t	Tensile stress in reinforcing element (F/L^2)
σ_v	Vertical stress (F/L^2)
σ_y	Tensile yield stress (F/L^2)
σ_1	Major principal stress (F/L^2)
σ_3	Minor principal stress (F/L^2)
τ_m	Maximum frictional stress along reinforcing element (F/L^2)
τ_{ult}	Ultimate shear stress along reinforcing element (F/L^2)
ϕ	Angle of internal friction
ϕ'	Effective angle of internal friction
ϕ_f	Angle of skin friction between soil and reinforcing element

In accordance with ER 70-2-3, paragraph 6c(1)(b), dated 15 February 1973, a facsimile catalog card in Library of Congress format is reproduced below.

Al-Hussaini, Mosaid M

Effect of horizontal reinforcement on stability of earth masses, by Mosaid M. Al-Hussaini [and] Edward B. Perry. Vicksburg, U. S. Army Engineer Waterways Experiment Station, 1976.

1 v. (various pagings) illus. 27 cm. (U. S. Waterways Experiment Station. Technical report S-76-11)

Prepared for Office, Chief of Engineers, U. S. Army, Washington, D. C., under Project 4A161102AT22, Task A2, Work Unit 004.

Includes bibliography.

1. Membrane strips. 2. Reinforced earth. 3. Reinforcing materials. 4. Retaining walls. 5. Soil stability. 6. Steels. 7. Stress-strain relations (Soils). I. Perry, Edward Belk, joint author. II. U. S. Army. Corps of Engineers. (Series: U. S. Waterways Experiment Station, Vicksburg, Miss. Technical report S-76-11)
TA7.W34 no.S-76-11